Title
Facilitating Shared Haptic Experiences: Design, Engineering, and Perception

ISBN
9798186385448

Author
Dinulescu, Stejara Iulia

Publication Date
2026-03-25

University of California
Santa Barbara

Facilitating Shared Haptic Experiences: Design, Engineering, and Perception

A dissertation submitted in partial satisfaction
of the requirements for the degree

Doctor of Philosophy
in
Media Arts and Technology

by

Stejara Iulia Dinulescu

Committee in charge:

Professor Yon Visell, Chair
Professor Jennifer Jacobs
Professor Elliot Hawkes

June 2026

The Dissertation of Stejara Iulia Dinulescu is approved.

Professor Jennifer Jacobs

Professor Elliot Hawkes

Professor Yon Visell, Committee Chair

March 2026

Facilitating Shared Haptic Experiences: Design, Engineering, and Perception

Acknowledgements

This research presented in this document would not have been possible without tremendous support from collaborators, mentors, friends, and family.

First, I want to thank my PhD advisor, Dr. Yon Visell, for mentoring this research and supporting me in my growth as a scientist and writer. I want to thank my committee members, Dr. Jennifer Jacobs and Dr. Elliot Hawkes, for their incredible support and feedback during my years at UCSB; their courses inspired this research and contributed to my academic growth. I additionally extend my deepest gratitude and appreciation for my peers and collaborators from the RE TOUCH Lab – Neeli Tummala, Gregory Reardon, Dustin Goetz, Yitian Shao, Bharat Dandu, Anzu Kawazoe, Mengjia Zhu, Max Linnander, and Serena Lee – who have provided tremendous feedback on my research and inspired me to become a better scientist.

This work would not have been possible without the tremendous financial support and guidance from the University of California, Santa Barbara, the Media Arts and Technology Program, and the National Science Foundation throughout my PhD. I want to specifically thank Allyson Walker and Marcos Novak for their assistance during my years at UCSB.

A huge thank you to Kit Dunagan, whose unwavering support inspired my continued determination over the past several years. I additionally am extremely grateful to Nefeli Manoudaki, Iason Paterakis, and Mert Toka for their tremendous support and artistic collaborations, inspiring me to think outside the box and pushing me as an artist throughout my PhD. I lastly want to thank my family – Aurelia, Antonia, and Catalin Dinulescu – for their tremendous support and dedication, despite the distance, and my cat Nala and horse Bunny, who keep me motivated to persevere and enjoy the mundane.

Curriculum Vitæ
Stejara Iulia Dinulescu

Education

2026	Ph.D. in Media Arts and Technology (Expected) *University of California, Santa Barbara.*
2024	M.S. in Media Arts and Technology *University of California, Santa Barbara.*
2019	B.S. in Psychology B.A. in Creative Computation B.A. in Studio Art *Southern Methodist University.*

Publications

Journal Articles

1. M. Zhu, A. Ferstera, **S. Dinulescu**, N. Kastor, M. Linnander, E. W. Hawkes, Y. Visell (2023) *A Peristaltic Soft, Wearable Robot for Compression Therapy and Massage*. IEEE Robotics and Automation Letters.
2. M. Zhu, S. Biswas, **S. Dinulescu**, N. Kastor, E. W. Hawkes, Y. Visell (2022) *Soft, Wearable Robotics and Haptics: Technologies, Trends, and Emerging Applications*. Proceedings of the IEEE.
3. **S. Dinulescu**, T. Alvi, D. Rosenfield, C.S. Sunahara, J. Lee, B. A. Tabak (2021) *Self-Referential Processing Predicts Social Cognitive Ability.* Social Psychological and Personality Science.

Peer-Reviewed Conference Papers

1. **S. Dinulescu**, N. Tummala, G. Reardon, B. Dandu, D. Goetz, S. Topp, Y. Visell (2022). *A Smart Bracelet Supporting Tactile Communication and Interaction.* Proceedings of the IEEE, Haptics Symposium.

In Preparation

S. Dinulescu, D. Goetz, N. Tummala, S. Lee, J. Carpino, Y. Visell (2026) *An Inter-Manual Exoskeleton that Facilitates Guided Multi-Finger Grasping and Manipulation.*

S. Dinulescu, N. Tummala, S. Lee, Y. Visell (2026) *Haptic Shape Perception via Guided, Whole-Hand Exploratory Movements.*

Awards

2022	**Runner Up, Best Conference Paper** (Place 2/39) *IEEE Haptics Symposium*, Santa Barbara, CA
2021	**Graduate Research Fellowship** *National Science Foundation*
2020	**Honorable Mention, Most Promising Work-In-Progress** *IEEE Haptics Symposium*, Virtual Proceedings

Abstract

Facilitating Shared Haptic Experiences: Design, Engineering, and Perception

by

Stejara Iulia Dinulescu

Despite rapid advances in computing and multimedia, there is a digital divide surrounding our sense of touch: Existing technologies cannot facilitate the sharing of haptic experiences in the ways that are possible with other media. The challenges in realizing such technologies arise from the hand's biomechanical complexity and extensive sensory capabilities, as well as from the intrinsically active nature of touch interactions. This dissertation builds upon prior research on haptic perception and hand function to investigate opportunities for new haptic technologies and methods that can facilitate the sharing of haptic experiences.

After two chapters of introduction and background information, the third chapter addresses the need for the digital transcription of interpersonal touch communication through tactile sign languages (TSLs), used by people with multiple sensory impairments. It presents a wrist-worn smart bracelet that senses touch-evoked skin oscillations, extracts discriminative spatiotemporal features, and accurately classifies the 26 letters of the Deafblind Manual alphabet, an Australian TSL, while leaving the hand free for natural interaction. This chapter establishes that semantic touch gestures can be digitally encoded and recognized via remote sensing at the wrist, and it presents methodologies for integrating tactile communication with digital systems to bridge the haptic digital divide.

The fourth chapter moves from the context of sharing touch communication digitally to shared physical haptic interactions. This chapter presents the design, fabrication,

and evaluation of an inter-manual exoskeleton that passively couples two hands together, enabling the transfer of finger, thumb, and hand movements from one person (guiding) to another person (guided). This device creates an unusual sensorimotor condition in which the guiding participant retains motor control but lacks direct cutaneous contact with the object. Experiments assessing manual dexterity (peg-in-hole, shape stacking) show that the grasping and manipulation of small objects is facilitated under guided movement conditions with the exoskeleton, with minimal loss in task accuracy. However, task completion times were substantially longer in the guided condition than during self-directed movement. This device serves as both a functional mechanism for shared manual interaction and as an experimental platform for investigating sensorimotor consequences of guided haptic interactions with objects.

The fifth chapter uses the aforementioned inter-manual exoskeleton to investigate whether haptic perception of three-dimensional shape requires hand movements to be self-directed. The inter-manual exoskeleton enables the guided participant to receive cutaneous input from contacting objects, without self-directing finger and hand movements during the haptic interaction. In a haptic experiment using three-dimensional objects of complex surface features, guided participants discriminated object shape reliably above chance; however, self-directed exploration resulted in higher performance. These findings show that guided hand movements nevertheless support the haptic discrimination of complex three-dimensional objects.

The research presented in this dissertation contributes to a deeper scientific understanding of the sensorimotor system; specifically, how guided movements affect haptic perception and hand function during grasping and manipulating objects (Chapters 4 and 5). Additionally, it provides technical methodologies that integrate the sense of touch across digital social interactions (Chapter 3). Ultimately, this dissertation positions the goal of sharing our rich, whole-hand touch experiences at the forefront of emerging haptic technologies and scientific inquiry.

Contents

List of Figures

List of Tables

Chapter 1

Introduction

Advances in multimedia computing, targeting predominantly auditory and visual sensory modalities, have transformed our social and digital interactions. We can now share images through social media, experience live streams, and engage with virtual or mixed reality with the simple click of a button and access to the internet. However, despite decades of research, no technology can capture, reproduce, or share the rich touch experiences that approximate those that we encounter in most daily activities. This persistent gap, which I refer to as the *haptic digital divide*, is not merely a technical limitation of sensors or actuators, but a consequence of the inherent biological complexity of the human hand, which functions as both a refined sensory organ and a dexterous manipulator of the physical environment. It has therefore proven challenging to develop haptic devices that facilitate sharing our rich haptic experiences with other people, outside of the original sensorimotor contexts in which they are felt.

The first challenge stems from the ability of the human hand to facilitate diverse functions across a myriad of contexts: We can grasp and manipulate small or heavy objects, gently shape lumps of clay into intricate, detailed sculptures, squeeze the hand of a friend to convey comfort or support, or communicate through tactile sign languages, where letters are spelled across the hand with combinations of tapping, pinching, and sliding gestures. The remarkable, dexterous abilities of the hand arise from the complex neural integration of tactile information, sensed via mechanoreceptors in the skin, kinesthetic information, sensed via receptors in the joints and muscles, and internal predictive models of anticipated sensorimotor consequences [11, 12, 13, 14, 15, 16]. Our ability to coordinate movements is therefore intrinsically linked to what we feel.

Second, the human haptic sense is an inherently active sensory modality [17, 18, 19]. During haptic perception, our self-directed hand movements elicit specific tactile signals from the interaction, enabling the rapid haptic identification of objects and their properties (such as shape, size, texture, weight, hardness, and temperature) [20, 21, 9, 22, 23, 17]. These tactile signals are highly dependent on how objects are explored; for example, we move our hands across object surfaces to feel texture, we lift objects to perceive weight, and we press into objects or deform them to feel compliance. What we feel is therefore intrinsically linked to how we move our hands.

The interdependencies between haptic perception and hand function, as illustrated above, have made it challenging to capture and share our rich touch experiences to date, as sharing a haptic experience is not as simple as capturing and replaying what we feel via the skin, outside of the hand's kinematic context. In order to further the broader goal of sharing of haptic experiences, new technologies, capable of mediating collaborative haptic interactions, must be developed. This dissertation presents the motivation, design, fabrication, and evaluation of two wearable haptic devices that enable shared touch experiences between two people, alongside contributions made to the scientific understanding of the human haptic sense.

In the third chapter, the shared experience of tactile communication is examined. Touch plays an essential role in communication with individuals affected by multiple sensory loss, many of whom use modes of touch communication that can be broadly described as tactile sign languages (TSLs). When communicating through TSLs, one person touches the hand of another person using distinct tactile lexicons to spell out sentences with expression and nuance, similarly seen with verbal languages. Few technologies exist today to support such interactions. This chapter directly addresses a current need for supporting digital tactile communication for those with multi-sensory impairments by presenting a smart bracelet that can digitally capture and accurately classify letters of the Deafblind Manual alphabet, an Australian tactile sign language. Such wearable tactile transcription devices are a promising avenue for increasing the accessibility of digital touch interactions for those with multiple sensory loss, who communicate via TSLs. This research also presents tangible haptic input methodologies that can be applied more broadly towards bridging the current haptic digital divide, furnishing new paradigms for human-computer interaction via self- and interpersonal-touch contact.

In the fourth chapter, an inter-manual exoskeleton is developed to facilitate physical shared haptic interactions with objects. Here, the shared haptic experience is the physical, manual guidance of one hand by another hand, resulting in the transfer of kinematic postures from the guiding to the guided hands. As a consequence of this guidance, the haptic sense is partitioned across two people, where one person can directly touch the objects, and the other person can directly control performed movements. Evaluation of the exoskeleton indicates that small objects can be successfully grasped and manipulated under guidance, as shown through two manual dexterity tasks. The device further serves as a platform for scientific investigation into haptic perception under guided, multi-finger movements, explored subsequently.

In the fifth chapter, a shared haptic perceptual experience is investigated: The question of interest is whether hand movements when perceiving objects are still sufficiently informative when they are guided by another person, rather than self-directed. The inter-manual exoskeleton, presented in the fourth chapter, is employed here, where one person guides the multi-finger movements of another person in exploring the surfaces of two objects, which contain complex surface features, and judging whether their shapes are the same or different. Findings indicate that guided movements support complex three-dimensional shape discrimination, suggesting that hand movements may not need to be deliberate to be perceptually informative.

The design, development, and evaluation of these two haptic devices contribute to greater scientific knowledge of our human haptic sense and present tangible outcomes towards a future where our sense of touch can be shared between two people. The following two sections further detail the contents and contributions of this dissertation.

1.1 Overview

The second chapter of this dissertation integrates interdisciplinary theories and experimental findings from the fields of haptic engineering, neuroscience, psychophysics, and perception to describe what is known about the human hand function and the haptic sense, contextualizing the research contributions in the subsequent chapters. The second chapter begins with a review of our sensorimotor system, followed by investigations into contextual differences between active, exploratory touch and passive, guided touch. It further reviews how our sense of agency over body movements and haptic experiences arises cognitively, and it culminates with design considerations for wearable devices that interface with the hand for haptic interaction.

The subsequent chapters of this dissertation (Chapters 3-5) present the design, fabrication, evaluation, and contributions of two haptic technologies towards the goal of sharing haptic experiences between two people. In one case, the focus is on the specific context of interpersonal tactile communication; in another case, the context of collaborative inter-manual, multi-finger guidance is addressed (including the more kinematically complex thumb, which has been a challenge to address to date). These wearable devices progress the overall vision of sharing haptic experiences and may additionally serve as experimental platforms for fundamentally investigating human haptic perception and hand mobility.

The third chapter identifies a current need for haptic sensing technologies that can support digital tactile communication for people with multiple sensory loss, who employ lexicons of semantic touch gestures, known as tactile sign languages, for interpersonal communication. A smart bracelet is developed using four sensors worn at the wrist to capture and analyze vibrations that are elicited in the skin from touch gestures performed on the hand. Here, the hand is left free to support tactile and manual interactions. The smart bracelet can accurately classify ($> 90\%$) the 26 letters of the Australian Deafblind Manual tactile sign language, despite a limited dataset. The first digital input device of its kind for users who communicate via tactile sign languages, this work shows how existing modes of tactile communication can be integrated with information technologies using currently available sensing methods and algorithmic approaches.

The fourth chapter presents the design of a passive, inter-manual exoskeleton, coupling the hands of two people, that enables the hand of one user to guide multi-finger grasping and manipulation by the hand of another user. The device is designed to provide the guiding hand with sufficient direct control, and to afford sufficient mobility, to enable successful grasping and manipulation of small objects using the guided hand's fingers, without the need for actuation or control electronics. The design was informed by an idealized kinematics analysis, along with ergonomic considerations, mobility requirements, and avoidance of occlusion. The functionality of the device was assessed during experiments that coupled the hands of pairs of participants in representative manual dexterity tasks. One participant guided motion, using vision, and the other remained passive and compliant. Results show that manual dexterity tasks can be successfully performed with the inter-manual exoskeleton, albeit with significantly slower performance when compared to individual (self-directed movement) conditions. Such an inter-manual exoskeleton can be used to prototype and evaluate the design of multi-finger kinesthetic interfaces and may find use in scientific experiments on haptic perception.

The fifth chapter examines how haptic shape discrimination varies when hand movements are self-directed or guided by another person, using the inter-manual exoskeleton presented in the previous chapter. Participants in either self-directed or guided movement conditions judge whether two objects (3D-printed bell peppers) are the same, regardless of their orientations, and report their confidence in provided responses. Results indicate that although performance is higher during self-directed movements, guided movements nevertheless support complex three-dimensional object perception. While haptic object perception relies on exploratory procedures (i.e., patterns of hand movements that depend on the haptic attributes of interest), our results suggest that the hand movements need not always be deliberate, although further research is warranted. Exploratory findings on subjective experiences during guided multi-finger movements indicate that such shared haptic experiences may change feelings of body ownership or awareness in the guided hand, opening up avenues for future research inquiry.

Chapter Six concludes the dissertation, presenting future research opportunities for digital and inter-manual technologies that enable shared haptic experiences.

1.2 Contributions

This dissertation presents the following contributions, summarized by chapter:

- The first chapter motivates the research in this dissertation through a proposal that diverges from conventional approaches to haptic interaction design: that of designing systems that facilitate the sharing of haptic experiences, rather than systems that enable virtual haptic experiences of a single person.

- The second chapter of this dissertation presents an interdisciplinary literature review, synthesizing information from the fields of haptics, neuroscience, engineering, human-computer interaction, and cognitive psychology to contextualize the research presented across the next three chapters. Additional in-depth background relevant to the constituent research is given within the relevant chapters.

- The third chapter presents a smart bracelet for facilitating tactile communication and interaction, specifically the transcription of tactile sign language communication that is used by numerous people worldwide who are Deafblind. The methodology presented here can transcribe tactile sign language with high accuracy and points toward future possibilities for sharing tactile communication digitally. This research has won two awards at the IEEE Haptics Symposium (2020 and 2022), the former being Honorable Mention for Most Promising Work-In Progress Award, and the latter being runner-up for Best Paper Award.

  - This chapter presents the first characterizations of skin oscillations evoked across the hand during signing, providing new insight into what the hand feels during communication via tactile sign languages.
  - This research demonstrated that tactile sign language letters can be discriminated by sensing these skin oscillations. This discrimination is possible even when employing only a few sensors, located at wrist.
  - The prior finding informed the design of a smart bracelet worn at the wrist that integrates just four miniature accelerometer sensors.
  - The device enables TSL transcription with per-letter accuracies of greater than 90%.

- The fourth chapter presents a distinct approach to facilitating shared haptic experiences – the design of an inter-manual exoskeleton that enables guided, multi-finger grasping and manipulation.

  - This research demonstrates an unconventional approach to haptic design by presenting a kinematically designed mechanism that enables the hand of one user to guide movements and manipulation by another user's hand, without the need for actuators or control electronics.
  - Using this inter-manual exoskeleton, participants are able to complete representative, standardized manual dexterity tasks (peg-in-hole and shape-stacking) by guiding manipulation of another hand.
  - This device facilitates new experimental paradigms for investigating haptic perception and hand function, and it could additionally aid the design and fabrication of multi-finger haptic technologies for hand guidance.

- The fifth chapter utilizes the shared haptic approach presented in the prior chapter to investigate haptic discrimination of three-dimensional objects with complex surface features under guided movement conditions.

  - During guided, rather than self-directed, hand movements, participants were nonetheless able to discriminate complex haptic shapes. This is significant because established accounts of haptic object perception generally assume that hand movements are deliberately-produced and self-directed to facilitate perception. The results of this chapter show that this is not entirely the case.
  - Subjective experiences during such shared haptic experiences may result in changes of body awareness of guided users, although further investigation is needed.

Chapter 2

Considerations for The Human Haptic Sense

This chapter reviews prior literature from the fields of neuroscience, haptic engineering, psychophysics, and cognitive psychology as a general context for the research presented in this dissertation. More detailed overviews on the topics of each chapter (Chapters 3-5) are presented in their respective introduction sections. This chapter summarizes the sensorimotor complexities inherent in the human haptic sense and investigates several contexts for haptic interaction (i.e., active, exploratory touch versus passive, guided touch paradigms). Furthermore, it discusses engineering principles and design considerations for wearable haptic systems, including sensing and actuation technologies, and explores additional considerations for assistive haptic devices. This chapter provides the research context and motivations for the smart bracelet assistive device, presented in the third chapter, and the inter-manual exoskeleton that enables guided hand movements, presented in the fourth chapter and employed in the fifth chapter.

2.1 Preface

The English word *haptic* originates from the Greek words *haptikós*, meaning "able to touch/come into contact with" and *háptein*, meaning "to grasp/to fasten" [24, 25, 26, 27].

Haptics is defined by the Oxford English Dictionary as "of the nature of, involving, or relating to the sense of touch, the perception of position and motion (proprioception), and other tactile and kinesthetic sensations." As seen through the etymology and definition of "haptic," there exists inherent couplings between 1) our cutaneous sense, where information is perceived through receptors in the skin, 2) our proprioceptive sense, where relative position of the kinematics of the body is conveyed via receptors in the muscles and joints, and 3) our ability to coordinate and plan movements of the hand, eliciting deliberate information from hand-object interactions [20, 21, 28, 29, 30, 18, 31]. The field of haptic engineering is therefore an interdisciplinary one, combining perception and psychophysics, neuroscience and neurobiology, and electrical, mechanical, and materials engineering to develop devices targeting the human haptic sense. This chapter's purpose is to highlight the complexities of the human haptic sense by presenting relevant theories and experimental findings from existing literature. These complexities and considerations have made it difficult to develop devices that can preserve and share our rich touch experiences.

2.2 Our Sensorimotor System

Our haptic modality is highly refined. Incoming information from thousands of tactile receptors (over 10,000 per hand) are integrated and processed in the brain's somatosensory cortex, the primary region for processing sensations felt via the skin [13, 11, 12, 31, 32]. These sensations are intimately coupled to the kinesthetic conditions with which they were experienced, and our perception of the tactile interaction is a product of sensory and motor processing in the brain [28, 33]. For example, when we open a door by manipulating a doorknob, the ways in which we move our hands will deform our skin and other tissues. This results in our perception of the shape, texture, size, and resistance of the doorknob. We then coordinate our resulting hand movements, which includes increasing our grasping force until our fingerpads do not slip against the surface, and activating the necessary muscles to turn the wrist. Haptics is thus the coordinated process of touch perception and action, with the hand as our primary sensorimotor effector for contacting the world around us [12, 32, 9, 17].

There are four classes of tactile receptors in the glabrous skin of the hand, which respond to different aspects of mechanical stimulation (such as vibration, skin stretch, motion, etc.) [13, 33]. The mechanoreceptors, embedded in the skin at various depths, send electrical impulses (i.e., spikes) up the body of the cutaneous afferent (i.e., peripheral nerve cell). These electrical impulses are passed through the cuneate nucleus (spinal cord), brain stem, thalamus, and finally converge within the primary somatosensory cortex of the brain. Here, incoming sensory information is integrated and processed into perception.

Cutaneous afferents are characterized as slowly adapting (SA) when responding to a sustained stimulus, or rapidly adapting (RA) when responding to a change in stimulus (i.e., start and end of a vibration). The four mechanoreceptor types, as described by Saal and Bensmaia [13], are as follows:

- Slowly adapting type 1 afferents (SA1, terminate in Merkel disks) respond to skin deformations and forces.
- Slowly adapting type 2 afferents (SAII, terminate in Ruffini cylinders) respond to skin stretch and are thought to encode information about hand conformation.
- Rapidly adapting afferents (RA, terminate in Meissner corpuscles) respond to low-frequency vibration and motion across the skin.
- Pacinian corpuscle afferents (PC, also rapidly adapting) respond to a wide range

of vibration frequencies.

While these afferents have been traditionally seen to provide non-overlapping streams of tactile information to the brain, known as functional sub-modality segregation, Saal and Bensmaia have shown that populations of receptors across these four classes are excited by most tactile stimuli (i.e., sub-modality convergence) [13]. Our gestalt perception of incoming sensory information is thus an integrated product of responses from populations of multiple mechanoreceptor types throughout the duration of contact with the stimulus.

In response to perception of tactile stimuli, we often move our bodies to accommodate and execute an intended action (described as deliberate or self-directed movement) [20, 34]. Our ability to grasp objects, or even perform a simple hand posture such as a pinching movement, is a result of coordinated muscle activations, constrained by the musculoskeletal system [28, 33, 35, 36, 37, 16]. The conformations of bones in our bodies, along with tendons, flexor and extensor muscles, and ligament tissues, dictate our range of movement, which can be expressed by degrees of freedom (DOF) and evaluated kinematically. The unique conformation of the human hand, specifically the prehensile thumb enabling abduction, adduction, extension, and flexion movements, is a structural reason for our tremendous abilities to grasp and manipulate objects within a wide range of sizes and weights.

Along with performing locomotion, muscles are additionally thought to provide sensory inputs to the brain in order to prevent over-extension and injury, as well as dynamically sense position in space (i.e., proprioception) [38, 33]. Furthermore, it has been shown that cutaneous afferents are either directly or indirectly connected to circuits involved with core locomotion, thus modulating these afferent signals [39, 40]. When picking up a glass of water, we make quick corrective adjustments to our grip force to prevent the object from slipping without overexerting the muscles. These adjustments in grip force are a result of strain patterns at the fingertip, sensed by mechanoreceptors in the skin [13, 29]. In turn, unexpectedly changing these strain patterns at the fingertip by altering the compliance of a surface can elicit the illusion of finger movements [28].

To further illustrate sensorimotor couplings, when the hand is anesthetized, thereby preventing cutaneous information from reaching the brain, our ability to regulate grip force and perform coordinated movements degrades tremendously [41, 42, 43]. A deeper discussion of the multi-sensory integration that occurs in the central nervous system can be found in research using functional magnetic resonance imaging (fMRI) by Kavounoudias et al., where proprioceptive and/or tactile afferents were stimulated to produce kinesthetic illusions (i.e., sensations that the body is moving) [44]. It is therefore understood that the neural integration of cutaneous sensations, felt via the skin, and proprioceptive information from our musculoskeletal system, provides the basis for our keen sense of touch and dexterity of locomotion.

It has also been observed that perception of specific object properties, such as texture, shape, weight, or compliance, requires the deliberate employment of categorical hand movements [20, 21, 9, 23, 17]. If we were to perceive the weight of something, we would need to grasp or hold the object in some way, and perform a lifting motion. In contrast, to perceive texture, we would need to perform scanning motions over an object's surface with our fingertips. While these hand movements can be performed with variance in speed, force, and other properties, they can be categorically grouped into 6 distinct motions, referred to as exploratory procedures by Lederman and Klatzky [20]. These exploratory procedures reflect the optimal movements needed to acquire pertinent sensory information via the skin – when employed deliberately, objects can be identified within several seconds of the interaction [22]. Other researchers have followed up on this seminal body of work, utilizing computational analyses of hand dynamics and contact conditions for identifying or categorizing these six exploratory procedures [45, 46], all of which have corroborated and contributed to the discussions started by Lederman and Klatzky's 1987 seminal work on hand movements during haptic object perception.

There is a general assumption that our perception of touch is superior when we maintain the deliberate ability to plan, coordinate, and execute our hand movements, as we receive sensory inputs to the skin that are a direct result of the ways in which we choose to move [17, 47]. However, it remains unclear the degree to which cutaneous sensation or internal motor coordination and execution is needed for goal-oriented tasks. The following section reviews distinctions between "active" (i.e., self-directed, exploratory touch) and "passive" touch (i.e., touch received under conditions of non-volitional movement or static contact), representing two distinct contexts of haptic interactions.

2.3 Active versus Passive Touch

In 1962, Gibson highlighted phenomenal and experimental differences between *touching* and *being touched* [47]. The semantics of the word "touching" indicate intentional movements originating from the self, and this haptic context has been referred to broadly as *active touch* in the literature. Conversely, "being touched" indicates receiving touch from an external agent, broadly referred to as "passive touch." Receiving touch can happen under a variety of conditions of kinesthesia – for example, a moving object can come into contact with a static hand, or touch can be received as we are subsequently moving, such as when your leg brushes by leaves on a bush, resulting in a tickling sensation and subsequent motor reflex response. A static hand contacting an object is referred to as passive static, and a hand that is moving via an external agent (i.e., guided by another person or by a robotic device) is referred to as passive movement (or passive-guided).

As illustrated here, touch can be experienced across two broad contexts, and resulting haptic perception is dependent on specific neural couplings of incoming sensorimotor information available during the experience. During active touch, the central nervous system (CNS) utilizes internal predictive models (i.e., efference copies) during motor coordination and planning to predict the sensory consequences of a motor command [37, 16]. As a result, functional magnetic resonance imaging (fMRI) shows that active touch involves a broader network of activation, including the primary motor cortex (M1), the supplementary motor area (SMA), and the cerebellum, which are less involved or silent during passive touch [48]. It is thus imperative to understand the contributions of cutaneous sensation, kinesthetic sensation, and motor control during haptic perception and action.

Active Haptic Perception	**Active Kinesthetic Perception**
Kinesthetic Agency + Cutaneous Activation + Kinesthetic Activation *Hand intentionally touches object.*	Kinesthetic Agency + No Cutaneous Activation + Kinesthetic Activation *Hand moves above object.*
Passive Haptic Perception	**Passive Kinesthetic Perception**
No Kinesthetic Agency + Cutaneous Activation + Kinesthetic Activation *Hand is moved over object.*	No Kinesthetic Agency + No Cutaneous Activation + Kinesthetic Activation *Hand is moved above object.*
Tactile Perception	
Kinesthetic Agency Cutaneous Activation No Kinesthetic Activation *Object is moved over static hand.*	

Table 2.1: Conditions of haptic perception, as outlined by Klatzky and Lederman [9].

Lederman and Klatzky distinguish five unique contexts of haptic perception, which arise from different couplings of the following variables: 1) the presence or absence of motor control during movement, which we refer to as kinesthetic agency (either *active* or *passive*), 2) contact between skin and surface (i.e., *tactile*, or otherwise noted as *cutaneous*), and 3) sensed locomotion conditions of the body (i.e., *kinesthetic*), present during movement [9]. Depicted in Table 2.1, these categories are found to be more fluid in practice; for example, a manual interaction can involve stages of passive haptic perception and active kinesthetic perception.

Researchers have been able to investigate how we perceive specific object properties, such as curvature [49, 50], compliance [51], roughness [52], general shape [53, 54], and others, under these different haptic conditions. To best isolate variables and decrease interpersonal variability in hand movements, the conducted experimental paradigms restrict or prescribe the method of contact with the object's surface; oftentimes, interactions are restricted to simple virtual environments with rudimentary replications of physical objects and their properties, limited to the use of one or two fingers, or emulate tool-based interactions, such as manipulating a pen or controller. Regardless, such research has served as a foundational source of understanding for the human haptic sense; examples of such systems for decoupling haptic perception and action are explored below.

The development of the Tactile Display System (TDS) [55] has enabled closer investigation of sensorimotor couplings within the human haptic sense, such as the ability to directly compare active (exploratory) and passive (guided) haptic perception. The TDS enables the recording and playback of one person's deliberate finger movements in a two-dimensional plane to another person, who cannot self-direct finger movements. In perceptual experiments with raised line drawings, they found that cutaneous stimuli presented to the skin during passive-guided conditions are just as informative for haptic perception as during active tactile exploration [56, 57, 58], despite prior assumptions about the superiority of active touch [47, 59].

This body of work is critical in beginning to isolate inherently coupled components of the haptic sense. While similar studies have been attempted within virtual environment contexts using force feedback devices that reproduce single-finger or general hand trajectories [60], no study to date has examined the reproduction of whole-hand (i.e., multi-finger) movements with three-dimensional objects in this decoupled fashion. See the fourth and fifth chapters of this dissertation for the design and functional assessment of an exoskeleton device that decouples cutaneous sensation from control over hand movements, which enables the evaluation of these nuances.

The above two sections have presented a "bottom-up" overview of the haptic system, examining how incoming sensory information from the skin, muscles, and ligament tissues is critical for haptic perception and dexterous manipulation. The final section of this chapter will examine what happens at the cognitive level when we are in control over our body movements, which I refer to as intact *kinesthetic agency*. This "top-down" cognitive variable is critical to consider when investigating the nuanced couplings of haptic perception and action.

2.4 Sense of Agency

The *Sense of Agency* (i.e., SOA) refers to the feeling that we are in control over our actions and their consequences [1, 61, 62]. In reference to our body and its movements, *kinesthetic agency* – or limb locomotion, originating from and executed by the self – is experienced when an intended motion, such as extending a finger, leads to expected perceived sensorimotor consequences.

Several theories exist to explain the occurrence of our kinesthetic SOA. The comparator model [1] (Fig. 2.1 A) attributes our sense of agency as arising from internal sensorimotor prediction models called *efference copies*, which are compared against incoming perceived sensorimotor consequences to determine whether an action was initiated by the self or by an external source [1, 61]. Engaging in self-directed and self-coordinated movements, such as reaching for our coffee mug in the morning, and receiving expected sensory feedback from the object and movements of our own body, results in a sense that we have planned, initiated, and followed through with the action. Studies have shown that self-touch, including tickling, is perceived to be less intense than externally-originated touch [63, 64], due to the filtering of expected sensorimotor consequences, and thus sensory attenuation can provide an implicit metric of studying sense of agency elicited from a haptic experience [1, 61].

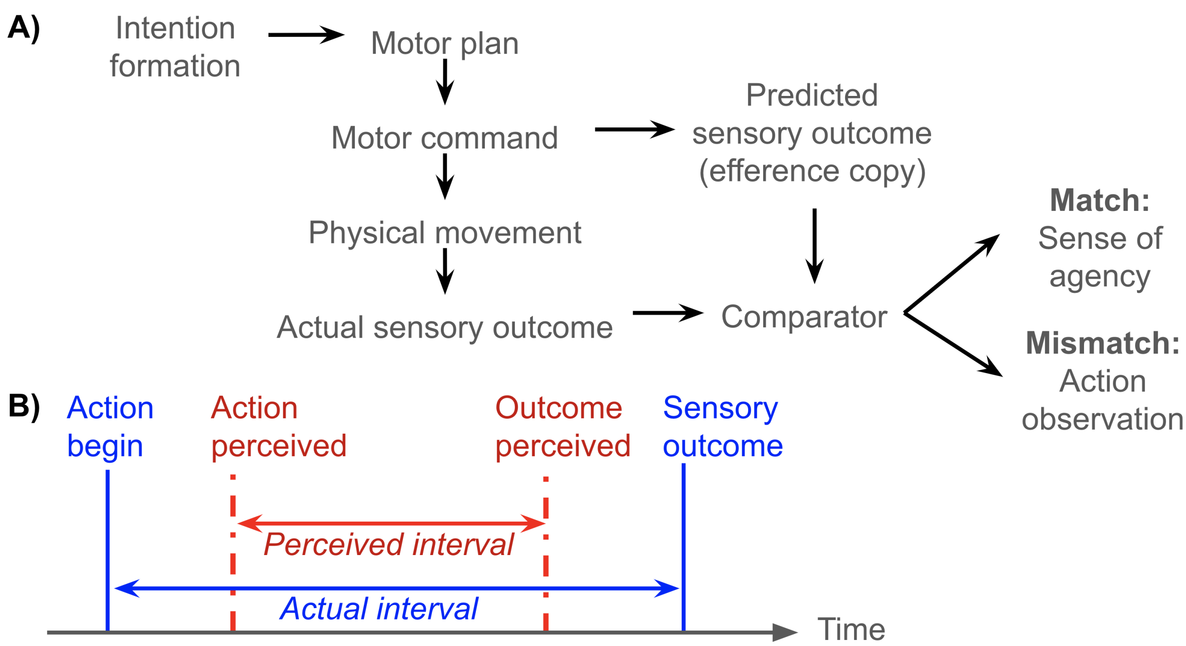

Figure 2.1: **Two Models of Sense of Agency** A) The comparator model states that our sense of agency arises from sensorimotor predictions (efference copies) and consequences. B) The theory of apparent mental causation. We perceive our actions as originating from the self when the distance between the actual and perceived intervals of action and causation is minimized. Figures adapted from [1], © 2016 Moore, licensed under Creative Commons 4.0.

Research has also found that when we perform a voluntary action, the perceived time frame between action and its consequence is shifted toward each other [65]. This perceptual change, called intentional binding, can be measured and used as another implicit metric of agency [1]. This experimental finding supports the theory of apparent mental causation, illustrated in Fig. 2.1B. This theory attributes our perceived sense of agency to arise from temporal couplings between intention and action, rather than subconscious sensorimotor predictions and consequences (as described by the comparator model) [66]. Illustrated in Fig. 2.1B, this perceptual dependence may explain why our sense of agency can be so fallible.

Moore's Bayesian cue integration theory integrates both of the above models. It states that our sense of agency is based on various weighted sources, with more reliable sources of information dominating the gestalt experience [1]. Our sense of agency is therefore generally understood to arise from sensorimotor, perceptual, and neural consequences and couplings; it is of critical importance to leverage this knowledge when designing haptic systems or devices administering tactile stimuli or motion guidance to the body.

Our sense of agency can further be subdivided into two phenomenal experiences, which can be thought of in terms of lower-level and higher-level cognitive processes [1, 62]. Our *Feelings of Agency* (FOA), are the lower-level, non-conscious feelings of control that we have over our actions, rooted in our body's natural sensorimotor processes as described above. Our *Judgments of Agency* (JOA) come from a higher-level cognitive process that is engaged when making attributions of agency to the self or others, and can be thought of as the context knowledge relating to the action. A preserved sense of agency is one where our FOA and JOA are in alignment.

While we may feel as though we can trust our sense of agency, research has shown that our feelings and/or judgments of agency can be disrupted, for example, when a performed action or consequence was not expected but logic implies self-causation [1, 62]. An example of this is when you knock something over without realizing it, but attribution of agency is placed on you because you are the only person in the room who could have knocked over that object at that time. More serious disruptions in agency have been seen in illnesses such as schizophrenia, where thoughts and actions are perceived as originating externally to the self (such as intrusive thoughts and auditory, visual, or tactile hallucinations) [67]. Our sense of agency can also be disrupted in a sensorimotor context [61]; for example, some people experience a medical condition called Phantom Limb, where they feel sensations from their amputated or missing limb (for example, pain) or feel as though their phantom limb can still be moved.

However, an important distinction must be made here between sense of *ownership* and sense of *agency*, as both are integral to self-experience and are present in the self-concept of our bodies [61]. Ownership is experienced as identification of belonging to the self (i.e., "mine-ness"), whereas agency is experienced as originating from the self. While sense of ownership and sense of agency are not independent and both impact our sense of self and our interactions, the scope of this dissertation focuses on *kinesthetic agency*, which refers to a sense of control over one's own limb movements, which originate from the self. Kinesthetic agency is important to consider when developing haptic devices that interface with the body, which will be summarized in the following section.

2.5 Designing Wearable Systems for Haptic Interaction

Emerging research in haptic engineering has focused on the design, development, and evaluation of wearable technologies (i.e., worn on the body, non-tethered). While traditional systems have prioritized touchable and graspable modalities of haptic interaction, such methodologies often limit the user to a restricted kinematic workspace. In recent years, there has been a distinct shift toward soft wearable robotic and haptic devices that leverage compliant materials to improve comfort, ergonomics, and portability considerations [68]. To adequately address design goals when developing haptic devices that interface with the skin and are worn on the body, it is imperative to select technologies that are most appropriate for the application at hand.

2.5.1 Wearability Considerations

An overview of wearability considerations for haptic devices interfacing with the body, as defined by Pacchierotti et al., are summarized below [69]:

- **Form Factor:** “Wearable devices should alter the body size of the wearer as little as possible” [69]. This consideration is determined relative to the body part on which the device is worn; for example, fingertip devices must be of significantly smaller form factors than devices worn on the arm. Furthermore, devices should be designed to fit the body part on which it is worn, rather than obstructing or protruding from the limb. Choice of actuator mechanisms are critical here, as oftentimes, actuators are the bulkiest components of wearable haptic devices.

- **Weight:** “Wearable devices should tire the wearer as little as possible” [69]. The weight of the assistive wearable device should be appropriate for the strength of the corresponding musculoskeletal structures of the body part on which the device is worn, and should additionally limit the potential for fatigue with continued use over time.

- **Impairment:** “Wearable devices should limit the motion of its wearer as little as possible” [69]. Haptic devices should ensure appropriate kinematic compatibility with the body part on which they are worn, without restriction or strain. Haptic devices designed for the hand, such as hand exoskeletons for guiding movements of the fingers, are optimally placed on the dorsal rather than palmar areas of the hand, leaving the fingerpads and palm free for direct skin-object contact. In contrast, haptic devices that provide tactile stimulation are usually placed at the distal fingerpads, where tactile acuity is highest. Furthermore, haptic devices should be able to accommodate a variety of limb sizes without hindering functionality.

- **Comfort:** “Wearable devices should be comfortable to wear and easy to adapt to the wearer limb size and shape” [69]. When wearing haptic devices, discomfort can be caused by sharp edges, rough surfaces, tight fabric bands, and hot parts from mechanical actuation or power sources. To accommodate these common issues, soft and conformable parts should be utilized wherever possible; however, there exists a tradeoff between comfort and functionality, as oftentimes, haptic devices must be pressed into the skin or fixed tightly to ensure proper function. Furthermore, care must be taken to ensure that high torques or shear forces are minimized during use of the device.

2.5.2 Sensing

The contents of this section have been adapted from [68], © 2022 IEEE. Reprinted, with permission, from:

Mengjia Zhu, Shantonu Biswas, **Stejara Iulia Dinulescu**, Nikolas Kastor, Elliot Wright Hawkes, Yon Visell, “Soft, Wearable Robotics and Haptics: Technologies, Trends, and Emerging Applications,” *Proceedings of the IEEE*, vol. 110, no. 2, pp. 246-272, 2022.

Sensors are critical to the functionality of haptic and robotic systems, enabling them to detect or perceive environmental stimuli, perform controlled movements, and manipulate their environments. Common sensing tasks include tracking the kinematic configuration and movements of the robot, sensing contact forces, and collecting environmental information, such as the geometry and configuration of nearby objects. In the last few decades, a large number of soft, wearable, and conformable sensors to detect strain, pressure, gesture, light, temperature, motion, and many other variables have been developed for wearable robotics applications. Data collected from these sensors can be used to control the behavior of the robotic system in a physical environment, through actuation-integrated feedback control, motion or task planning, or to provide application-dependent information, including the affordance of interactivity, as in the sensing of motion or kinesthetic inputs from a user in relation to objects in a virtual environment. It is imperative to select sensors that best suit the design goals of the intended system, several of which are briefly reviewed below. For a more extensive review, see [68].

- **Capacitive sensing** is based on capacitive coupling, which is the transfer of electrical energy by means of charged surfaces coupled through electric fields. A simple example of a capacitive sensor is a parallel capacitor with a soft dielectric material whose softness enables the device geometry, and thus capacitance, to change in response to applied mechanical displacements, stresses, forces, or strains. The capacitance of such a device is the ratio of change in electric charge to electric potential, depending on the device geometry and the dielectric constant of the materials. In simple devices, capacitance sensing is performed via charge or current sensing, while in more refined approaches, the capacitive device forms part of an oscillating circuit whose resonant frequency is sensed electronically in order to measure capacitance.

- **Resistive sensing** is based on changes in electrical resistance of a current path in response to mechanical stimuli. A simple example of such a device involves changes in the electrical resistance of a soft, conductive channel or wire in response to strain or changes in length. In a conductive channel, the resistance R increases with length, l, and decreases with cross-section area, A, i.e. $R = \rho l/A$, where ρ is volume resistivity, a material parameter.

- **Piezoelectric sensors** convert mechanical stresses, such as from strain, force, or pressure, into changes in electrical signal.

- **Accelerometers** measure changes in acceleration, typically within three dimensions (x, y, z).

Capacitive and resistive sensors can be designed to achieve high sensitivities and have been integrated into wearable gloves and electronic skins for measuring strains, pressures, shear deformations, or curvature [70, 71]. They are predominantly attractive for their ability to integrate into soft, stretchable electronic form factors, although capacitive sensors involve additional design considerations because their capacitance is affected by the dielectric properties governing electric fields in their nearby environment, and not merely by their geometric and mechanical state. [68].

Piezoelectric sensors and accelerometers can be worn directly on the skin to measure responses of the skin and muscles. Harrison and colleagues employed small cantilevered piezoelectric films to turn the hand and forearm into a digital input interface when employed with a wearable projector [72]. Shao et al. developed a 126-channel accelerometer array, placed over the hand, to measure oscillations of the skin [73] during tactile contact with objects. These two works were seminal pieces of inspiration for the smart bracelet supporting transcription of tactile sign languages, presented in the third chapter.

2.5.3 Actuation

The contents of this section have been adapted from [68], © 2022 IEEE. Reprinted, with permission, from:

Mengjia Zhu, Shantonu Biswas, **Stejara Iulia Dinulescu**, Nikolas Kastor, Elliot Wright Hawkes, Yon Visell, "Soft, Wearable Robotics and Haptics: Technologies, Trends, and Emerging Applications," *Proceedings of the IEEE*, vol. 110, no. 2, pp. 246-272, 2022.

Among the most intensively investigated technologies for soft robotics are actuators, which convert supplied energy into mechanical work to produce substantial displacements, forces, thermal, or other responses. Actuators that produce forces or displacements also produce mechanical stresses and heat that must be carefully considered in relation to ergonomic requirements, safety, and operating performance. Soft materials are intrinsically insulating, which can result in more severe thermal management challenges than are encountered in many conventional mechatronic systems, further amplifying the challenge of designing actuators for many soft robotic systems.

Below are examples of commonly used actuation methods in haptic devices, many of which can also be integrated into robotic devices (such as hand exoskeletons) [68]. Each class of actuators can be driven to provide small skin displacements, such as skin stretch, or larger forces applied to fingers or a limb.

- **Vibrotactile actuators** are small speaker-like devices that produce vibrations by converting electrical signals into mechanical displacements. These devices include eccentric rotating mass actuators (ERM), linear resonant actuators (LRA), piezoelectric actuators, or electromagnetic actuators. These actuators are often used in haptic devices, interfacing with the hand and arm, due to their low cost and ease of integration. For comprehensive reviews of vibrotactile actuators and their numerous applications, see [74, 75].

- **Electrotactile actuators** use electrical pulses to apply voltages to the skin, producing complex, tactile sensations that are not mediated by a single mechanoreceptor. Electrotactile stimulation can evoke the feeling of material properties (roughness, softness, and temperature) [76, 77]. However, there are additional safety considerations to be addressed when employing electrotactile actuators, as electrotactile stimulation may cause skin irritation, burns, electric shock, and discomfort over time [76].

- **Servo motors** operate as closed-loop actuators that integrate a motor (linear, rotary, stepper, etc.), a feedback sensor (such as an optical encoder), and a control circuit to achieve high-precision position and torque control. DC motors are commonly used in wearable devices interfacing with the skin of the fingers, hand, and arm [69, 78].

- **Electroactive polymers actuators (EAPs)** change size or shape in response to applied electric fields. EAP actuators are most commonly used in tactile devices that apply localized mechanical stimuli to the skin. These actuators produce low forces (on the order of millinewtons, mN) and low displacements (on the order of μm), but may be actuated at high frequencies (approaching 100 Hz). Piezoelectric polymer EAPs, which have been used in wearable applications, produce relative displacements when an electric field is applied. This occurs due to molecular dipole alignment. For a more comprehensive review of EAPs in soft wearable robotic applications, see [68].

- **Dielectric elastomer actuators (DEAs)** are a class of EAPs that can be designed to be rapidly actuated through electrostatically generated Coulomb forces between electrodes separated by elastic dielectric materials. Voltage requirements are often on the order of several kilovolts (kV) or more. This can create design challenges, since electrical discharge through the air or other materials is possible at distances of a few millimeters. For the same reason, safety requirements, such as current limiting, insulator design, and suitable grounding strategies, are often required. Risks are higher if the electrically active regions of such devices could, through failure or misuse, produce current paths that traverse the torso, since even electrical currents less than one milliampere (mA) across the heart create risks of cardiac fibrillation. This can be avoided by confining the electrically active region of a device to a single limb, for example, and avoiding potential current paths to ground through other body regions. For a more comprehensive review of DEAs in soft wearable robotic applications, see [68].

- **Shape memory alloy (SMA) actuators** have been used in many robotic systems, including soft, wearable devices. SMA actuators are engineered alloys, such as NiTi, that undergo thermally-controlled phase changes between two different atomic-ordered (crystalline) structures. These changes produce macroscopic actuation in the form of displacement, shape, or force. Because actuation is achieved without any need for motors, mechanical actuators, or fluidic sources, SMA actuation systems can be designed to be compact, quiet, and lightweight. The phase changes that produce SMA actuation are generated via active heating and, less often, through active cooling. Because these materials are conductors, electrical power, from infrastructure or batteries, provides a convenient method for dynamic heat delivery, although other heat sources are also used. These advantages also imply performance drawbacks that affect SMA actuation, and that also affect other thermally-dependent actuation methods (such as nylon filament actuators, for example). While SMA actuators can be rapidly driven to their contracted phase, the speed at which these transitions can be reversed is limited by heat transport out of the SMA structure, typically via convection, radiation (when surrounded by air), or conduction (if encapsulated in another liquid or solid medium). The rate at which cooling can be achieved depends on the temperature of the ambient medium and the size and geometry of the SMA actuators. Because SMA structures must often be massive enough to produce sufficient force, in many cases, this reversal of contraction requires more than one second. Thus, it is challenging to employ SMA actuation in applications that require high mechanical power to be produced, such as in force assistance or force feedback applications. In addition, due to the thermal mode of actuation, care must be taken in using SMA actuators close to the skin. For a more comprehensive review of SMAs and their use in wearable haptic and robotic systems, see [68].

- **Cable-driven actuation** utilizes cables – filaments, wires, or tendons – to supply forces or displacements, often via remotely positioned motors. Cables can often be selected to be thin and flexible and are thus suitable for integration in many soft, wearable devices. The forces and displacements, or mechanical work, that can be produced using such actuation schemes depend on the motor characteristics and routing details, but are often large when compared with other soft actuator technologies. Because of their capabilities and their use of standard electromagnetic motors, such actuation methods have been used in many wearable robotic systems, including devices for rehabilitation, haptics, or other applications. In these applications, they may supply mechanical work needed for haptic force feedback, force assistance, tactile cues such as compression or skin stretch, or for driving a supernumerary limb. For an example of a cable-driven actuation system that elicits tactile sensations of virtual objects by impeding motion, see [79]. For a more comprehensive review of cable-driven actuation methods, see [68].

- **Fluidic actuators** use encapsulated gaseous or liquid fluid media to supply mechanical forces or displacements, and are among the most widely used in soft robotics. One reason for this is that fluid volumes or channels can often be integrated within soft polymer materials that can be efficiently fabricated, yielding intrinsically compliant actuated structures. Fluidic actuators can produce forces, displacements, or work densities that span a large range, depending on their design and operating range of fluid volumetric displacement or fluid pressure. Indeed, conventional fluidic actuators include high-force industrial hydraulics and miniature devices for displacing biological fluids. Forces that can be produced depend on the device geometry and configuration, but typically increase monotonically with operating pressures and with the characteristic cross-sectional area of the fluid channel. For an example of a soft, fluidic muscle actuator that can lift fairly heavy loads or provide compression stimulation to the forearm when integrated into a sleeve form factor, see [80]. For a more comprehensive review of fluidic actuators for soft robotic and haptic wearable applications, see [68].

The above examples are non-exhaustive, but nonetheless display the breadth of opportunity in providing tactile or kinesthetic stimulation via a haptic device. When designing a haptic device that utilizes methods of actuation, considerations must be made to the type of actuator that would best suit the needs of the system. For example, vibrotactile actuators are cheap, easy to use, and safer to the body than electrotactile actuators, which have additional safety considerations when driving the electrical pulses that stimulate receptors in the skin [68]. Alternatively, the type of actuator may be chosen based on the amount of force needed to be supplied to the body – cable-driven devices can provide larger forces and displacements than fluidic actuators or servo motors [68].

Another class of haptic devices that should be mentioned here includes force-feedback devices, such as the Omega (by Force Dimension), Novint Falcon [81], Delta [82], and PHANTOM [83]. When holding the end effector, which resembles a handle and knob that is gripped by the hand, these desktop devices can sense and drive the position, orientation, and acceleration of hand motion via encoders and actuators across six degrees of freedom. An emerging area of interest with these devices includes developing virtual haptic environments, where one can feel the impact of bumping into a virtual wall [84]. These environments employ an active touch paradigm, where one explores the virtual space via the manipulandum and experiences changes in stiffness, acceleration, and damping forces, which give the illusion of interacting with real objects. Such force-feedback devices have also been used to passively guide users through mazes [85] or investigate haptic perception of virtual objects under guided conditions (recording and playback of active exploratory trajectories) [60].

2.5.4 Wearable Hand Exoskeletons

Wearable hand exoskeletons and robotic gloves have been recently developed for several applications, such as motor rehabilitation, assisting with tasks, and providing haptic feedback to the hand. Many examples of mechatronic exoskeletons that can actuate movements of the fingers have emerged over the recent years, with technologies ranging from high-impedance, rigid architectures that can produce high forces to the fingers (i.e., 20-30 N) to soft, compliant systems that address wearable needs such as portability and conformability to the body. For more comprehensive reviews of hand exoskeletons, for applications such as rehabilitation and assistance, see [10, 86, 87].

Li et al. categorize hand exoskeletons in three broad groups, based on their transmission methods: rigid (i.e., linkages, gears, etc.), flexible (i.e., springs, cables, tendons, etc.), and soft (i.e., fabric-based or fiber-based pneumatic actuation, soft variable stiffness actuators, etc.) [10]. While rigid transmission exoskeletons are valued for their abilities to generate high forces, they must be properly aligned with the kinematics of the body to prevent joint misalignment or discomfort during use. Soft transmission exoskeletons are valued for their conformability and compliance, and often result in devices with lighter weights and lower costs. An overview of hand exoskeletons, reviewed by Li et al. and grouped by transmission type, is reproduced from their review paper [10] in Table 2.2.

Such exoskeletons can additionally be categorized based on their afforded interactions with the user. Li et al [10] describe two categories of interactions, based on algorithmic control of the exoskeleton. Active human-robot interaction is where robot feedback is adaptive to the user's hand movements, providing resistive or assistive feedback based on how the user moves their hand, whereas passive human-robot interaction is where the robot drives movements of the user's fingers without the user's ability to resist or change the trajectory. Passive human-robot control algorithms utilize methods such as open-loop control, closed loop control (i.e., proportional-integral-derivative control), impedance control, or admittance control. In contrast, active human-robot control algorithms utilize either mechanical control, relying on mechanical sensing methodologies (such as force or position sensing, optical tracking, etc.), or bioelectric control strategies, relying on biosensing methods (such as surface electromyography, electroencephalography, etc.). For a more comprehensive review of control methodologies for active or passive robot-human control, see [10, 142].

2.5.5 Additional Considerations for Assistive Haptic Devices

Designing assistive haptic systems necessitates nuanced and ethical approaches that prioritizes the specific physiological and cognitive needs of the end user. A user-centric design approach, proposed by Lei et al., describes three critical aspects of designing assistive haptic devices for the visually impaired [143]:

- **Participatory design** prioritizes a collaborative approach between end user and

Table 2.2: Mechanical Design Features of Some Typical Hand Exoskeletons, reproduced from [10] © 2024 IEEE.

Author	Fingers	Transmission	Placement	Actuation	Force	Weight	App.
Schabowsky [88]	5	Linkage	Dorsal	DC	N/A	N/A	Rehab.
Ho [89]	5	Linkage	Dorsal	Linear DC	N/A	500 g	Rehab.
Ueki [90]	5	Linkage	Dorsal	DC	N/A	N/A	Rehab.
Ben-Tzvi [91]	5	Linkage	Dorsal	DC	20 N	275 g	Haptic
Leonardis [92]	5	Linkage	Dorsal	DC	30 N	N/A	Rehab.
Jo [93]	5	Linkage	Dorsal	SEA	3.5 N	298 g	Haptic
Sarac [94]	4 (I-L)	Linkage	Dorsal	Linear DC	1.485 Nm	300 g	Assist.
Gabardi [95]	1 (T)	Linkage	Dorsal	DC	N/A	N/A	Rehab.
Hong [96]	1 (I)	Linkage	Lateral	DC	10 N	172 g	Assist.
Jo [97]	4 (I-L)	Linkage	Dorsal	Linear DC	N/A	156 g	Rehab.
Li [98]	1 (T)	Linkage	Dorsal	DC	12 N	206 g	Rehab.
Li [99]	2 (T, I)	Linkage	Dorsal	DC	12.7 N	128 g	Assist.
Yang [100]	5	Linkage	Dorsal	DC	1.498 Nm	863 g	Rehab.
Xu [101]	5	Linkage	Lateral	SEA	10 N	383 g	Assist.
Lai [102]	5	Linkage	Palmar	DC	7.47 N	356 g	Rehab.
Michikawa [103]	5	Linkage	Dorsal	Pneumatic	8.0 N	300 g	Haptic
Liang [104]	5	Linkage	Dorsal	Linear DC	10 N	376.5 g	Rehab.
Dragusanu [105]	5	Flexible	Dorsal	Linear DC	N/A	N/A	Assist.
Li [106]	2 (T, I)	Flexible	Dorsal	DC	N/A	250 g	Rehab.
Chiri [107]	1 (I)	Flexible	Dorsal	DC	N/A	250 g	Rehab.
Jones [108]	1 (I)	Flexible	Dorsal	DC	20 N	N/A	Rehab.
Ma [109]	2 (I, M)	Flexible	Lateral	DC	10 N	180 g	Haptic
Cempini [110]	2 (T, I)	Flexible	Dorsal	DC	N/A	270 g	Rehab.
Agarwal [111]	1 (I)	Flexible	Dorsal	SEA	0.3 Nm	80 g	Rehab.
Popov [112]	4 (T-R)	Flexible	Dorsal	DC	16 N	250 g	Assist.
Rose [113]	4 (T-R)	Flexible	Dorsal	DC	40 N	220 g	Assist.
Kang [114]	2 (I, M)	Flexible	Dorsal	DC	10.3 N	104 g	Assist.
Pu [115]	5	Flexible	Dorsal	DC	N/A	900 g	Assist.
Sun [116]	1 (I)	Flexible	Dorsal	DC	N/A	N/A	Rehab.
Butzer [117]	5	Flexible	Dorsal	DC	6.4 N	148 g	Assist.
Tran [118]	3 (T-M)	Flexible	Dorsal	DC	6.3 N	131 g	Assist.
Chen [119]	5	Flexible	Dorsal	SEA	14 N	200 g	Rehab.
Kim [120]	5	Flexible	Dorsal	DC	N/A	N/A	Assist.
Sui [121]	5	Flexible	Dorsal	SMA	14.3 N	490 g	Rehab.
Li [122]	2 (M, R)	Flexible	Dorsal	Linear DC	10.0 N	N/A	Assist.
Daemi [123]	2 (T, I)	Flexible	Dorsal	DC	N/A	N/A	Rehab.
Tadano [124]	5	Soft	Dorsal	PAM	0.5 Nm	550 g	Assist.
Polygerinos [125]	5	Soft	Dorsal	Pneumatic	N/A	285 g	Rehab.
Zhao [126]	5	Soft	Dorsal	Pneumatic	10 N	N/A	Rehab.
Yap [127]	5	Soft	Dorsal	Pneumatic	11.3 N	99 g	Rehab.
Yun [128]	3 (T-M)	Soft	Dorsal	Pneumatic	22.35 N	350 g	Rehab.
Wang [129]	5	Soft	Dorsal	Pneumatic	1.6 N	N/A	Rehab.
Heung [130]	5	Soft	Dorsal	Pneumatic	N/A	207 g	Assist.
Takahashi [131]	5	Soft	Palmar	Pneumatic	8 N	N/A	Assist.
Wang [132]	3 (T-M)	Soft	Dorsal	Pneumatic	4.09 N	93.7 g	Haptic
Ge [133]	5	Soft	Dorsal	Pneumatic	47.9 N	128 g	Assist.
Kim [134]	2 (I, M)	Soft	Dorsal	Pneumatic	11.76 N	71.2 g	Rehab.
Feng [135]	5	Soft	Dorsal	Pneumatic	N/A	569 g	Assist.
Li [136]	5	Soft	Dorsal	Pneumatic	N/A	87 g	Rehab.
Jadhav [137]	5	Soft	Dorsal	Pneumatic	7 N	N/A	Haptic
Gerez [138]	5	Soft	Palmar	Pneumatic	N/A	120 g	Assist.
Lai [139]	5	Soft	Dorsal	Pneumatic	13.57 N	107 g	Assist.
Wang [140]	5	Soft	Palmar	Pneumatic	11.95 N	44.03 g	Haptic
Liu [141]	5	Soft	Dorsal	Pneumatic	7.74 N	N/A	Rehab.

research development teams, where explicit and implicit knowledge of end users are valued and determined rather than assumed.

- **Inclusive design** minimizes unconscious exclusion of impaired users during the consideration of mainstream or able-bodied users.

- **Emotional design** prioritizes the emotional needs of the user alongside basic technological requirements. For example, aspects of social inclusion, personal safety, and feelings of agency or vulnerability must be additionally addressed.

Assistive haptic devices may be designed to facilitate sensory substitution, where environmental data from a missing modality (i.e., vision or auditory information) is re-encoded into tactile or kinesthetic cues [143]. Assistive haptic devices may also provide motor assistance to augment force production when biological capabilities are compromised [92, 144, 117, 145, 86, 87]. Examples of assistive haptic devices that have motivated the research contributions in this dissertation are reviewed below, explicitly chosen due to their user-centric design approaches.

The Rice Haptic Rocker administers skin stretch feedback on the upper arm to convey kinesthetic feedback from the opening and closing of a prosthetic hand [78, 146, 147, 148]. Skin stretch stimulation has been shown to provide feedback that resembles a kinesthetic, or movement, cue (i.e., a tugging sensation on the skin that has magnitude and direction). The Rice Haptic Rocker employs a servo motor and custom hemisphere-shaped end effector that stretches the skin of the upper arm, which is mapped to the opening/closing of a prosthetic hand (Pisa/IIT SoftHand). By adding tactile feedback from the prosthetic hand, re-routed to the upper arm via this device, usage of the prosthetic hand improved in user studies. This example further illustrates the intricate couplings of sensation and action, where kinesthetic cues can be delivered via tactile sensation.

The HaptiComm is a hardware and software platform for Deafblind users, designed to reproduce the sensations generated during communication via tactile sign languages [149, 150]. The HaptiComm employs an array of linear actuators to provide tactile and kinesthetic sensations to the skin and is able to adaptively present most tactile signs across tactile sign languages, used by those who are Deafblind for communication. This work provides a critical example of an output device enabling shared digital communication in the tactile domain.

In the next chapter, I present research that addresses an additional barrier for digital tactile communication for those who are Deafblind – the lack of digital transcription methodologies for tactile sign languages. We take inspiration from the HaptiComm's accessible design principles and have openly collaborated with Deafblind haptics researcher Sven Topp, anthropologist and linguist Jeraldine Milroy, who focuses on Deafblind communication, and Dr. Basil Duvernoy, who led the device development of the HaptiComm.

Chapter 3

A Smart Bracelet Supporting Tactile Communication and Interaction

The contents of this chapter contribute towards the goal of enabling an existing mode of communication, shared touch communication via tactile sign languages, to interface with digital technologies for supporting social interactions. Despite significant advancements in the digital transcription and translation of verbal languages, a profound technological gap remains in the tactile domain. Currently, no established methodology exists for the digital capture of tactile sign language. To address this limitation, this chapter introduces an assistive haptic wearable designed to sense and translate touch interactions into semantically classifiable data. Such wearable sensing technologies represent a promising digital haptic future, where the skin becomes a digital input interface for interpreting remote touch interactions and supporting digital tactile communication.

Stejara Dinulescu, Neeli Tummala, Greg Reardon, Bharat Dandu, Dustin Goetz, Sven Topp, Yon Visell, "A Smart Bracelet Supporting Tactile Communication and Interaction," *2022 IEEE Haptics Symposium (HAPTICS)*, 2022.

Abstract

The sense of touch can convey semantic and emotional information in social or computer-mediated interactions. Touch plays an essential role in communication with individuals affected by multiple sensory loss, many of whom use modes of touch communication that can be broadly described as tactile sign languages. Few technologies exist today to support such interactions. Here, we present a smart bracelet for facilitating tactile communication and interaction. The smart bracelet captures and analyzes vibrations that are elicited in the skin via touch gestures performed on the hand. We demonstrate the utility of this system for supporting communication via the Deafblind Manual alphabet, which is a tactile sign language. This smart bracelet can classify signed letters with greater than 90% per-letter accuracy. These results show how existing modes of tactile communication can be integrated with information technologies. This work may furnish new paradigms for human-computer interaction via self- and interpersonal-touch contact.

3.1 Introduction

The skin is a highly expressive medium used for perceiving and interacting with the world, including communication through touch. Indeed, touch interaction can convey significant meaning, intent, and sentiment. The diverse repertoire of touch interactions encountered in everyday settings, including interpersonal touch, contrasts starkly with the limited communicative and expressive range of touch found in most computing systems today. In some interpersonal interactions, including those involving individuals with multiple sensory impairments such as deafblindness, touch is the principal medium of communication [152, 153, 154]. Several languages, organizations, and educational systems exist to support the needs of individuals with deafblindness, but there exists a lack of accessibility for digital communication, which is crucial to address due to its ubiquity. However, current interaction paradigms primarily lie in the audiovisual domains. New technologies are needed that can enable individuals with all ranges of sensory abilities to engage with information technologies and digital resources.

Here, we present a smart bracelet for supporting tactile communication and interaction (Fig. 3.1A). This system captures vibration signals elicited in the skin by touch contact gestures performed on the hand; these gestures could be initiated by the wearer or by another person. The captured vibrations are analyzed using signal processing and machine learning methods that can recognize, from a designated lexicon, which gestures are performed (Fig. 3.1B1). We demonstrate the ability of this system to capture and classify touch gestures from the Deafblind Manual alphabet (Fig. 3.1C), a tactile sign language (TSL) used by individuals in Australia who are deafblind, in order to support digital tactile communication.

While several researchers have investigated *output* technologies for reproducing TSL [155, 156, 150, 157], the present work is, to the best of the authors' knowledge, the first *input device* specifically directed at supporting digital TSL communication. Such a device could address important unmet needs, such as those of transcribing information conveyed via TSL communications in court proceedings, emergencies, policy forums, scholarly meetings, or moments of personal or historical significance, especially where transcripts might otherwise be unavailable. Our TSL input device enables the letter-by-letter translation of touch gestures performed on the hand. One might, for example, use the palm of one's own hand to enter text, take notes, or send a text message normally requiring a standard phone interface (Fig. 3.1B2). Such a system could assist individuals with limited vision, for whom usage of mobile devices can be challenging.

In other applications, smart bracelets like the one presented here could also support

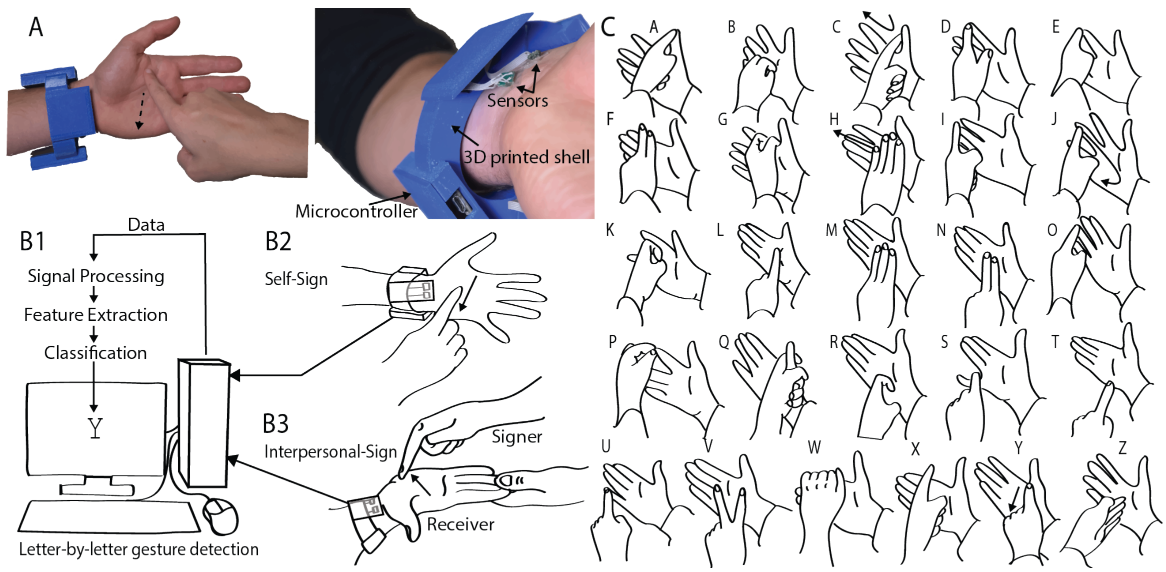

Figure 3.1: **Overview of Smart Bracelet System for Classifying Tactile Sign Language:** A) Wrist-worn acoustic sensing interface to encode and detect touch gestures on the hand. B) System overview and envisioned applications for detection of touch gestures on the skin. B1) Touch signals signed on the palm are transmitted to a PC via serial communication with the microcontroller. The data is processed and features are extracted to be used for classification. B2) Wearable interface enables self-signing on the palm of the hand to encode semantic meaning for note-taking purposes, sending a remote text message via touch, or transcription/record-keeping in the tactile domain. B3) Wearable interface translates interpersonal touch gestures as they are being signed. This could facilitate learning of TSL gestures, transcription of conversations in the tactile domain, and translation of TSL in real-time when the wearer is uncertain of the semantic mappings of the alphabet. C) The 26 letters of the Deafblind Manual alphabet.

the training of TSL interpreters. When combined with an output device capable of reproducing TSL gestures, such a smart bracelet could provide a means of TSL communication over the internet, including remote TSL interpretation, improving access to such services by many individuals. When combined with computer translation algorithms, such a smart bracelet could also facilitate conversation between individuals who communicate via different languages, including deafblind individuals who may not use the same TSL (Fig. 3.1B3). Indeed, a diverse variety of TSLs are used around the world [150].

3.1.1 Deafblindness and Tactile Communication

Research and development in automatic speech recognition and language processing over the past 50 years has yielded algorithms and systems for capturing, computationally understanding, and interacting with computers via speech. More recently, analogous methods to speech recognition have been used to support computer-based communication by detecting hand poses during visual sign languages, such as American Sign Language [158]. To date, little attention has been given to achieving similar goals in tactile communication, particularly TSLs.

A recent report by the World Federation of the Deafblind indicates that between 0.2-2% of people are impacted by sensory impairment of both vision and hearing. Deafblind individuals use a variety of languages for tactile communication, depending on their region, community, and individual factors, such as the onset and severity of sensory impairment. Many TSLs exist today supporting critical daily activities and social interaction [149]; in addition, many of the TSLs are letter-based semantic touch communication methods. Here, we demonstrate a system for supporting TSL communication, specifically utilizing the Deafblind Manual alphabet, which involves the performance of touch gestures, including tapping, lightly pinching, and sliding on the surface of the hand. Each of the 26 gesture patterns corresponds to a letter in the English alphabet [150] (Fig. 3.1C).

Other technologies for supporting communication by individuals with visual and auditory sensory loss include Braille interfaces, emerging methods for tactile graphic displays, and more commonly available screen-based accessibility features for those with low vision. However, such methods do not support the communication needs of all individuals who are deafblind. More recently, researchers have engineered systems to translate text or speech into tactile patterns [155, 156], including TSL gestures [150, 149, 159]. However, the authors are not aware of any prior efforts to facilitate or develop a computational encoding of tactile input. A system such as the one presented here could support TSL communication by enabling transcription, analysis, or reproduction of TSL interactions.

3.1.2 Capturing Touch Gestures via Vibration Signatures

Touch interactions with the skin elicit vibrations that travel far from the point of contact, encoding information about the contact location and nature of the gesture [160, 73, 161, 162, 163]. This physical process makes it feasible to collect information about tactile interactions using vibration sensors that are positioned remotely from the contact location. Human-computer interaction research has utilized such processes to provide means of computational input via contact with the skin, as in the Skinput device [72]. Many other sensing methods can be used for capturing information from skin contact, including capacitive, electromyography, ultrasound, force, and other sensing techniques [164, 165, 166, 167]. However, the propensity of touch-elicited vibrations to travel great distances in the skin and the efficiency with which such signals can be captured electronically via low-cost, readily available sensors makes this approach particularly attractive for interactive device engineering, especially in settings where it is preferable to leave the hand unencumbered.

3.1.3 Summary of Contributions

We present a smart wrist wearable for capturing and recognizing touch gestures that occur on the hand during skin-to-skin contact. To inform the design of this smart bracelet, including the number and placement of sensors, we captured the signal profiles of a subset of letters of the Deafblind Manual alphabet with high spatial resolution using a sensor array encompassing the whole hand. By analyzing this data, we identified that even letters that are highly similar to one another in tactile sign contain unique signal profiles, even when measured at locations removed from the gesture contact. Informed by this finding, we designed a compact, wrist-worn device to capture these propagating signals without hindering natural manual movements and tactile interactions. To demonstrate the utility of this system for tactile communication, we illustrate the capacity of our device to classify 26 different touch gestures—in this case, the letters of the Deafblind Manual alphabet. We find that the device can accurately discriminate between different touched contact locations (e.g. digit II, digit V, or palm) and between different types of touch contact (e.g. slides, impulses, pinches, or squeezes). We show using simple, supervised machine learning methods that such a device is able to identify these 26 different gestures with above 90% accuracy, even when trained on a small dataset.

3.2 Whole-Hand Sensing

3.2.1 Materials and Methods

In a first experiment, we surveyed the whole-hand mechanical responses produced during the signing of a subset of letters from the Deafblind Manual alphabet. We used two 42-channel, 3-axis accelerometer arrays (Model LI3DSH, ST Microelectronics) [73]. We captured data at a rate of 1300 Hz via a field-programmable gate array (FPGA) based multichannel data acquisition board, with firmware on the FPGA and software on a Windows PC. We affixed each accelerometer in the array to the skin via doubled-sided adhesive, with one array attached to the dorsal side of the hand and the other to the palmar (Fig. 3.2B).

We captured the skin acceleration for 10 trials of 9 letters of the Deafblind Manual alphabet (A, D, E, F, I, M, N, O, U), signed on the palmar side of the hand through interpersonal touch (i.e one person signs on the hand of another person). Letters were chosen for high frequency of use (i.e. vowels) and letter similarity (i.e. M and N, D and E). Because the palmar surface of the hand was also covered with sensors, we slightly shifted the signed location of M and N to avoid interfering with the sensors. The palm was held facing upwards, with the forearm stabilized against the edge of a table at chest-level to minimize noise from spurious hand movements. The data consisted of ten, 84-channel 3-axis acceleration signals for each letter. The data was de-meaned and bandpass filtered, then compressed to a single axis by computing the magnitude of the vector. We then computed the RMS of the acceleration magnitude.

To determine the spatial distribution of acceleration energy for each gesture class, we compute root mean square (RMS) acceleration over all trials. We interpolated these data using coordinates obtained from an anatomically plausible 3D hand model using squared distance weighting. We analyzed the differences between letters using this data and also computed the mean pairwise absolute correlation (Pearson's r) between the RMS acceleration of all trials and of all letters.

3.2.2 Results

Each tactile gesture class yielded distributions of RMS acceleration that reflected the contact location and the nature of the gesture (single touch - A, E, I, O, U and multi-touch - D, F, M, N) (Fig. 3.2A). For example, the peak RMS acceleration of the letter E was localized to the point of contact. Multi-touch gestures tended to deliver high RMS acceleration (relative to the peak RMS acceleration for that gesture) to locations far from the point of contact, reflecting that the contact location on the hand was much larger (2-3 times the size of the contact for single touch gestures). Furthermore, all gestures delivered energy to the wrist; the amount of RMS acceleration delivered at the wrist was a function of the distance from the contact location (e.g. the contact location for E is much further from the wrist than for M/N).

The tactile gestures elicited vibration patterns that were consistent across gesture instances (Fig. 3.2B), and were qualitatively distinct from the other gestures. Consistent with the observations of the whole-hand patterns (Fig. 3.2A), some gestures produced similar distributions of RMS acceleration and thereby high correlations (i.e. M/N and D/E/F). For the subset of data captured by the ten accelerometers located on the wrist, averaged within-gesture mean absolute correlations of the RMS acceleration (0.94) were substantially larger than across-gesture correlations (0.48). These results suggested that acceleration information captured at the wrist could be used to classify varied tactile gestures.

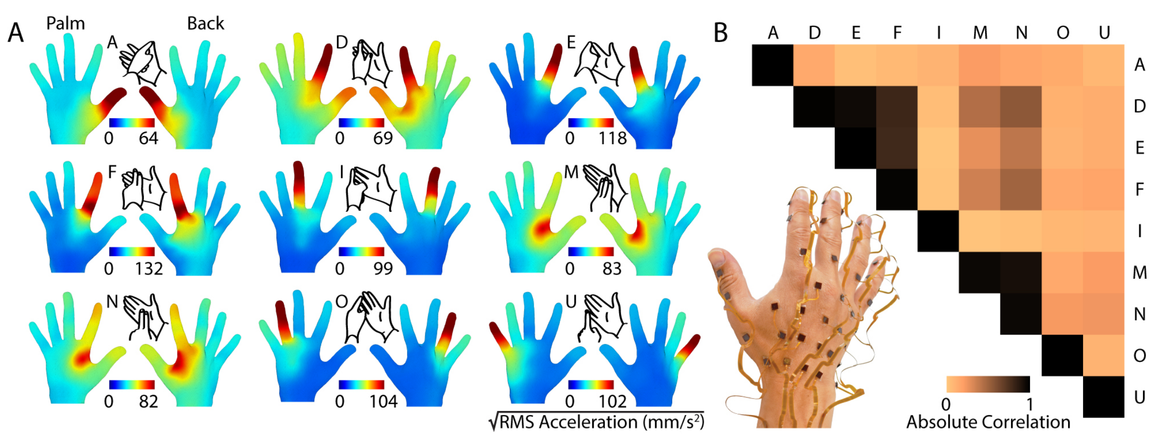

Figure 3.2: **Whole Hand Sensing:** A) Measured whole-hand mechanical responses for a subset of the Deafblind Manual alphabet. We found that the contact is not only reflected in skin responses at the touched location, but also that this energy propagated outwards to regions on the skin, on both sides of the hand, far from the point of contact. B) We found that the tactile gestures produced consistent, repeatable patterns of RMS acceleration across the hand (mean absolute correlation > 0.95 within trials of the same gesture), while yielding very low correlations when comparing across trials of different gestures.

3.3 Wrist-Worn Interface

Informed by the preceding findings, including the extent to which similar information could be captured via sensors at locations removed from the point of contact with the hand, we designed a smart bracelet using a minimal arrangement of sensors located at the wrist. We evaluated the utility of this device for classifying touch contact gestures performed on the hand, in the form of TSL gestures.

3.3.1 Materials and Methods

3.3.1.1 Device Design

The device was composed of an ABS shell enclosing two Adafruit Feather M0 WiFi microcontrollers. It employed a total of four 3-axis analog accelerometers (Analog Devices ADXL335) (Fig. 3.1A). Each sensor was adhered to the skin. Pairs of sensors were positioned 25 mm apart on both the palmar and dorsal sides of the wrist (Fig. 3.3A), at locations determined from the preceding experiment. The casing for the electronics was designed to avoid mechanically disturbing the sensing elements. The data was captured at a sampling frequency of 1250 Hz and at a resolution of 12 bits using the onboard ADC of the microcontroller.

3.3.1.2 Collection of TSL Data

We collected accelerometer measurements during TSL touch contact in each of two conditions: one in which the signer performed gestures on their own hand (self-sign, or SS, depicted in Fig. 3.1B2) and one in which the signer contacts another person's hand (interpersonal-sign, or IS, depicted in Fig. 3.1B3). The palmar surface of the hand, held outstretched and flat, was facing upwards throughout data collection, with the dorsal side of the forearm stabilized against the edge of a table to minimize disturbance from unintentional limb movements. In both conditions, we recorded 40 trials of each of the 26 letters.

3.3.1.3 Signal Processing and Feature Extraction

The data for each letter were segmented, lowpass filtered at 250 Hz, and compressed from 3 axes to 1 axis using principal component analysis (PCA). After compression, the data for each trial was normalized independently,

$$y_{c,n} = \frac{y_{c,n}}{\max_{\{c,n\}} |y_{c,n}|} \tag{3.1}$$

where n is the sample number and c is the channel number. This preserved the inter-channel differences between accelerometers, while also reducing inter-trial variability of the same gesture and improving the consistency of the feature estimates across gestures.

For every trial, we computed time-domain, frequency-domain, and spectro-temporal features for all 4 channels of each analyzed segment, yielding 96 features per trial. The time-domain features were peak-to-peak amplitude

$$PTP_c = |\max_n y_{c,n} - \min_n y_{c,n}| \tag{3.2}$$

and mean absolute deviation

$$MAD_c = \frac{1}{N} \sum_{n=1}^{N} |y_{c,n} - \bar{y}_c| \tag{3.3}$$

where $\bar{y}_c$ is the mean of signal $y_{c,n}$. This yielded a total of 8 time-domain features per segment.

For the second set of features, we computed the Discrete Fourier Transform (DFT) of each of the normalized signals, $Y_{c,k} = \mathcal{F}\{y_{c,n}\}$, where $\mathcal{F}$ is the DFT. From the frequency-domain representation of the signal, we computed the spectral centroid

$$SC_c = \frac{\sum_{k=1}^{N} f_k |Y_{c,k}|}{\sum_{k=1}^{N} |Y_{c,k}|} \tag{3.4}$$

where f_k is the center frequency of bin k and $|Y_{c,k}|$ is the magnitude of bin k for channel c. In addition, we computed the center frequency of the DFT bin with the largest magnitude for each channel c,

$$F_c = f_{k^*} \text{ s.t. } k^* = \arg\max_k |Y_{c,k}| \tag{3.5}$$

We computed the mean and standard deviation of the DFT bins over a 50 Hz bandwidth. Let the bandwidth $b_i \in \{[0\ \ 50], [50\ \ 100], [100\ \ 150], [150\ \ 200], [200\ \ 250]\}$ for $i = 1, ..., 5$. We associate the set of bins K_i whose center frequencies lie within bandwidth b_i and compute:

$$\mu_{c,b_i} = \frac{1}{|K_i|} \sum_{k \in K_i} |Y_{c,k}| \quad , \tag{3.6}$$

$$\sigma_{c,b_i} = \sqrt{\frac{1}{|K_i|} \sum_{k \in K_i} (|Y_{c,k}| - \mu_{c,b_i})^2} \tag{3.7}$$

where $|K_i|$ is the size of set K_i. This produced 40 features (2 measures $\times$ 5 bandwidths $\times$ 4 channels), for a total of 48 frequency-domain features.

Finally, we composed a set of spectro-temporal features to capture temporal variations in the spectral envelope of the signal. We computed the Short-Time Fourier Transform (STFT) of the signals (window size K=256 samples, 50% overlap, Hanning window), yielding a matrix of Fourier coefficients ($M \times K$) for each channel c where each of the M rows is the DFT of the signal over different times. We computed the mean and standard deviation of the measure μ_{c,b_i} (see Eq. 3.6) for each row of the Fourier matrix. Let $\mu_{c,b_i,m}$ be the mean of bandwidth b_i for channel c for row m. We compute

$$\mu_{c,b_i}^{STFT} = \frac{1}{M} \sum_{m=1}^{M} \mu_{c,b_i,m} \quad , \tag{3.8}$$

$$\sigma_{c,b_i}^{STFT} = \sqrt{\frac{1}{M} \sum_{m=1}^{M} (\mu_{c,b_i,m} - \mu_{c,b_i}^{STFT})^2} \tag{3.9}$$

This yielded another set of 40 features (2 measures × 5 bandwidths × 4 channels). All features (temporal, frequency, and spectro-temporal) were concatenated to form a 96-dimensional vector, used to train the machine learning model and classify the 26 different tactile gestures.

3.3.1.4 TSL Classification

To distinguish the 26 letters of the Deafblind Manual alphabet via our smart bracelet, we pass computed features into three common supervised machine learning classification models: a support vector machine with a linear kernel (SVM), logistic regression with PCA (LR), and a random forest model (RF). To minimize bias during training and classification, we employed a 10-fold cross-validation procedure with a 90-10 train-test split. During each classification run, we computed the mean and variance of each feature in the training data and used these sample moments to whiten both the training and testing data. We performed classification for each mechanical dataset separately (SS and IS conditions, 40 trials per letter) and on both datasets (combined condition, 80 trials per letter).

3.3.2 Results and Discussion

3.3.2.1 Mechanical Signal Profiles

We found that the measured signals (Fig. 3.3B) yielded noticeably different time-domain acceleration responses, which became more prominent when we grouped the gestures by palm taps (Fig. 3.3B1), finger taps (Fig. 3.3B2), slides (Fig. 3.3B3), and pinches/grabs (Fig. 3.3B4). We found that tapping gestures yielded transient signals that decayed rapidly, while slides and pinches/grabs decayed at much slower rates in the skin. This likely reflects the variation in contact conditions between the gestures, for which slides and pinches/grabs occur at much longer time scales. We found that finger taps delivered less energy to the wrist when compared to palm taps, reflecting that the properties of the skin, which is a highly damped medium, play a role in encoding the distance from the contact location to the wrist, thereby differentiating the measured tactile gestures. Finally, we found that sliding gestures, regardless of contact location, tended to deliver less energy to the wrist, but that this energy was nonetheless measurable and informative.

3.3.2.2 TSL Classification

When utilizing data from all four sensors, the SVM classifier consistently outperformed the RF and LR classifiers in the SS and IS conditions, with average accuracies greater than 93% across cross-validation folds; in the combined condition, the RF classifier slightly outperformed the others at close to 90% average accuracy across folds (Table 3.1). High performance using SVM is promising for real-time applications, as a trained SVM model can easily be implemented on a micro-controller without the need for additional computational power. In the following analysis, we focus on the performance of the SVM model.

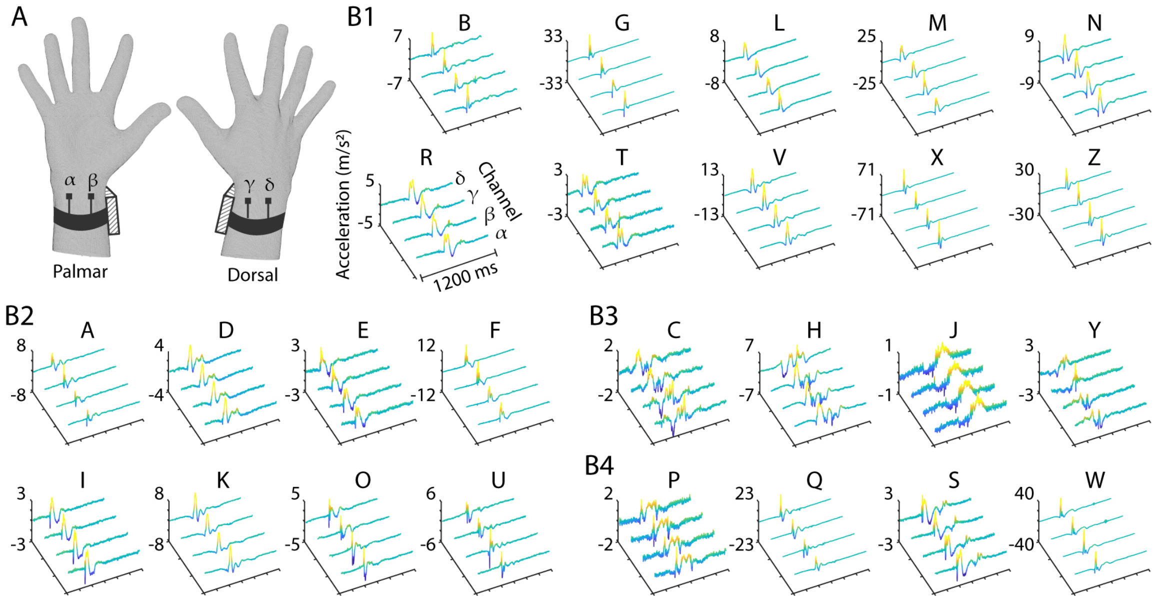

Figure 3.3: **Four-Channel Sensing:** A) Wrist-wearable device using four accelerometers affixed to the skin to capture mechanical vibrations produced during tactile fingerspelling. B) Measured accelerometer signals produced during a single trial of each letter of Deafblind Manual alphabet. Palm tap and finger tap gestures (B1 and B2, respectively) produced transients that rapidly decayed. Finger taps tended to deliver less energy to the wrist when compared to palm taps, reflecting the difference in distance between the point of contact and the sensor. Sliding or pinching/grabbing gestures (B3 and B4, respectively) produced signals that tended to decay at a much slower rate on the skin, reflecting that the gesture occurs over a longer time scale than the tap gestures.

We further analyzed classification performance using different subsets of sensor channels (Fig. 3.3A) to determine the minimal number of sensing element required for robust classification. The subsets considered include all four channels $(\alpha, \beta, \gamma, \delta)$, two channels on the palmar side of the wrist (α, β), two channels on the dorsal side of the wrist (γ, δ), one channel on the palmar side of the wrist (α), and one channel on the dorsal side of the wrist (γ). Table 3.2 summarizes the average classification accuracies across cross-validation folds for the SS, IS, and combined datasets. The use of all four channels yields the highest classification accuracies, but the employment of just two sensors maintains robust performance (above 85% in the single subject conditions), indicating that they

	Classifier		
Dataset	SVM	RF	LR
SS	93.9	88.7	90.6
IS	93.7	92.2	91.0
Combined	86.3	89.4	76.1

Table 3.1: Average Classification Accuracy (%) Across Datasets and Models for 4-Sensor Configuration

	Sensor Configuration					
Dataset	$\alpha, \beta, \gamma, \delta$	α, β	γ, δ	α, γ	α	γ
SS	93.9	86.5	86.8	87.1	76.3	73.8
IS	93.7	88.3	85.4	87.1	75.0	75.4
Combined	86.3	76.8	75.6	78.4	61.6	64.3

Table 3.2: Average Classification Accuracy (%) Across Datasets and Sensor Configurations for SVM Model

are sufficient for detecting various sets of tactile gestures. Mounting the sensors on the palmar or dorsal side of the wrist does not significantly change classification accuracies. On the other hand, classification accuracy drops significantly when using only one sensor, indicating that inter-channel differences encode relevant classification information that cannot be discarded. Close inspection of the signals shown in Fig. 3.3B shows differences in the phase and shape of signals between channels, most evident in the sliding gestures.

We found that the most commonly misclassified letters were L and N, which is expected due to the similarity of the tactile gestures; N is signed with two fingers in the center of the palm whereas L is signed with one finger in the same location (Fig. 3.5). Additionally, R and T are commonly mislabeled, as they are both taps occuring near the same palmar location: T with one finger and R with two fingers. Other commonly misclassified letter pairs include G and X, and W and Z. The former are gestures performed with the signer's whole hand, producing high acceleration signals at the palm; the latter produce similar high energy signals, but occur at different locations on the hand.

We also examined classification accuracy within each gesture grouping shown in

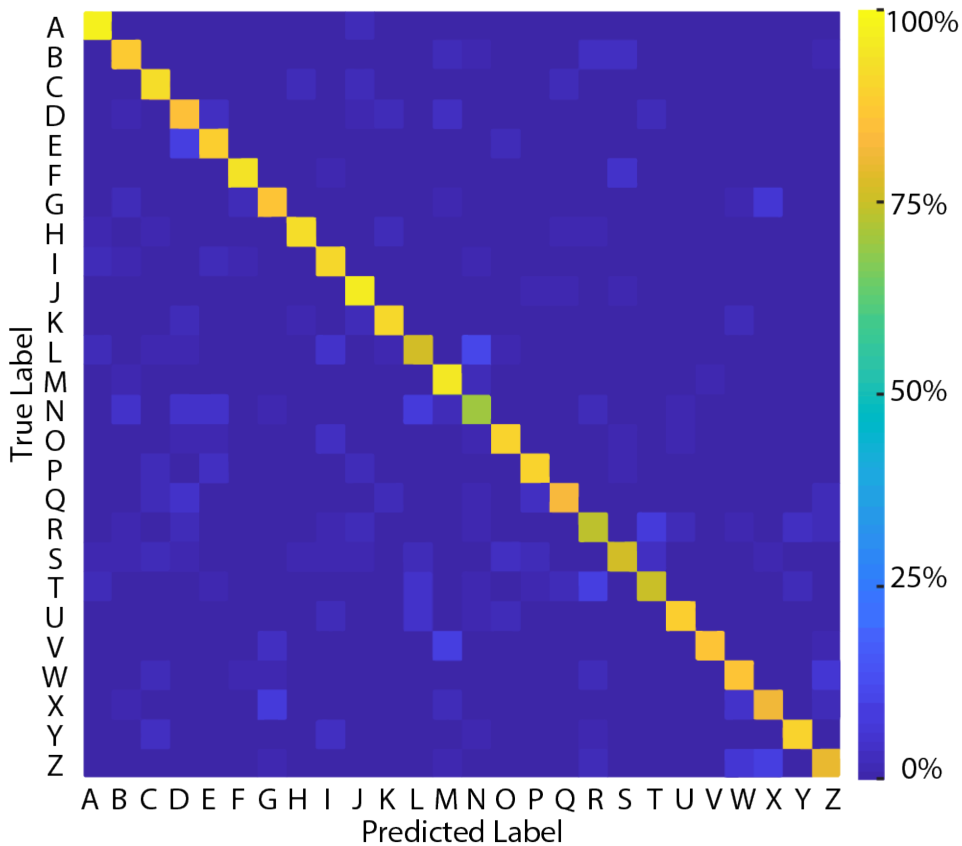

Figure 3.4: **Classification Results:** Confusion matrix for the linear SVM Classifier on the combined dataset, with per-letter accuracies along the diagonal. On the off–diagonal, type I (false positives) read column-wise and type II (false negatives) read row-wise. Commonly misclassified letter pairs can often be grouped into the subsets introduced in Fig. 3.3. For example. {E,D} are both taps on digit II, and {G, X, Z}, {L, N}, and {R, T} are all taps on the palm.

Fig. 3.3B (i.e. palm taps, finger taps, slides, and pinches/grabs) for the combined dataset in the four channel configuration, averaged across cross-validation folds. Sliding gestures are classified with the highest accuracy (92.8%), likely because they produce the most distinct mechanical signals. Finger taps are also accurately classified (90.8% accuracy) and are generally only misclassified as other finger taps, likely because the captured signals often possess similar magnitudes and temporal profiles. Similarly, palm taps (81.1% accuracy) are accurately recognized and are typically only misclassified as other palm taps. This is expected when considering the similarity between many of the palm taps;

for example, L, M, N, and V are all signed in the middle of the palm but with different finger placements. Finally, pinch or grab gestures (83.8% accuracy) are somewhat more likely to be misclassified as other types of gestures due to their heterogeneous nature.

Regardless of the classifier, dataset, or sensor configuration, we observe accuracies above 60%, which is significantly higher than chance (3.9% for 26 classes). In the majority of SS and IS conditions, accuracies are above 90% when using four sensors, regardless of classifier used. This indicates that accuracies approaching 100% can likely be achieved via standard techniques such as lexicon-based models that are widely used in natural language processing and automatic speech recognition. Further improvements might also be achieved through the use of state-of-the-art multi-layer neural network classifiers.

3.4 Conclusion

We present a smart bracelet system that transforms the skin into a touch gesture input interface. The bracelet can classify touch gestures of the Deafblind Manual alphabet, via integrated wrist-worn sensors, with significantly higher-than-chance accuracy. Our approach demonstrates the success of minimal accelerometer-based sensing that leaves the hand unencumbered for manual interactions and movements. Measurements from a whole-hand sensing array were used in an initial exploration to identify a subset of four sensors that are able to capture enough salient information in a touch gesture, thus reducing cost and complexity. We demonstrated the utility of this device for supporting tactile communication via TSL. We present analyses of an experiment in which we captured and accurately classified signal profiles for all 26 letters of the Deafblind Manual alphabet, demonstrating promising uses of such systems for supporting tactile communication.

The smart bracelet can be used for input via tactile gestures performed on the hand of the user by the user, which could be useful for note-taking, transcription, or textual communication. Such a device could support interpersonal tactile communication by individuals who prefer using touch over other modalities, in addition to encoding touch in the digital domain. These findings may also enhance the utility of output devices for tactile communication. Utilizing input and output devices in conjunction could support communication between two or more individuals, including people who may communicate via different TSLs.

While we have demonstrated the capability to accurately classify the 26 gestures of the Deafblind Manual alphabet, more remains to generalize features for classification of larger mechanical datasets consisting of various TSL signers, receivers, and alphabets. Further investigation into individual differences between subjects, such as hand size, signing speeds, and emotion (i.e. happy, angry) conveyed through TSL, will be experimentally investigated.

We further envision supporting real-time classification of TSL, where signing occurs as fast as five letters per second [150]. In these cases, intentional or accidental movements of the hand (such as finger motion from a previously performed tactile gesture) must not interfere with signals captured from the sensors. Thus, further data capture and signal processing methods will be explored, examples of which include capturing data from two devices worn on both the signer's and receiver's wrist, or capturing false positive dataset examples (such as muscle contractions, finger twitches, etc.) to help identify gestural noise versus salient gesture data. We will additionally explore multi-layer classification and feature optimization by additional meta-analysis of similarities and differences between tactile signals in a gesture set, as well as natural language processing as previously applied in speech technologies. Such advancements are expected to improve accuracy and robustness, aiding applications in natural communication. This system holds promise for supporting tactile communication, including scenarios where it is paired with a haptic communication output device, to address communication needs of individuals who are deafblind.

3.5 Acknowledgments

The authors thank Basil Duvernoy, Jeraldine Milroy, and Yitian Shao for their feedback. The authors acknowledge support from the University of California, Office of the President, National Science Foundation (NSF) Fellowship No. 2139319 to Dinulescu and Goetz, and NSF award 1751348 to Visell. Any opinion, findings, and conclusions or recommendations expressed in this material are those of the authors and do not necessarily reflect the views of the NSF.

3.6 Supplemental Figure

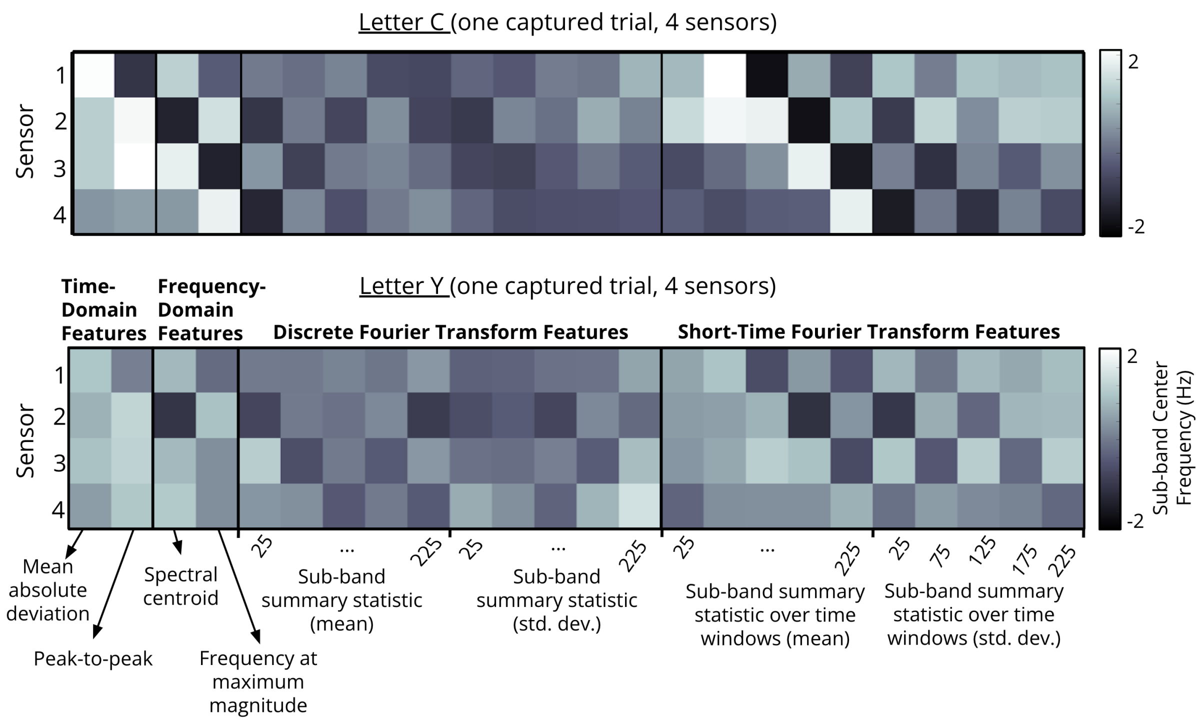

Figure 3.5: **Features across Letters C and Y:** Here, we depict feature representations of two letters (C and Y) of the Deafblind Manual tactile sign language. Despite both letters being performed with sliding gestures, their feature profiles remain visually distinct. These unique spatiotemporal signatures, when extracted via our methodologies, can be classified with high accuracy, despite a limited dataset.

Chapter 4

An Inter-Manual Exoskeleton that Facilitates Guided Multi-Finger Grasping and Manipulation

This chapter presents an unconventional model for sharing physical haptic experiences through an inter-manual exoskeleton that enables the hand of one person to guide multi-finger grasping and manipulation actions by another person's hand. This instrument was designed to facilitate scientific experiments on shared haptic manipulation and perception, as exemplified in the experiments presented in Chapters 4 and 5. It may also find use as a tool for prototyping and evaluating the design of multi-finger kinesthetic (force-feedback) interfaces for the human hand. Such multi-finger mechatronic devices are complex, and require careful mechanism design, sensing and actuation considerations, and significant time investment. The design reported here can be readily reproduced using standard 3D-printing and fabrication methods, and thus may contribute to further research investigating multi-finger guided haptic interactions. To facilitate this, the digital design files for this device will be made public when this work is published.

The contents of this chapter are in preparation:

Stejara Dinulescu, Dustin Goetz, Neeli Tummala, Serena Lee, Jack Carpino, Yon

Visell, "An Inter-Manual Exoskeleton that Facilitates Guided Multi-Finger Grasping and Manipulation," *In preparation.*

4.1 Abstract

We present the design of a passive, inter-manual exoskeleton, coupling the hands of two people, that enables the hand of one user (leader) to guide multi-finger grasping and manipulation by the hand of the other user (follower). We designed this instrument to provide the leader hand with sufficiently direct control, and to afford sufficient mobility, to enable tasks involving the grasping and manipulation of small objects with the fingers, without the need for actuation or control electronics. The design was informed by an idealized kinematics analysis, which we formalize in this paper, along with ergonomic considerations, mobility requirements, and avoidance of occlusion. We evaluated the utility of this device using experiments that coupled the hands of pairs of participants in representative hand function tasks. One participant guided motion, using vision, and the other remained passive and compliant. We found that participants were able to execute peg insertion and shape stacking tasks by using our inter-manual exoskeleton to guide a different hand. We compared this inter-manual condition with a control condition involving a single hand, finding that completion rates were similar to those obtained in the guided condition, but that completion times were substantially longer in the guided condition. This instrument can be used to prototype and evaluate the design of multi-finger kinesthetic interfaces, and may find use in scientific experiments on haptic perception.

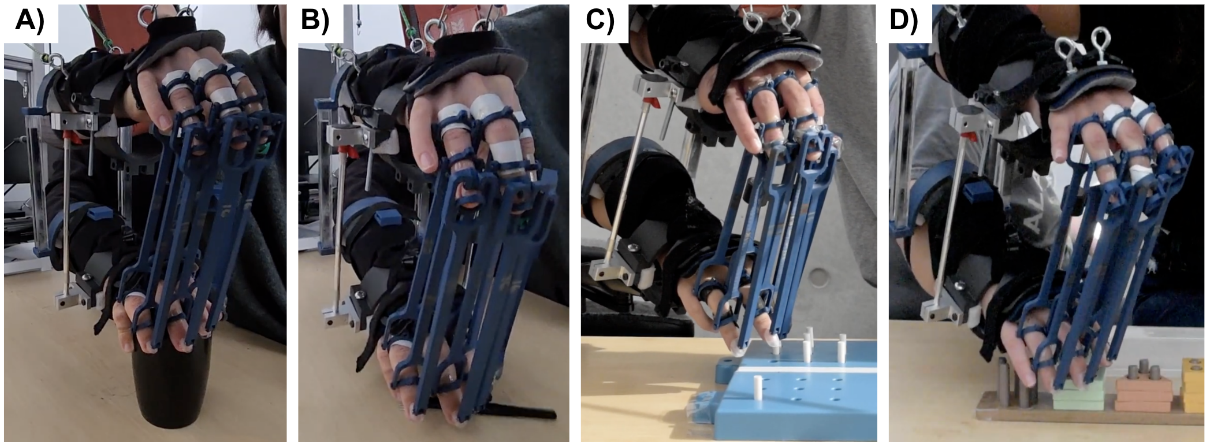

Figure 4.1: **Our inter-manual exoskeleton enables collaborative grasping:** A) One participant's hand (top) guides another participant's hand (bottom) to grasp a cup. B) Hand-coupled participants grasp a set of tweezers. C) Hand-coupled participants perform the peg-in-hole experimental task. D) Hand-coupled participants perform the shape-stacking experimental task.

4.2 Introduction

We present an inter-manual, dual-user exoskeleton that enables one person to guide the whole-hand and multi-finger movements of the other person via plastic coupling links worn on the fingers, thumb, wrist, and forearm (depicted in Fig. 4.1). With this device, two people can share simultaneous experiences of grasping and manipulating objects, with components of the haptic sense partitioned between them. Here, one person (guiding, or "leader" hand) retains the ability to direct and coordinate their hand movements, but cannot feel the objects themselves, and the other person (guided, or "follower" hand) cannot self-direct their hand movements, but can feel the objects. The device enables us to examine the sensorimotor consequences of collaborative grasping, showcasing how such inter-manual, multi-finger guidance paradigms can provide insight into human hand coordination when aspects of the haptic sense are partitioned between two people.

It is well understood that incoming sensory information, felt via populations of mechanoreceptors in the skin and proprioceptive receptors in the joints and muscles, rapidly and subconsciously modulates subsequent outgoing motor coordination of the fingers [11, 12, 17, 14, 15]. For example, when we grasp an object, critical information regarding contact timing, pressure distribution, and the onset of frictional slips are conveyed via the skin; this feedback allows for the near-instantaneous and subconscious adjustment of grip forces, ensuring that an object is held with enough pressure to prevent dropping it [41, 168]. This intricate coupling between sensation and action in the central nervous system indicates that incoming streams of cutaneous sensation are a fundamental component of the internal control loop required for stable grasping and manipulation of objects [38, 14, 15, 37, 16].

There has been a recent rise in the development of hand exoskeletons for motor rehabilitation (for comprehensive reviews, see [169, 170, 87, 86]), where movements of the hands and fingers are not self-directed but instead actuated by robotic devices that operate via force-feedback or electrical muscle stimulation [144, 145, 117, 171, 92]. Here, the internal control loop required for coordinating functional grasping of the hand is delegated to pre-programmed, task-specific control algorithms that lack the adaptive variability inherent in human motion and may be unstable [169, 142]. Furthermore, the challenge of mechanically coordinating the many degrees of freedom (DOF) of the hand (fingers and thumb) requires significant design optimizations; researchers must often make tradeoffs between functionality (i.e., high-complexity joint control) and practical wearability considerations (i.e., comfort, ergonomics, and ease of use) [170]. To bypass these algorithmic and mechanical constraints, new methods for human-human guidance, enabled by haptic devices, are being explored.

One approach to replicating finger trajectories between two people is the Tactile Display System [55], which tracks one user's fingertip movements as they actively explore raised-line drawings and replays the exact spatio-temporal motion trajectory to a second guided participant. This platform enabled exploration of the contributions of cutaneous and kinesthetic sensory information to perception and attention of two-dimensional haptic stimuli [56, 57], but was constrained to planar (2D) movements with a single finger.

Prior work most closely related to ours lies in human–human haptic guidance and upper-limb rehabilitation: several studies have shown that direct physical coupling between two people can shape ongoing motor behavior and sometimes learning [172, 173]. Applied rehabilitation protocols sometimes use manual or hand-over-hand guidance for functional hand posture; however, we found little prior work investigating settings allowing one person to directly guide another person's whole-hand grasp during functional manipulation tasks.

While many researchers have investigated motor-based exoskeletons, few examples exist in which a hand is guided by a non-motorized exoskeleton. One example, the DigituSync of Nishida et al [174], bears similarities to the inter-manual exoskeleton presented here. Like our system, the DigituSync relies on a passive mechanism linking the two hands in a top-bottom configuration, and avoids the use of electronic actuators (and control algorithms) that are required for motorized hand exoskeletons, and that contribute to the complexity, bulk, and performance challenges encountered by such devices [87, 86]. However, whereas our system is designed to enable a leader hand to guide five-digit movements of a follower hand, with sufficient kinematic transfer to enable grasping, the DigituSync system was designed to facilitate the transmission of forces from only four fingers, neglecting the thumb, which is essential for most grasping tasks. In addition, the DigituSync transfers force only in flexion and extension, neglecting abduction and adduction, and thus is not suitable for general grasping tasks. Furthermore, that system does not constrain the palmar regions and forearms to be parallel in the manner that ours does, which can lead to kinematic distortion.

4.2.1 Contributions

The primary contributions of this work are twofold. First, we present the kinematic design and fabrication of an inter-manual exoskeleton that mechanically couples the right hands of two individuals through passive mechanical linkages. This inter-manual exoskeleton enables a guiding hand (top hand, i.e., "leader") to drive the whole-hand, finger, and thumb movements of a guided user (bottom hand, i.e., "follower") during haptic interactions with objects. By leveraging passive linkage mechanics rather than actuators or control algorithms, the system enables guidance of finger and thumb without latency or instability, while remaining relatively robust to small anatomical variations between participants.

Second, we evaluate the functionality of this device through two experiments assessing guided grasping and manipulation, and the findings from these experiments contribute to the scientific understanding of how hand movements are coordinated when sensory information received via skin-object contact is unavailable. Here, cutaneous sensation from the objects is only directly available to the follower hand, and only the leader hand can plan, coordinate, and execute deliberate hand movements to complete the experimental tasks. We evaluate experimental accuracy and completion time metrics between solo (individual, no device) and coupled (hand-matched pairs, with device) conditions. Our results demonstrate that the inter-manual exoskeleton enables a leading hand to pick up objects via a follower hand, similar to using a highly dexterous tool, without directly experiencing cutaneous sensations from skin-object contact. Such an inter-manual, multi-finger guidance device serves as a platform for experimental investigation into human hand function under collaborative, guided movement conditions.

4.3 Mechanism Design and Kinematics

We designed the exoskeleton to enable one hand (the leader hand, L) to guide movements of the hands and fingers of a second person (follower hand, F). Only L is driven in the coupled mechanism, while F remains compliant (undriven). We designed the mechanism under the assumption that L and F have similar, but not identical, hand morphology (dimensions, finger lengths, etc.). In our experiments, we ensured this was approximately true by recruiting participants with closely matched hand dimensions.

To aid the design of the mechanism, we formulated an idealized kinematic model that could be theoretically analyzed in order to inform the selection of attributes of the mechanism to facilitate guidance. We base this treatment on a kinematic parallelism condition, in which the corresponding phalanges of L and F remain parallel in orientation. When satisfied, this condition would ensure that the hand posture of F that achieves grasping during object contact (e.g. form or force closure on an object) matches that at L, thus minimizing kinematic distortion between the two. While this idealized parallel kinematic condition is aligned with our primary interest in facilitating grasping, and is convenient in making the kinematic analysis tractable, it introduces several idealizations and assumptions that are incompatible with the realization of a practical device integrating with the human hand. A condition of strict parallelism is likely also excessively rigid, due to the ability of humans to perform sensorimotor tasks with the hand (or tools) in the presence of significant disturbances.

There are several reasons for this. First, to support guided manipulation, which is our primary objective, it is important to avoid occluding large areas of skin, such as would be required in order to achieve precise kinematic control. Second, it is impractical to established fixed anchor points on most of the hand surface, due to the high shear deformability of the skin. For example, even with a brace in distributed skin contact along the phalanx, modest forces less than a few newtons are sufficient to displace the skin by millimeters in multiple shear directions. Third, as related below, grasp occlusion and other effects complicate the control of thumb kinematics. Fourth, even after selecting participants for matched hand sizes, it is impossible to ensure identical segment lengths. Therefore, our goal here is to facilitate guidance by the leader (via vision), rather than to control kinematics.

Nonetheless, a formal description of the kinematics proved useful in designing this device. We emphasize that we do not claim this device enforces parallel kinematics across the hands. Our evaluation is instead functional. Indeed, individuals exhibit a remarkable ability to accommodate kinematic differences in manual control tasks [175]. The next section describes the kinematics motivating our design in greater detail.

4.3.1 Idealized Kinematic Objectives for Parallel Lead-Follow Guidance

Let the five digits of the right hands of L and F be indexed by $j \in \{1, \dots, 5\}$. Let each corresponding phalanx pair have identical segment length (our experiment relaxes this condition). Each digit may be modeled as a serial kinematic chain originating at a base joint, consisting of the carpometacarpal (CMC) joint for the thumb ($j = 1$) and the metacarpophalangeal (MCP) joints for the fingers ($j = 2 \dots 5$) respectively. Let the phalanges of each digit j be indexed by k. For the fingers ($j = 2, \dots, 5$), $k = 0$ represents the metacarpal phalanges (MC), $k = 1$ represents the proximal phalanges (PP), $k = 2$ represents the medial phalanges (MP), and $k = 3$ represents the distal phalanges (DP). For the thumb ($j = 1$), $k = 1$ represents the metacarpal phalanx (MC), $k = 2$ represents the proximal phalanx (PP), and $k = 3$ represents the distal phalanx (DP).

Let $\{0\}$ be the world frame with $\hat{z}$ as its vertical axis. Let $T^X_{j,k} \in SE(3)$ denote the world pose of the k-th phalanx of the j-th digit for hand $X \in \{L, F\}$. Each can be represented by a homogeneous matrix:

$$T^X_{j,k} = \begin{bmatrix} R^X_{j,k} & p^X_{j,k} \\ 0 & 1 \end{bmatrix}, \; X \in \{L, F\} \tag{4.1}$$

where the phalanges, k, are numbered from proximal to distal. $R^X_{j,k} \in SO(3)$ is a rotation and $p^X_{j,k} \in \mathbb{E}^3$ is a translation. Our design positions the leader hand (L) above the follower hand (F), at constant displacement $p_0 = d\,\hat{z}$. The configurations of a pair of hands so displaced is parallel if the pose of each phalanx satisfies

$$T^L_{j,k} = T_d\, T^F_{j,k} \tag{4.2}$$

where T_d is the constant translation

$$T_d = \begin{bmatrix} I_3 & d\,\hat{z} \\ 0 & 1 \end{bmatrix}$$

As noted above, since we are interested in guiding prehensile manipulation with the fingertips, we focus on the distal phalanges. A pair of corresponding distal phalanges is parallel and displaced by distance d in the $\hat{z}$ (vertical) direction if it satisfies

$$T^L_{j,3} \;=\; T_d\, T^F_{j,3} \tag{4.3}$$

The high mobility and expansive workspace of the thumb ($j = 1$) make our objective challenging to achieve with a practical mechanism that preserves thumb mobility over the required range of grasping configurations. Thus, for the thumb, we relaxed the constraint (3) to apply only in position, and not necessarily in orientation, thus allowing the distal phalanx orientations to differ,

$$p^L_{1,3} = p^F_{1,3} + d\,\hat{z} \quad \text{(thumb, } j = 1\text{)} \tag{4.4}$$

In practice, as explained below, in our implementation, the distal phalanges of the thumbs remain close to parallel, due to our mechanism design and due to the single degree of rotation freedom at the IPJ joint of the thumb.

4.3.2 Mechanism Design for Fingers, $j = 2, 3, \ldots, 5$

The mechanism design for each finger is independent and illustrated in Fig. 4.2. At the proximal end of each digit, a rigid constraint is imposed across the forearm, wrist, and palmar surface (metacarpals). This is represented by a base constraint link c_0 of length d, ensuring that the condition of Equation 4.2 is satisfied for the MC phalanx ($k = 0$) of each finger.

We proceed in proximal to distal order with each corresponding pair of phalanges of L and F. We first address flexion and extension; abduction and adduction at the MCP joint are treated below. The digits of L and F may be treated, in flexion, as planar serial mechanisms.

The mechanism of our exoskeleton introduces additional constraint linkages and joints that realize a closed kinematic chain across the corresponding L and F fingers. Proceeding by induction for any finger, from proximal to distal: we first introduce a constraint link c_1 with length d oriented in the $\hat{z}$ direction. c_1 terminates on either end at revolute joints on the respective PP phalanges, at a distance $l_{j,1}/2$ halfway along the phalanx from the respective proximal joint $\theta_{j,1}$. A parallelogram is formed by c_0 and c_1 and the equal-length segments of the PP phalanges of L and F on the proximal side of c_1. Thus, phalanges PP of L and F satisfy the condition of Equation 4.2. This construction pro-

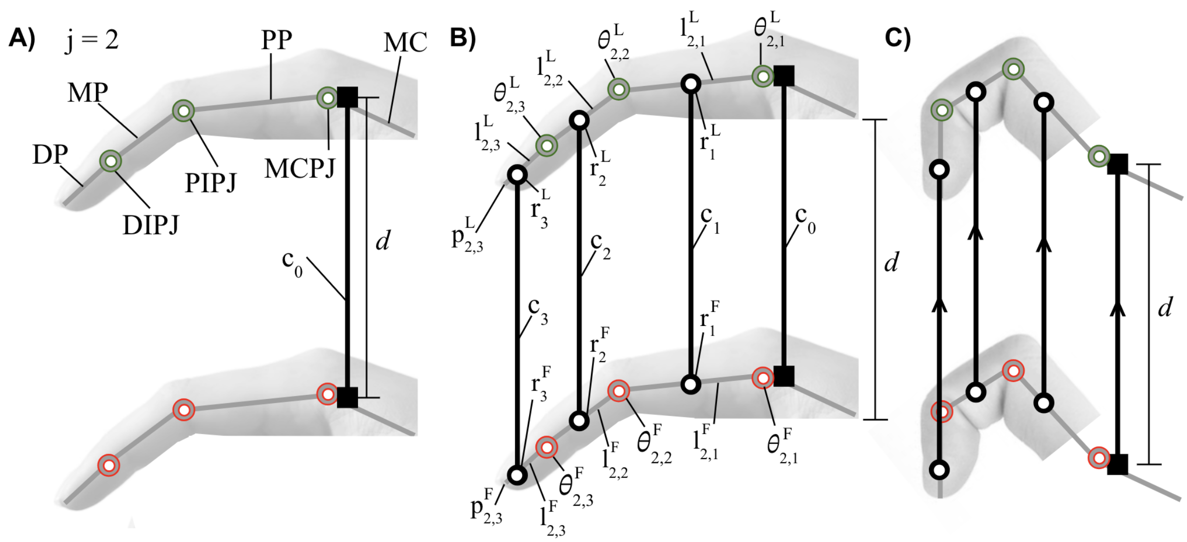

Figure 4.2: **Kinematic constraints of digits $j = 2 \cdots 5$ imposed by the proposed serial four-bar linkage mechanism:** We design a coupling mechanism for the non-thumb fingers to enable one finger to guide the posture of another finger. A) The underlying kinematic structure of the index finger contains a distal phalanx (DP), distal interphalangeal joint (DIP), medial phalanx (MP), proximal interphalangeal joint (PIP), proximal phalanx (PP), metacarpophalangeal joint (MCP), and metacarpal (MC). We first consider two uncoupled index fingers, initially constrained by a rigid coupling link c_0 of length d, representing the base coupling constraints between the palm, wrist, and forearm. B) We impose a set of coupling links c_1, c_2, c_3 on the PP, MP, and DP of L and F, which can rotate in 1DOF to accommodate finger extension/flexion. All four coupling links $c_0 \cdots c_3$, imposed on the underlying kinematic structure of the finger, constrain the follower finger to match the posture of the leader finger via a series of four-bar parallelogram planar mechanisms. C) An example of matched posture between the leader and follower fingers during flexion. The coupling links $c_0 \cdots c_3$ remain parallel, ensuring that the movements of the follower finger match those of the leader finger.

ceeds in the same fashion with the MC phalanges replaced by the PPs, and the PPs replaced by the MPs, and with the addition of a new constraint c_2 terminating on MP at identical distances $l_{j,2}/2$ of F and L, ensuring that the MP phalanges of L and F also satisfy (4.2). Repeating this construction one further time, with the addition of constraint c_3, ensures that the distal phalanges also satisfy the condition of Equation 4.2, as desired.

Our design decouples finger mobility in flexion/extension and abduction/adduction, so this analysis holds across the range of motion of the respective finger. In detail, constraint c_0 ensures that the MCP joints are displaced by d on a line parallel to the $\hat{z}$ axis. Furthermore, the revolute joint at c_3 is fixed to the fingernail such that each phalanx and the distal phalanges are also displaced by $d\,\hat{z}$. Consequently, as the fingers abduct or adduct about the MCP joint, flexion of the coupled fingers is always in in a plane whose normal vector is in the $x-y$ plane (orthogonal to vertical).

In summary, the mechanism design ensures that the kinematic conditions of Equations 4.2 and 4.3 hold for each leader-follower pair of fingers ($j = 2, 3, 4, 5$).

4.3.3 Mechanism Design for Thumb ($j = 1$)

As noted above, due to the high mobility and expansive workspace of the thumb ($j = 1$), which can pronate in opposition to the fingers for grasping, it is challenging to design a mechanism that ensures parallel configuration of the coupled thumbs without producing interference. Furthermore, motion involving components of pronation or rotation about the thumb's axis is difficult to control via a practical mechanism, because the skin covering the phalanges is highly mobile, impeding the establishment of a fixed mount on each phalanx as was achieved with the other digits. We modeled, analyzed, designed and prototyped several solutions for the thumb, none of which performed satisfactorily. These challenges motivated the design used in our exoskeleton, which relaxed the distal phalanx parallelism condition (Equation 4.3) to apply only in position, not orientation.

Specifically, our kinematic condition for the thumbs is as follows: we designate corresponding points $p^F_{1,3}$ and $p^L_{1,3}$ near the nail on the thumb tip that must satisfy Equation 4.4. Thus, the thumb tip phalanx positions are displaced by $d\,\hat{z}$, but can differ in orientation. In practice, the distal phalanges of the thumbs remain close to parallel, because

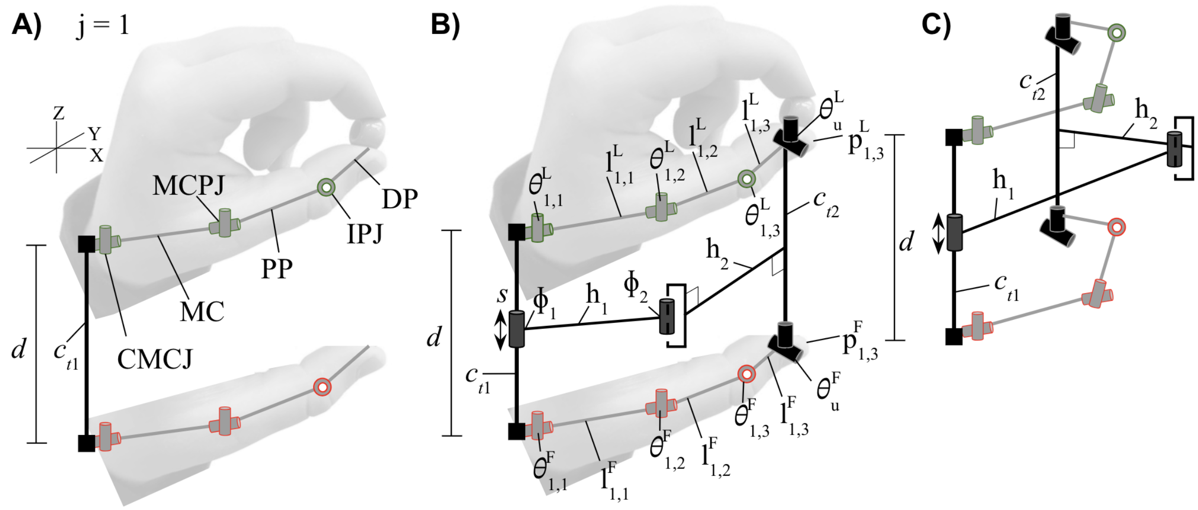

Figure 4.3: **Kinematic constraints of the thumb digit $j = 1$, imposed by the proposed coupling mechanism:** Our design goal is to enable a leader thumb to guide a follower thumb, such that the position of the thumb tip is matched and displaced by a vertical distance (relaxing orientation constraint). A) Each thumb has a carpometacarpal joint (CMCJ), a metacarpal (MC), a metacarpophalangeal joint (MCPJ), a proximal phalanx (PP), an interphalangeal joint (IPJ), and a distal phalanx (DP). The CMCJ and MCPJs are modeled to be universal joints (2-DOF) and the IPJs are modeled to be rotary joints (1-DOF). The two uncoupled thumbs are initially fixed at the base joint (CMCJ) by a distance d with coupling link c_{t1}. B) Our slider-double-hinge (s, h_1, h_2) mechanism and u-joint coupler $(c_t 1, \theta_u^L, \theta_u^F$ mechanism enable the leader thumb to guide the follower thumb. C) We illustrate the position of the thumb coupling mechanism when the leader thumb performs adduction movements.

the residual degree of freedom at the IPJ has a limited range of motion.

The mechanism design for the thumbs is thus distinct from that for the fingers and illustrated in Fig. 4.3. Proximal to the carpometacarpal joint (third from the thumb tip), it imposes a rigid constraint grounded at the wrist and palmar surface, which are fixed. This is represented by a base constraint link c_{t1} of length d parallel to $\hat{z}$. A second constraint, c_{t2} bridges points $p_{1,3}^L$ and $p_{1,3}^F$, which are just above the nail. c_{t2} terminates in universal joints on each end. A hinge mechanism couples the two constraints. One hinge link, h_1, terminates with a sliding revolute joint s on c_{t1}. The other, h_2, is rigidly coupled to the midpoint of c_{t2} at the distal end and to the revolute joint at the end of h_1 on the proximal side. By inspection, this mechanism preserves 3 spatial degrees of freedom: With s fixed, the distal end of h_2 can translate in a plane orthogonal to the $\hat{z}$ axis. Motion in $\hat{z}$ is accommodated by sliding at s. This ensures that condition 4.4 is preserved as $p^L_{1,3}$ translates. The universal joints at the ends of c_{t2} accommodate 2-axis rotation at either thumb. Because rotation of the universal joints is about $p^F_{1,3}$ and $p^L_{1,3}$, which lie near the midpoint of the distal thumb phalanx, and due to the constrained lengths of the thumb phalanges, the distal phalanges have limited unconstrained mobility in orientation in practice.

As part of our design process, we verified that the mechanism for fingers and thumb are free from singularity and interference, across the range of motion employed here, using numerical kinematic studies and prototyping.

4.4 Design and Fabrication of the Inter-Manual Exoskeleton

Our device was fabricated with mechanical parts from McMaster Carr, as well as 3D-printed with carbon-fiber reinforced PETG material using a Bambu X1 Carbon 3D-printer with AMS. Our process enables the quick production of thin and stiff linkages that can appropriately transfer posture between leader and follower hands. Mechanism components were designed in CAD using Solidworks 2024 (licensing provided by the University of California, Santa Barbara's Mechanical Engineering Department). The resulting fabricated mechanism, when worn by two people, is depicted in Fig. 4.4A.

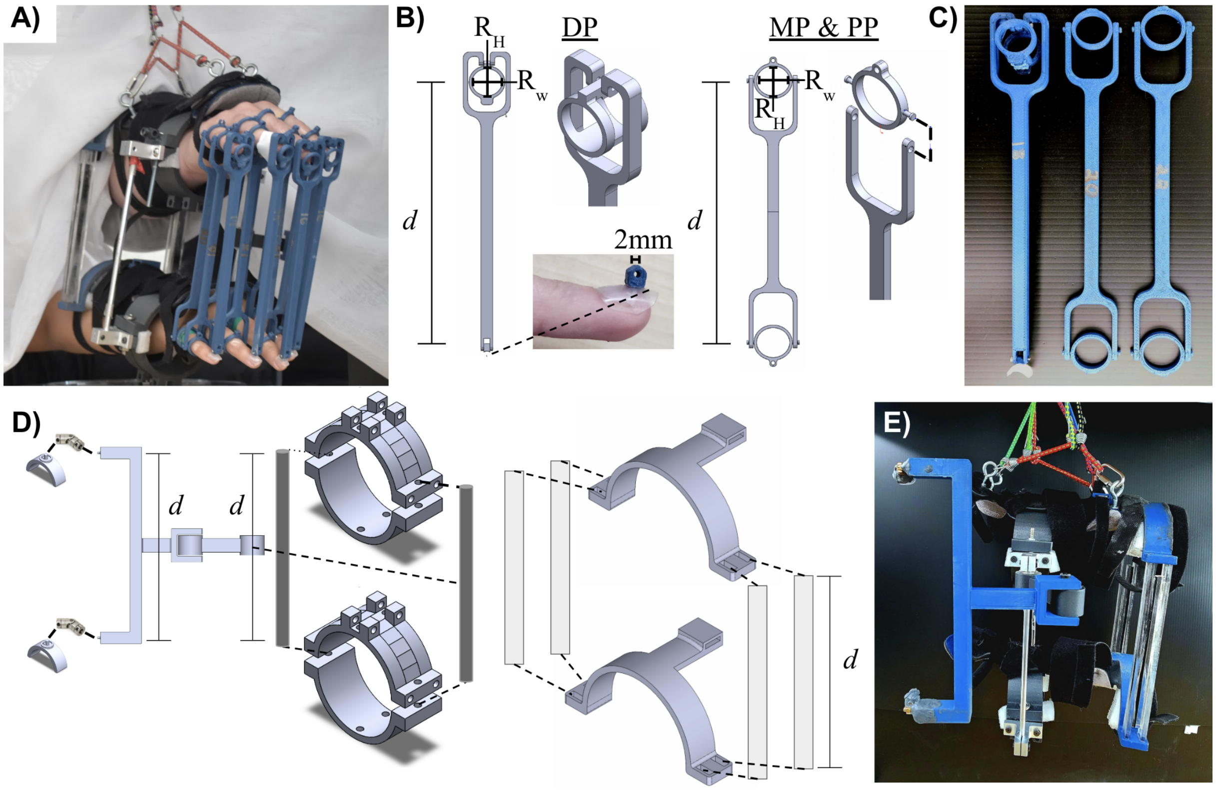

Figure 4.4: **The design and fabrication of the inter-manual coupling device:** A) We fabricated a whole-hand coupling mechanism between two people, which enables one hand (top of the device, leader hand) to guide the multi-finger and thumb movements of another compliant, follower hand (bottom of the device). B) CAD models of 1-DOF linkages that couple digits $j = 2 \cdots 5$. The coupling linkages for the medial and proximal phalanges (MP, PP) are composed of two rings, rotating in 1DOF within a rigid links of length $d = 200mm$. The coupling linkages for the distal phalanges include a rigid finger cage for the leader hand and a fake nail with a rotary joint, mounted to the fingernail of the follower hand, via UV-cured manicure gel. C) The resulting fabricated finger links (distal, medial, and proximal phalanges), when worn between two hands, can reproduce finger extension and flexion of the joints of the digits, as well as transfer abduction/adduction of the metacarpal joint. D) CAD models of the thumb and wrist constraint mechanism. The device employs a brace with rigid linkages fixing the two arms with a vertical distance of $d = 200mm$. The thumb coupling mechanism employs a slider and double-hinge design, terminating in two u-joints, to enable one thumb to guide the movements of another thumb. D) The fabricated mechanism for the wrist and thumb, using carbon-fiber reinforced PETG and linear motion shafts from McMaster Carr. The forearm and wrist components of the device are suspended via a bungee system, supporting the leading hand.

4.4.1 Wrist and Forearm Coupling Mechanism

Our device employs two braces that fix the forearms, wrist, and palm of the hand of each participant (Dorsal Carpal Tunnel Splint made by RCAI). Such braces are intended to address discomfort from arthritis or carpal tunnel, or to brace the wrist during strain injuries. Here, our use of the braces restrict wrist flexion. We connect the two braces in a vertical configuration through the use of linear motion guides (200 mm in length) and two sets of 3D-printed bracelet components. There is one full bracelet at the base of the wrist (80 mm diameter) and one half-bracelet design at the forearm (100 mm diameter). Velcro straps fix the device to the forearm and palm in three locations. The thumb coupling mechanism is mounted to the linear guides at the wrist and explained further below. The wrist coupling mechanism design (CAD models) and resulting fabricated mechanism are depicted in Fig. 4.4D and Fig. 4.4E, respectively.

4.4.2 Phalanx Coupling Links

We fabricated 3 coupling linkages with revolute joints for each finger, according to the design constraints shown in Fig. 4.2. The linkages for the MP and PP, depicted in Fig. 4.4B, are composed of a rigid vertical link of length 200 mm, connected to two ring structures and incorporating two rotary joints each (1-DOF). Each ring structure is fit to the corresponding phalanx of both leader and follower hands; the inner diameter of the rings vary in size by 2 mm ($R_w = [14, 16, 18, 20, 22, \cdots 26]$ mm, with the height of each ring $R_h = 0.9 \times R_w$. The horizontal thickness of the ring is 2 mm and the bracket is 4 mm, meaning about 12 mm of thickness is added to each finger by the linkage (6 mm on each side). The rotary joints must be positioned on each side of the ring such that they lie on the horizontal axis of the finger cross-section.

The distal phalanx coupling mechanism requires a different design, due to nail and cartilage material on the dorsal side of the finger, and must support adhesion to the fingertip under the high forces produced during functional grasping. To accommodate these design needs, we adhere a fake nail, connected to a small revolute joint, to the human nail with UV-cured manicure gel, leaving the fingerpads of the follower hand free to grasp objects without interference from the mechanism. For the leader hand, we designed a cage surrounding the distal phalanx to properly adhere the mechanism to the finger, without the need for fake nails. CAD models for the distal phalanx mechanism is depicted in Fig. 4.4B and the resulting fabricated linkage is depicted in Fig. 4.4C.

Placing two ring linkages on two coupled fingers, at the midpoint of medial and proximal phalanges, in addition to the distal phalanx linkage at the fingertips, results in the ability of a leader digit to guide the movements of a follower digit (non-thumb).

4.4.3 Thumb Coupling Mechanism

We fabricated our mechanism for the leader and follower thumbs according to the design requirements depicted in Fig. 4.3. The resulting CAD models and fabricated mechanism are depicted in Fig. 4.4D and E, respectively.

The fabricated thumb coupling mechanism is composed of a slider-double-hinge mechanism that terminates in two u-joints (outer diameter 7 mm, inner diameter 3 mm). The slider mechanism includes the linear guide from the rigid wrist coupling structure, of length 200 mm, in addition to a hinge arm of length $h_1 = 80$ mm. These components enable sliding in $\hat{z}$ and opening and closing orthogonally to $\hat{z}$. A second hinge arm of length $h_2 = 65$ mm, which also opens and closes orthogonally to $\hat{z}$, is attached to a rigid vertical linkage component of length 200 mm, which is coupled to the leader and follower thumb nails via 3D-printed thumb brackets. When two wrists are fixed into this coupling mechanism, and the thumb brackets are fixed to the thumb nails, the resulting mechanism can reproduce natural abduction, adduction, extension, and flexion of thumb movements between leader and follower thumbs.

4.5 Experiments

We evaluated the functionality of our inter-manual coupling mechanism in standard object manipulation tasks, drawn from hand functional testing and widely used in other research [176, 177]. Participants were tasked with completing a nine-peg-in-hole task (Experiment 1) and a shape stacking task (Experiment 2) using either their own hand (solo condition) or by guiding the hand of a second person (coupled condition).

4.5.1 Participants

We recruited eight right-handed participants (five female, three male) between 21 and 34 years old to participate in two experiments evaluating the functionality of our inter-manual exoskeleton. All eight subjects participated in both the solo and coupled conditions of the study. The study was approved by the Institutional Review Board of the University of California, Santa Barbara, and all participants provided written informed consent. No participants reported sensorimotor impairments that would affect grasping or manipulation of small objects.

For the coupled condition, the eight participants were matched into four pairs, with the constraint that corresponding phalanx lengths within each pair differed by less than 10 mm. Within each pair, participants were randomly assigned to be either the leader (top) hand or the follower (bottom) hand.

4.5.2 Experiments

Participants performed two manual dexterity experiments – peg-in-hole (Experiment 1) and shape-stacking (Experiment 2) – in both solo and coupled conditions. There is one practice trial before the captured experimental trial for each experiment, in line with manual dexterity clinical evaluations. Participants are instructed to complete the task as quickly and as accurately as possible. We recorded time-stamped video of the hands of participants completing the dexterity experiments in both conditions, and task accuracy and completion time metrics were extracted post-hoc.

4.5.2.1 Peg-In-Hole Experiment

The peg-in-hole experiment (Jamar 9-Hole Peg Test Kit, Superior Medical Equipment) consisted of two stages (Fig. 4.5A). During the Peg Insertion (P-I) stage, participants moved each of the nine pegs from a pegboard to its corresponding hole on a second pegboard. During the subsequent Peg Removal (P-R) stage, participants removed each peg from the second pegboard and placed it in a dish. A peg was considered a "miss" if it was placed in an incorrect hole during the Peg Insertion stage or dropped during either stage, and a "hit" otherwise.

4.5.2.2 Shape-Stacking Experiment

The shape-stacking experiment (S-S) involves four identical copies of five different shapes, which are sequentially stacked directly on top of the others in the same orientation on a pegboard (Fig. 4.5B). Each shape featured one or more circular cutouts (12 mm diameter) that allowed it to be stacked on the pegboard, with the number of cutouts varying by shape. The five shapes include: circle (45 mm diameter, 1 cutout), rectangle (25 mm x 50 mm, 2 cutouts), triangle (53 mm edge length, 3 cutouts), square (50 mm

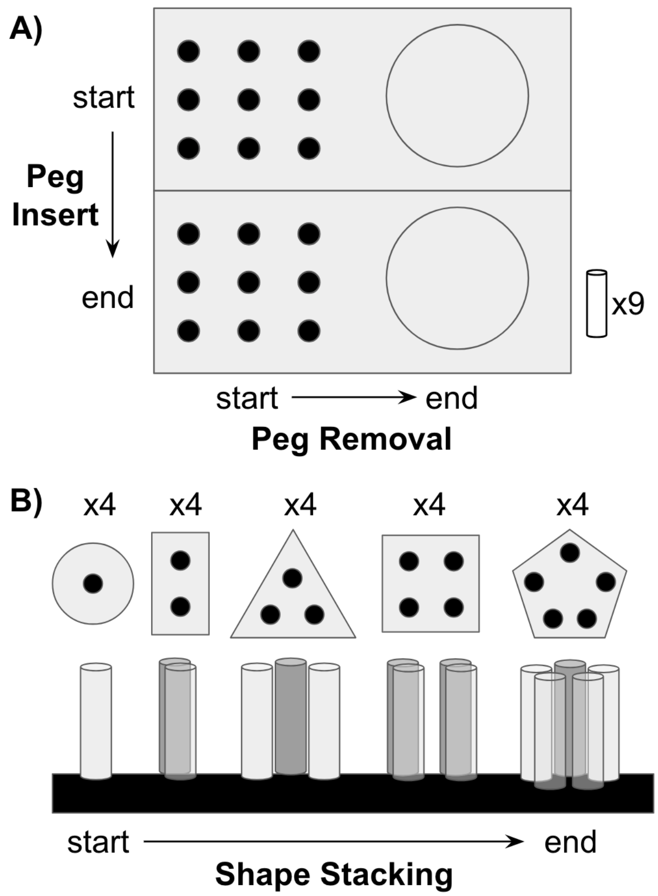

Figure 4.5: **The two experiments assessing manual dexterity:** A) Peg-in-hole: In the Peg Insertion (P-I) stage, each of nine pegs was moved from the top pegboard to its matching position in the bottom pegboard. During the subsequent Peg Removal (P-R) stage, pegs were removed from the bottom pegboard and placed in a dish. B) Shape-stacking: For each of five shapes, four identical copies were stacked sequentially in the same orientation on a peg board. Shapes contained one or more circular cutouts that allowed them to be mounted on pegs and were completed in order of increasing cutout count.

edge length, 4 cutouts), and pentagon (33 mm edge length, 5 cutouts). All shapes were 8 mm thick. Shapes were stacked in order of increasing cutout count (from circle to pentagon). Each copy of a shape was considered a "miss" if it was dropped or placed in an incorrect orientation on the pegboard, and a "hit" otherwise.

4.5.3 Experimental Protocol

The solo condition was completed within 15 minutes per participant, and the coupled condition was completed within 1 hour and 30 minutes. All eight participants took part in both solo and coupled conditions. During the solo condition, all participants had vision of the two tasks. During the coupled condition, only the leader hand had vision of the tasks. The order of tasks (shape-stacking or peg-in-hole) and experimental conditions (coupled or uncoupled) were randomized and counterbalanced. Participants were given a five-minute break between tasks.

Donning the device during the coupled condition took between 30-45 minutes per participant pair. The experimenter first secured the participants' wrists and forearms within the device. Then, the index, middle, and ring fingers were coupled at the proximal and medial phalanges with the appropriately-sized ring linkages. Next, the distal phalanges of the index, middle, and ring fingers were coupled with the appropriately-sized cage-and-fake-nail linkages. Lastly, the fake nails at each end of the thumb mechanism were attached to the leader and follower thumb nails. All fake nail components were attached with UV-cured manicure gel. Skin safe, double-sided adhesive was used to adhere the plastic links to the fingers and minimize play in the mechanism. The pinky fingers were not coupled, as pilot testing demonstrated they were not used for grasping and manipulation in either experiment.

4.5.4 Subjective Questionnaire

After the participants completed both solo and coupled conditions of the two experiments, they provided written responses to the following questionnaire:

- How comfortable was the device attached to your hand during the experiments? (Likert scale response from 1-10, followed by free response)

- How much mental effort did you have to engage in when completing the experiments with the exoskeleton? (Likert scale response from 1-10, followed by free response)
- If you were the leader hand in the experiments, please provide any comments you may have about what it felt like to perform the tasks via the other person's hand (when you were guiding the other hand)? (Free response)
- If you were the follower hand in the experiments, please provide any comments about what it felt like for the other person to perform the tasks with your hand (when your hand was guided)? (Free response)
- Any other feedback or comments? (Free response)

4.5.5 Analysis

We manually annotated the captured video to identify start and stop times on the experimental trial in each experiment, and from these data obtained the amount of time required to complete each manual dexterity task.

Peg-in-hole accuracy, on both P-I and P-R phases, is computed per participant by dividing the total number of hits by 9 and reported as a %. Shape-stacking accuracy is similarly computed by dividing the total number of hits by 20 (5 total shapes, 4 copies per shape) and reported as a %. Per-peg completion time for both P-I and P-R is computed by dividing total task time by 9. Per-shape completion time is computed by summing the time it takes for each participant to pick up and place each copy of one shape and dividing by 4; then, each of these averages (one value per shape per participant) is summed and divided by 5.

To determine whether accuracy and completion time are significantly different between solo and coupled conditions, we use Welch's t-tests (with a 95% confidence interval), corrected post-hoc using the Holm-Bonferroni method. Welch's t-tests were employed here, as our experimental groups have unequal variances and sample sizes.

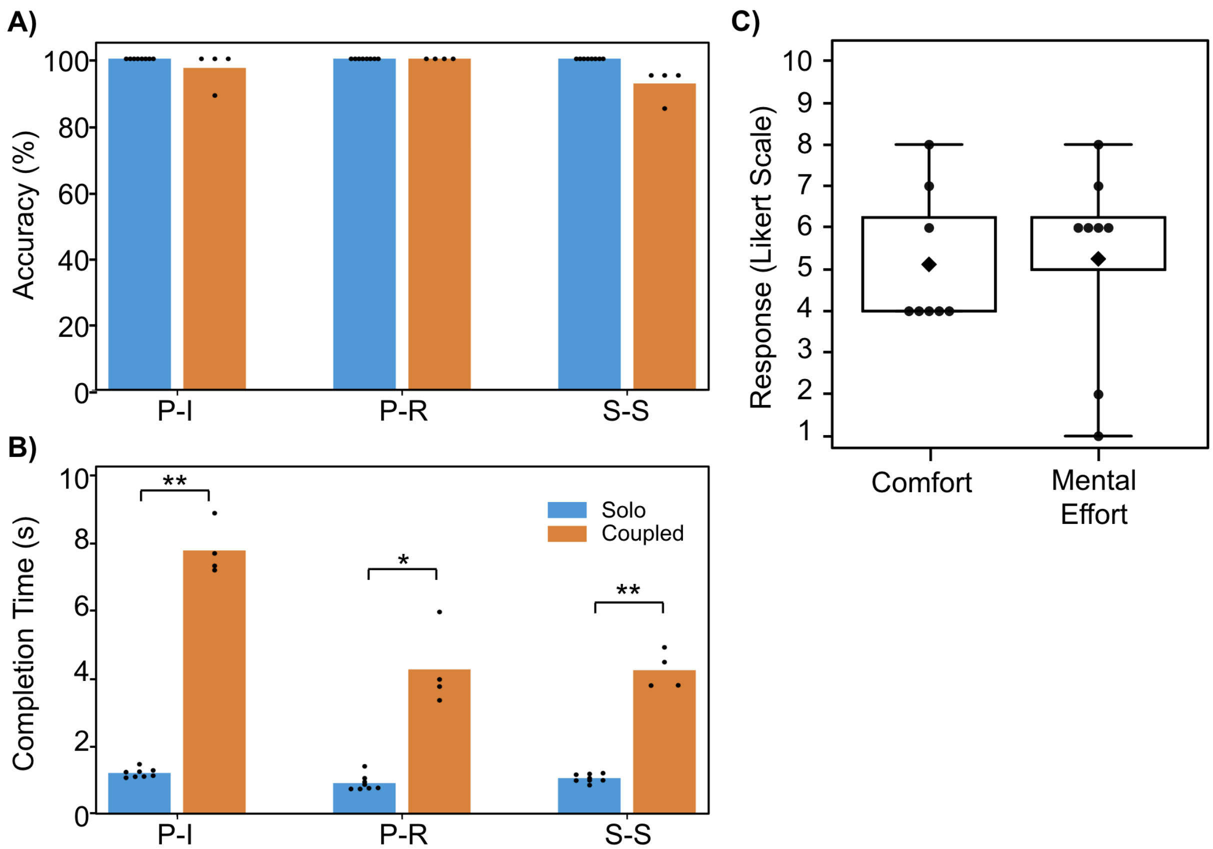

Figure 4.6: **Experimental results (accuracy, completion time, Likert-scale questionnaire responses):** We measure accuracy (A) and completion time (B) from solo participants and coupled dyads. No statistically significant difference was found in accuracy between solo and coupled conditions on either peg-in-hole or shape-stacking experiments. A significant difference in per-object completion time (average time to correctly place either one peg or one shape) was found between solo and coupled conditions. C) Participant responses to Likert-scale questions are depicted, which include comfort of the exoskeleton device (left) and how much mental effort was experienced while performing the experiments with the device (right). A score of 1 indicates extremely uncomfortable or extremely low mental effort, whereas a score of 10 indicates extremely comfortable or extremely high mental effort. Mean scores for both questions were 5.125 (around neutral).

4.5.6 Results – Accuracy and Completion Time

Mean accuracy in the solo condition across the two manual dexterity experiments (P-I, P-R, S-S) was 100%. Mean accuracy in the coupled condition was above 90% (P-I: 97.22%, P-R: 100%, S-S: 92.5%). Mean accuracy results (across condition and per participant or participant pair) are reported in Fig. 4.6A. Completion time per-peg or per-shape in the solo condition for all tasks was under 1.5 seconds (P-I: 1.20 s, P-R: 0.90 s, S-S: 1.05 s). In the coupled condition, completion time per-peg or per-shape was greater than 4 seconds (P-I: 7.78 s, P-R: 4.26 s, S-S: 4.25 s). Mean per-peg or per-shape completion times (across condition and per participant or participant pair) are reported in Fig. 4.6B. Comprehensive descriptive statistics for both accuracy and completion time metrics are reported in the supplementary material (Table 4.1).

Accuracy across all tasks was not found to be significantly different between solo and coupled conditions (P-I: $t = 1.000, p = 0.782$, P-R: both groups resulted in 100% accuracy, S-S: $t = 3.000, p = 0.173$). Conversely, we found statistically significant differences for completion time between solo and coupled conditions across all tasks (P-I: $t = -16.989, p = 0.002$, P-R: $t = -5.721, p = 0.038$, S-S: $t = -11.403, p = 0.006$). Comprehensive results from Welch t-tests with post-hoc correction can be found in the supplementary material (Table 4.2).

4.5.7 Discussion – Accuracy and Completion Time

We found that performance accuracy remained consistent across solo and coupled conditions during both peg-in-hole and shape-stacking experiments, demonstrating that the inter-manual exoskeleton enables the guided, functional grasping and manipulation of small objects. This occurs despite the leader lacking direct cutaneous contact with objects, relying on the visual system instead to coordinate the movements of the follower's fingers. This inter-manual device effectively partitions the human haptic sense between two individuals while preserving the hand's full functional capacity under passive guidance.

We additionally observed higher completion times in the coupled condition for both experiments; this indicates that while cutaneous sensation may not be necessary for the leader hand in successfully coordinating the grasping and manipulation of objects via the follower hand, it may significantly speed up the time it takes to perform these hand functions. However, this may be due to interference from the linkages and unfamiliarity of the experience, requiring periods of adaptation and motor learning. We evaluate our participants' subjective experiences while using our inter-manual coupling device below to investigate the possible contributions of other variables.

The findings we report appear to be consistent with prior studies of natural human hand function under digital anesthesia, which show that manual dexterity in grasping is significantly impoverished under digital anesthesia [41, 38, 178]. The same studies show that task completion is often possible under visual guidance, but incurs significant time delays. Our inter-manual exoskeleton reproduces these results without the use of digital anesthesia by enabling multi-digit guidance of one person's hand by another person.

The inter-manual exoskeleton makes it possible, under restricted conditions, to partition motor control and cutaneous sensory feedback between two participants, and thus could enable a host of experiments that are not accessible using other methods, including digital anesthesia, beyond manipulation tasks like those tested here. For example, this apparatus makes it possible to compare the perception of haptic object properties under conditions in which agency over exploratory movements is present or absent. Additionally, this apparatus can facilitate experiments in which object perception is tasked to the (top) leader hand, which possesses agency over exploration, with or without sensory input from vision, but does not have access to cutaneous information. Alternatively, by switching the role of the bottom hand to leader and the top hand to follower, this apparatus makes it possible to assess how proprioceptive information that is available to the top hand contributes to object perception, in the absence of motor control and cutaneous input from skin-object contact. A host of other possibilities exist that may enable further studies.

4.5.8 Questionnaire Responses

Responses for questions 1 and 2 (comfort of the exoskeleton, mental effort while using the exoskeleton) are reported in Fig. 4.6C. The mean response for both questions was 5.125, indicating a slightly above neutral response for comfort and a medium level of mental effort.

Regarding comfort of the exoskeleton (question 1), some participants (n = 2) reported a limited range of motion in closing their fingers together, due to lateral interference from the brackets. Other responses included the fake nail tips being slightly too long when grasping the small pegs (n = 1), slight pulling sensations at the cuticle from the fake nail of the DP linkage (n = 1), and some upper arm and body discomfort/fatigue towards the end of the study (n = 4). One participant described the finger and thumb coupling links like wearing a glove.

Regarding mental effort during the tasks with the exoskeleton (question 2), follower participants described some level of effort in remaining passive, without resisting guidance forces from the top hand or making their own corrective movements while feeling the objects. Leader participants described effort in translating movements through vision from their own perspective, which required more concentration than moving with their own hand, particularly at the beginning of the study. One leader participant described this experience as playing a video game, where they could better coordinate the movements of the follower hand over time through use of vision.

Some participants who experienced the leader condition (question 3) felt as though they could almost feel the objects themselves, through the follower hand (n = 3), due to visual feedback from the task and cutaneous feedback felt via the plastic coupling links. One participant reported, "I was surprised to find that it almost 'felt' like I was physically grasping the objects with my own hand." Another leader participant reported that not having the sense of touch made it more difficult for them to complete the task, compared to using their own hand, especially during the peg-in-hole experiment (i.e., smaller objects requiring a higher level of fine motor coordination).

Some participants who experienced the follower condition (question 4) described how being guided through a movement felt similar to performing the movement themselves (n = 2). However, a break in the illusion occurred if the leader hand stumbled or made an error when picking up an object. Having tactile sensation, but not the ability to control their movements, felt strange for most follower participants, with two reporting the experience to be "interesting" and one reporting it to be disconcerting and invasive to their sense of agency over their own body.

Several responses (n = 3) to our request for additional comments (question 5) included reflections on agency and autonomy. One follower participant described their experience as "very extraordinary... It made me think about how much agency do I have in my daily life." Another follower participant wrote, "I guess I like my autonomy." One participant suggested a further coupling of the upper arms during future experiments.

4.6 Conclusion

We developed an inter-manual exoskeleton that enables one person to guide the whole-hand movements of another person in grasping and manipulating small objects. Here, a simultaneous haptic experience is shared between two users, with aspects of the haptic sense partitioned between them – the leader hand does not directly contact the objects being manipulated, and the follower hand cannot self-direct movements. Our design synchronizes movements of the forearm, wrist, and all five fingers, while accommodating the thumb's complex adduction and abduction. We note that parallelism between the two hands is not strictly enforced by our mechanism, and may be difficult to achieve in practice due to difficulties mounting the device to the the skin on certain parts of the hand, and due to wide ranges of digit morphologies between people.

We observed similar performance accuracy during two experiments between solo and coupled conditions, indicating that our device facilitates successful grasping and manipulation of small objects under guided movement conditions. However, we observed significantly different completion times between solo and coupled conditions across all tasks.

This is expected, given the limitations on the haptic sense on behalf of the leader hand. Here, there is a heavy reliance on the visual system for motor planning and coordination rather than the tactile sense, as cutaneous sensory streams do not contain information directly from object surfaces. This may cause disruption in the internal models used to predict sensorimotor consequences and guide subsequent hand movements, which may be mitigated with longer familiarization periods and more experience with the hand-coupling device. Like practicing an instrument, wielding another person's hand may become easier with time.

Additionally, mechanical factors such as structural interference from linkages, increased weight on the hand and forearm from the device, and fatigue over time may contribute to longer completion times in both experiments. Improvements to the device design and ergonomics, in addition to shortening the time it takes to don participants into the device, would help to eliminate these potential confounding variables. Furthermore, responses to our questionnaire indicate that follower participants, who did not control their finger movements during the tasks, experienced changes to their feelings of agency and autonomy over their hands. These qualitative results warrant further investigation into sensations of agency, body ownership, and embodiment during such guided, multi-finger experiences.

The present contribution addresses shared haptic grasping and manipulation, in which agency over the completion of the task was entirely allocated to the leader hand, which lacks cutaneous sensory input. An interesting question naturally arises as to what the follower hand feels, since they have access to cutaneous input that the leader hand lacks. Because haptic perception involves the integration of sensory input and movement, this question naturally leads to a host of other research questions about haptic object perception that may be possible to clarify using a device such as ours that partitions sensation and movement between two people. We aim to investigate this in future research.

4.7 Acknowledgements

The authors thank Max Linnander and Cole Bentley for their assistance. The authors acknowledge support from the University of California, Office of the President, National Science Foundation (NSF) Fellowship No. 2139319 to Dinulescu and Goetz, and NSF award 1751348 to Visell. Any opinion, findings, and conclusions or recommendations expressed in this material are those of the authors and do not necessarily reflect the views of the NSF.

4.8 Supplementary Materials

4.8.1 Summary Statistics

We compute summary statistics across our dataset, presented in Table 4.1. Solo accuracy across both experiments is 100 %. Coupled accuracy scores across both experiments vary between 85 % and 100 % ($\text{Mean}_{P-I} = 97.22\ \%, \text{Mean}_{P-R} = 100\ \%, \text{Mean}_{S-S} = 92.5\ \%$). Completion time in the solo condition ($\text{Mean}_{P-I} = 1.20\ s, \text{Mean}_{P-R} = 0.90\ s$, $\text{Mean}_{S-S} = 1.05\ s$) is between four and seven times faster than the coupled condition in both experiments ($\text{Mean}_{P-I} = 7.78\ s, \text{Mean}_{P-R} = 4.26\ s, \text{Mean}_{S-S} = 4.25\ s$).

Table 4.1: Summary Statistics of Accuracy and Completion Time Metrics for Peg Insert (P-I), Peg-Removal (P-R), and Shape Stacking (S-S)

Task/Metric	**Condition**	**Mean**	**Std Dev**	**Min**	**Max**	**Median**	**Mode**
P-I: Acc	Solo	100.00	0.00	100.00	100.00	100.00	100.00
	Coupled	97.22	5.56	88.89	100.00	100.00	100.00
P-I: CT	Solo	1.20	0.13	1.06	1.46	1.18	1.06
	Coupled	7.78	0.77	7.20	8.89	7.51	7.20
P-R: Acc	Solo	100.00	0.00	100.00	100.00	100.00	100.00
	Coupled	100.00	0.00	100.00	100.00	100.00	100.00
P-R: CT	Solo	0.90	0.23	0.73	1.40	0.81	0.73
	Coupled	4.26	1.16	3.35	5.96	3.87	3.35
S-S: Acc	Solo	100.00	0.00	100.00	100.00	100.00	100.00
	Coupled	92.50	5.00	85.00	95.00	95.00	95.00
S-S: CT	Solo	1.05	0.12	0.85	1.20	1.02	0.85
	Coupled	4.25	0.55	3.79	4.92	4.14	3.79

4.8.2 Statistical Analysis

Comprehensive results from our Welch t-tests for significance, with post-hoc Holm-Bonferroni corrections for multiple comparisons, are presented in Table 4.1.

Table 4.2: Welch T-Test Results with Holm-Bonferroni Correction for Solo versus Coupled Groups

Metric	***t*-statistic**	***p*-adj (Holm)**	**Sig**
P-I: Acc	1.000	0.782	
P-I: CT	−16.989	0.002	**
P-R: Acc	NaN	NaN	
P-R: CT	−5.721	0.038	*
S-S: Acc	3.000	0.173	
S-S: CT	−11.403	0.006	**

Significance codes: * $p < 0.05$, ** $p < 0.01$

Chapter 5

Haptic Shape Perception via Guided, Whole-Hand Exploratory Movements

The motivation and design of the inter-manual exoskeleton, presented in the previous chapter, was to clarify unexamined questions about haptic perception. Perception via touch is highly refined, able to readily discriminate numerous objects and their properties without sight. It is well established that the perception of haptic object properties relies on exploratory procedures – deliberate patterns of hand movements that are specifically employed to elicit salient cues about the desired property. Prior accounts characterize these exploratory procedures as deliberate hand movements, but the question of whether they need to be deliberate has not been assessed. This chapter exploits the unique shared haptic instrument of the previous chapter to investigate haptic shape discrimination under guided multi-finger movements and compare it to discrimination performance using self-directed movements. Here, shared physical haptic interactions, facilitated by inter-manual multi-finger guidance, are used to investigate scientific questions about the human haptic sense.

The contents of this chapter are in preparation:

Stejara Dinulescu, Neeli Tummala, Serena Lee, Yon Visell, "Haptic Shape Perception via Guided, Whole-Hand Exploratory Movements," *In preparation.*

5.1 Abstract

Haptic object perception relies on exploratory procedures – patterns of hand movements that depend on the haptic attributes of interest. Here, we examined how haptic shape discrimination varies when hand movements are self-directed or guided by another person. Guidance is facilitated by an inter-manual exoskeleton that couples two people's hands together, enabling one person to guide the multi-finger movements of another person. We conduct a two-alternative forced-choice perceptual discrimination task in which participants judge whether a pair of stimuli (3D-printed bell peppers) are the same object, regardless of their orientations. We found that when hand movements are guided, rather than self-directed, participants were nonetheless able to discriminate complex haptic shapes with 68% accuracy ($d' = 0.94$). When exploratory movements were self-directed, rather than guided, perceptual discrimination was better (80% accuracy, $d' = 1.73$). Our results suggest that although performance is higher during self-directed movements, guided movements nevertheless support complex three-dimensional object perception. While haptic object perception relies on exploratory procedures, our results suggest that the hand movements need not always be deliberate, although further research is warranted.

5.2 Introduction

The human hand is both a refined, sensitive organ and a highly dexterous, prehensile manipulator; the human haptic sense is thus a result of inherent couplings between sensory and motor systems [12, 18, 17]. When interacting with objects, neural signals from mechanoreceptors in the skin (cutaneous sensation) and kinesthetic receptors in the joints and muscles (proprioception) inform our subsequent hand movements [31, 14, 179]. These hand movements, referred to as "exploratory procedures," vary with the sensory input and the type of tactile information desired [20, 21]. While it has been well-established that our remarkable ability to perceive haptic object properties is a result of such deliberate hand movements, it remains unclear whether exploratory procedures must be self-directed to be haptically informative. Here, we investigate how haptic shape discrimination abilities are altered when hand movements are guided by another person.

During self-directed haptic exploration, the central nervous system employs internal prediction models of the sensory consequences of a motor command, referred to as efference copies [180, 38, 37, 16]. These efference copies are used to compare the predicted sensory feedback (movement reafference) to actual sensory feedback (exafference) in order to inform subsequent motor commands. When hand movements are guided, as with the inter-manual coupling method employed in this work, these internal predictive models are disrupted, potentially altering the ability to perceive object properties.

Several prior studies have examined motor coordination and hand function during haptic interactions that involve digitally anesthetising the fingers [41, 38, 178]. Here, we sought to investigate haptic perception under conditions where movements are not self-directed. In this case, the hand must still retain the ability to feel through the skin. Similar considerations have motivated other researchers to develop dual-user platforms that physically decouple outgoing motor commands from incoming sensory feedback. These devices enable one person to guide the finger, hand, or arm trajectories of another person, enabling the study of haptic perception under guided (i.e., passive movement) conditions. For example, Froese et al. [181] demonstrated that guided users can accurately perceive the length of virtual two-dimensional objects when their hand trajectory is reproduced from another person's deliberate, exploratory movements. The successful extraction of spatial features, such as distance, during guided movement suggests that haptic information remains accessible even without direct and deliberate motor control of the hand.

As another example, Richardson and Symmons developed the Tactile Display System (TDS), which imposed movements on a passive finger during exploration of embossed line drawings. Their results suggest that aspects of perception are conserved when movements are imposed, rather than self-directed [55, 56, 57]. However, the experiment involved a narrow task performed with a single digit, and involved the perception of two-dimensional patterns. Notably, the perception of two-dimensional shape via the finger is markedly less accurate than three dimensional object perception with the hand. Thus, it is unclear to what extent the results extend to multi-finger haptic perception of three-dimensional objects.

However, there remains a need to investigate the impact of guided whole-hand movements (movements of the fingers and thumb) on haptic discrimination of three-dimensional objects and their properties. This has proven challenging to date, due to the significant kinematic complexity of the human hand. Traditional methodologies for guiding the whole-hand movements of another person would require complex multi-digit coordination from sophisticated robotic devices and corresponding control algorithms [86, 87]. We circumvent this complexity by using the inter-manual coupling device, developed by Dinulescu et al. [182], that enables one person to guide the whole-hand (finger and thumb) movements of another person through the use of passive mechanical linkages. By removing the ability to self-direct multi-digit hand movements, we can investigate haptic shape perception of complex, three-dimensional objects under such guided conditions.

5.2.1 Contributions

We present the first experimental investigation of haptic perception of three-dimensional objects under conditions of guided multi-finger movements (i.e., exploratory procedures are externally driven and not self-directed). We employ the exoskeleton device presented by Dinulescu et al. [182], which enables one hand to guide the finger and thumb postures of another hand.

We show that in conditions where hand movements are guided in perceiving object shape, haptic discrimination accuracy is above chance. Furthermore, we show that haptic discrimination accuracy and discrimination sensitivity (d') are lower when hand movements are guided than when hand movements are self-directed. We observe no difference in response bias (c) between guided and self-directed movement conditions. These results indicate that guided hand movements can still inform the perceptual discrimination of three-dimensional object shape, even when the surface features of the objects are quite complex, although self-directed hand movements yield greater discrimination accuracies.

5.3 Methods

The experiment is based on pairwise haptic shape discrimination and was conducted in both guided and self-directed conditions, as described below. The experimental design and shape set were derived from prior studies [5, 7, 6], adapted to the unique conditions probed here.

5.3.1 Subjects

We recruited 6 participant pairs (12 total) for the Coupled-Guided Exploration (C-G) condition. Participant pairs were matched based on hand size, where phalanx lengths

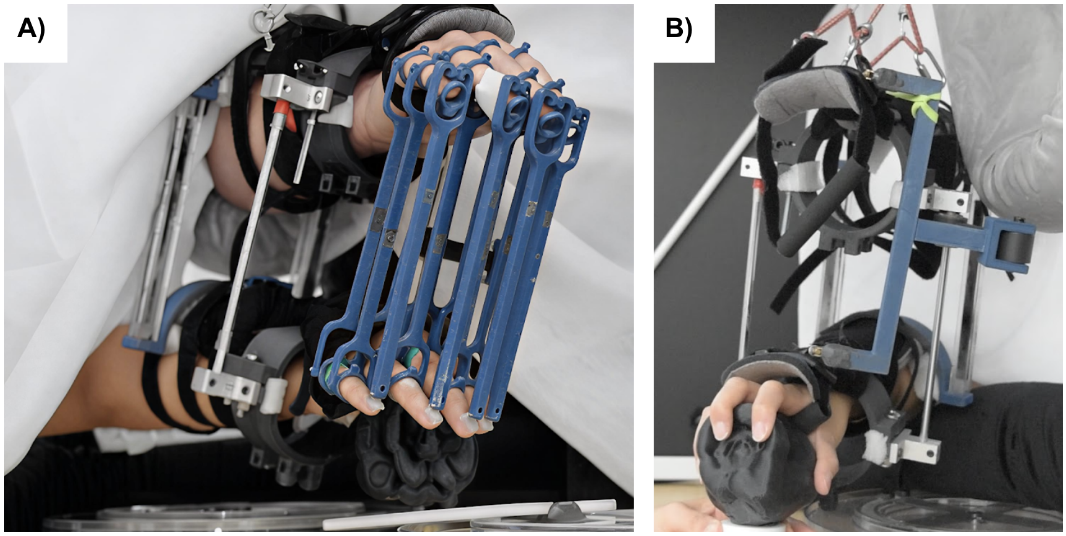

Figure 5.1: **Experimental Conditions:** A) The coupled-guided exploration condition (i.e., C-G) is performed by two participants wearing the inter-manual exoskeleton device. Participants in this condition are paired based on closely matched finger lengths and widths. During a two-alternative forced-choice (2AFC) task, the guided (bottom hand) participant does not have vision of the task and must respond whether two objects are the same or different, regardless of object orientation. In contrast, the guiding (top) hand can see the objects and is tasked with directly moving the responding (guided) hand's fingers to explore the surface of the objects. B) The solo–controlled (S-C) condition is performed by individual participants who can self-direct their hand movements during the same 2AFC task. Here, participants wear the coupling brace component of the exoskeleton device to control for occlusion and wrist restriction, without being coupled to another person.

differed by no more than 10 mm per participant. Participant pairs wore the inter-manual exoskeleton from Dinulescu et al. [182], which enabled one participant (top hand) to guide the hand movements of the other (bottom hand), as depicted in Fig. 5.1A. Two participant pairs were removed from data analysis due to adhesion issues of the device with the thumb and pinky (n = 1) and a mechanical mismatch of posture in the thumb mechanism due to mismatched distal phalanx morphology (n = 1). This resulted in a total of 4 coupled pairs used in data analysis for the C-G condition (mean age = 23.75, SD = 3.012, 4 female and 4 male participants).

We additionally recruited 7 participants for the Solo-Controlled (S-C) condition (mean age = 24.714, SD = 4.716, 5 female and 2 male participants). Here, participants wore the wrist/forearm brace component of the inter-manual exoskeleton to control for any potential restrictions from the device (i.e., wrist flexion/extension is prevented and the palm is partially occluded). Participants in this condition self-directed their hand movements, as depicted in Fig. 5.1B.

All participants were naive to the experiment and gave their informed consent before participation. The study was conducted with approval from the Institutional Review Board of the University of California, Santa Barbara. No participants reported difficulties with sensory or motor hand function.

5.3.2 Stimuli

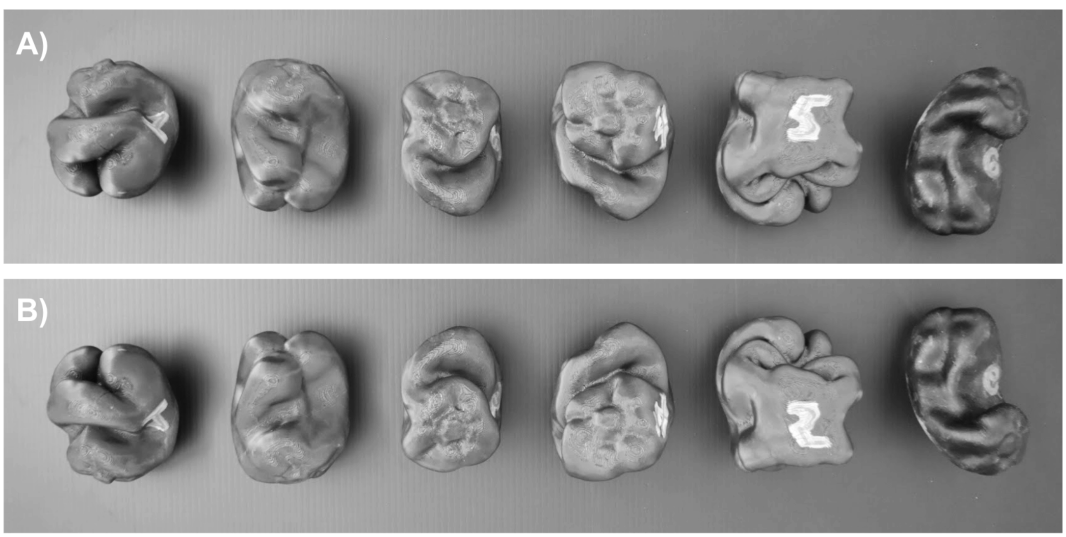

Figure 5.2: **Haptic Stimuli:** The stimuli used in this experiment are 3D-printed bell peppers. We use the first 6 out of the 12 original set of bell peppers used in prior experiments [2, 3, 4, 5, 6, 7] and created by Norman et. al [8]. A) The 6 bell peppers, presented in the first orientation condition (stem facing away from the participant). B) The 6 bell peppers, presented in the second orientation condition (stem facing towards the participant).

The stimuli were a subset of the first six bell peppers from the original set of twelve developed by Norman et al. [8] for visuohaptic perception of object shape and used in several subsequent research experiments [2, 3, 4, 5, 6, 7]. Each of the six bell pepper stimuli were unique in size and exact shape (surface features). Two copies of each of the six stimuli (12 shapes in total) were 3D-printed with PLA using a Bambu X1 Carbon 3D printer, after being scaled to 80% of their original size. Small magnets and a circular platform were attached to the bottoms of the stimuli, such that they could be temporarily fixed to a flat magnetized surface during the duration of a trial and replaced for the next trial. The stimuli, depicted in Fig. 5.2, were presented in one of two possible orientations (stem facing towards or away from the participant).

Stimuli were occluded from view of responding participants using a curtain in all conditions. In the coupled condition (C-G, with device), the guiding hand had vision of the haptic stimuli, but the guided hand did not.

5.3.3 Device

The guided exploration (C-G) experimental group employed the inter-manual coupling exoskeleton developed by Dinulescu et al.; we briefly describe the design of the device here, but for more comprehensive description, refer to [182].

The device (shown in Fig. 5.3) was designed such that two participants' right hands were arranged in a vertical configuration, separated by a distance of 200 mm. The exoskeleton consists of three main components: wrist/forearm coupling (rigid linkages), finger couplings (rotary joint linkages), and thumb coupling (universal joints, two hinges, and a sliding mechanism). The plastic links for the digits, as well as the wrist and forearm bracelet fixtures, were 3D-printed with carbon-fiber reinforced PETG, using a Bambu X1 Carbon with AMS. Linear motion shafts (McMaster Carr) were used between the 3D-printed wrist bracelets for the sliding component of the thumb coupling mechanism. Laser-cut acrylic was used as the final rigid coupling link between the forearms.

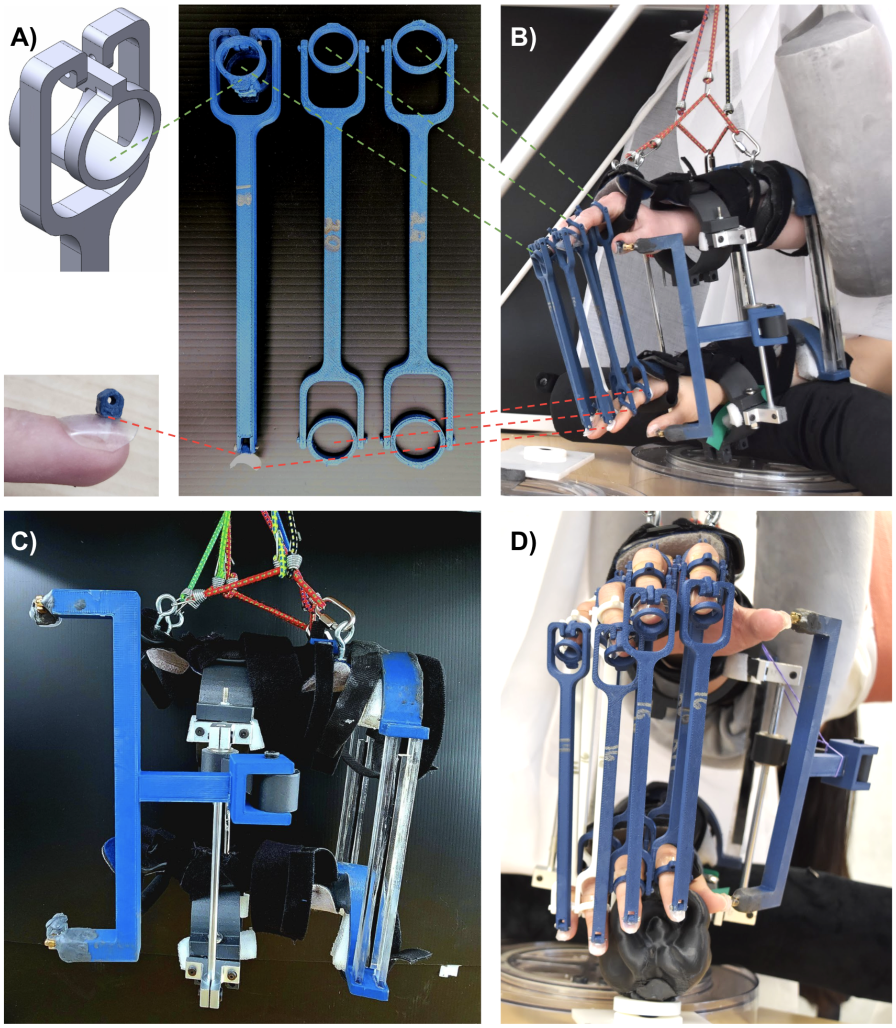

Figure 5.3: **Guidance Device:** The inter-manual exoskeleton used in the Coupled-Guided Exploration (i.e., C-G) condition, enabling one person (top hand) to guide the hand movements of another person (bottom hand). A) The coupling linkage mechanism for the non-thumb digits. The proximal and medial phalanges of two people are coupled together by the ring-linkages, and the distal phalanges are coupled via a cage-structure for the guiding hand and a fake nail with a rotary joint for the guided hand, leaving the fingerpads free for exploration. B) The coupling linkages on the fingers form a serial chain of four-bar parallelogram mechanisms that transfer finger extension and flexion from guiding to guided hands. C) The rigid wrist and forearm coupling structure, as well as the thumb coupling mechanism (double-hinge mechanism, terminating in two universal joints). D) The full hand coupling mechanism enables the transfer of whole hand movements, from guiding (top) to guided (bottom) hands during haptic object exploration.

The wrist and forearm coupling mechanism operates as a base constraint, fixing the hands of both participants at a vertical distance of 200 mm. This enables the forearms and palms of each participant to move as one rigid body. The coupling mechanism consists of two braces (Dorsal Carpal Tunnel Splint made by RCAI) that are coupled via 3D-printed bracelet components, laser cut acrylic links, and linear motion shafts. The mechanism prevents wrist extension and flexion and supports the forearms of both participants. Velcro attachments fix the coupling exoskeleton to the forearms and palms of each participant. This component of the mechanism is depicted in Fig. 5.3C.

The device further employs rigid links with rotary joints (Fig. 5.3A) to reproduce extension, flexion, abduction, and adduction movements of the non-thumb digits. To couple the medial and proximal phalanges, plastic links (length 200 mm, 1-DOF rotation per phalanx) were attached to the fingers using double-sided adhesive. To couple the distal phalanges, a fake nail, UV-cured with manicure gel, was temporarily attached to the guided participant's fingernail, leaving the fingerpad free, and the guiding finger was fit into a "cage"-like bracket and secured with double-sided adhesive. When all finger linkages are attached to distal, medial, and proximal phalanges, the coupling mechanism forms a kinematic chain of four-bar parallelogram linkage mechanisms, in series, as depicted in Fig. 5.3B.

The thumb coupling mechanism (Fig. 5.3C) employs two universal joints and a double-hinge-slider design to restrict position of the guided thumb relative to the guiding thumb (orientation matching is not a fixed constraint). The double-hinge-slider mechanism, originating from the leftmost linear motion shaft at the wrist, terminates in universal joints attached to fake nails, which are fixed to both thumb nails via UV-cured manicure gel.

Attaching the exoskeleton device to the hands of both participants took between 30 and 45 minutes for all five fingers; the complete exoskeleton, coupling the right hands of two participants, is shown in Fig. 5.3D. To avoid encumbering participants with holding the weight of the apparatus and hands in a raised position, while still accommodating movement, the weight of the system was supported from above using elastic bands attached to a metal frame surrounding the experimental region. The forearms of each participant were supported via small cushions.

5.3.4 Procedure

We investigated haptic discrimination of object shape using a two-alternative forced-choice (2AFC) task. Two haptic stimuli (A and B) were presented for 5 seconds each, separated by an inter-stimulus interval (ISI) of 3 seconds. Responding participants, who did not have vision of the task, then discriminated whether stimuli A and B were the "same" (i.e., exact match of object shape and size, regardless of orientation) or "different" (i.e., stimuli A and B were unique shapes, regardless of orientation). In the guided condition (C-G), guiding hand participants were asked to move their hands in the same manner as if they were the ones feeling the objects, whereas in the solo condition (S-C), participants were asked to freely explore the objects.

Each participant (S-C) or participant pair (C-G) performed 48 shape discrimination trials in the experiment (24 "same" trials and 24 "different" trials). Within the 24 "same" trials, 12 stimuli were presented with the same orientation (Same/Same category) and 12 trials were presented with different orientations (Same/Dif category). The same can be seen for the 24 "different" trials, where 12 trials were presented with same orientations (Dif/Same category) and 12 trials were presented with different orientations (Dif/Dif category). The 48 trials were presented in a random order for each participant or participant pair.

5.3.5 Captured and Computed Metrics

We captured two metrics in each trial: response accuracy (either 0 for incorrect or 1 for correct) and confidence in perceptual judgment (continuous, on a scale of 0-100%). The main analysis for this work concerns response accuracy; analyses for confidence judgments can be found in the supplementary material.

From per-trial accuracy scores, we computed discrimination sensitivity (d'), a standard metric used in signal detection theory that, in our case, quantifies a participant's ability to distinguish stimuli A and B as either "same" or "different." We further computed response bias (c), which indicates whether a participant's response was biased towards "same" ($c > 0$) or "different" ($c < 0$).

5.3.6 Primary Statistical Analysis

5.3.6.1 Discrimination Accuracy

Statistical testing was completed with Matlab R2025b and the Statistics and Machine Learning toolkit. Our main hypotheses for captured accuracy metrics across Solo-Controlled (S-C) and Coupled-Guided (C-G) conditions were as follows:

- Accuracy in the solo-controlled (S-C) condition is greater than chance (50%). $H_0 : P_{S-C} = 0.5$.
- Accuracy in the coupled-guided exploration (C-G) condition is greater than chance (50%). $H_0 : P_{C-G} = 0.5$.
- Accuracy in the C-G condition is not significantly different from the S-C condition. $H_0 : P_{S-C} = P_{C-G}$.

We fit a generalized linear mixed effects (GLME) model with a binomial error distribution and a logit link on per-trial accuracy data. Condition (S-C or C-G) and Category

(Same/Same, Same/Dif, Dif/Same, or Dif/Dif) were included as fixed effects, and Subject (i.e a unique participant or participant pair) was included as a random effect.

To test if discrimination accuracy in S-C or C-G conditions was significantly different from chance ($H_0 : P_{S-C} = 0.5, \quad P_{C-G} = 0.5$), we performed two F-tests on a linear contrast of the GLME model coefficients. Because the GLME utilized a logit link function, the null hypothesis was evaluated by testing the combined estimate of the intercept and the condition coefficient (-1 for S-C, 1 for C-G) against a logit-transformed chance value ($\text{logit}(0.5) = 0$). This contrast allowed for a post-hoc assessment of absolute performance within the specific experimental condition, accounting for the random-effects structure of the model.

We further conducted a one-way ANOVA to compare discrimination accuracy across S-C and C-G groups. The F-statistic was calculated using the residual mean square error, with $df_{\text{residual}} = n - m$, where n is the total number of observations and m is the total number of groups. Assumptions of normality and homogeneity of variance were verified.

5.3.6.2 Discrimination Sensitivity (d') and Response Bias (c)

We investigated whether discrimination sensitivity (d') and response bias (c) were significantly different in the guided movement condition (C-G) than the self-directed movement condition (S-C). Our hypotheses are below:

- Mean d' values in the S-C condition do not differ significantly from mean d' values in the C-G condition ($H_0 : \mu^{d'}_{S-C} = \mu^{d'}_{C-G}$).
- Mean c values in the S-C condition do not differ significantly from mean c values in the C-G condition ($H_0 : \mu^{c}_{S-C} = \mu^{c}_{C-G}$).

To test the above hypotheses, we performed two Mann-Whitney U-Tests on discrimination sensitivity (d') and response bias (c) metrics between S-C and C-G conditions.

We further computed the effect size r from the following equation:

$$r = 1 - \frac{2U_{stat}}{n_1 n_2} \tag{5.1}$$

5.3.7 Subjective Questionnaire

Following the experiment, participants in the C-G condition completed a 16-item subjective questionnaire comprising both 10-point Likert scale responses and free responses (presented in Table 5.1). Some questions were tailored to the specific role of either the guiding or guided hand.

The first four questions assessed comfort of the device and the mental effort required for the task, replicating metrics used in our prior work [182]. Based on previous observations of upper-limb fatigue in the guiding participants, we integrated a sling for mitigating shoulder fatigue for the guiding hand, and a dedicated arm rest for mitigating forearm fatigue for the guided hand, in this experiment. Comfort and mental effort were evaluated on scales ranging from 1, representing completely uncomfortable or not mentally challenging, to 10, representing extremely comfortable or extremely challenging.

Questions 5 through 7 capture distinct subjective experiences of each role. For guided participants, these items evaluated the extent to which the device-mediated guidance facilitated or hindered their perceptual judgments, on a scale from hindered greatly (1) to extremely helpful (10). Conversely, the questions for guiding participants evaluated their subjective confidence in the manual guidance they provided to their partner, on a scale from not confident at all (1) to extremely confident (10).

The final group of questions (8-16) employed a consistent Likert scale, where 1 represented completely disagree and 10 represented completely agree. Questions 8 through 10 investigated the perceived origin of movement and the sense of causation for both guiding

Table 5.1: Post-Study Subjective Questionnaire (C-G Condition Only)

Metric	**Participant**	**Question**	**Method**
Comfort	All	1. How comfortable was the device attached to your hand during the experiment?	Likert (1-10)
		2. Please elaborate on your comfort level below:	Free Response
Mental effort	All	3. How much mental effort did you have to engage in when completing the tasks with the device?	Likert (1-10)
		4. Please elaborate on your mental effort below:	Free Response
Guidance	Guided	5. To what extent did the guidance of your hand help or hinder your judgments?	Likert (1-10)
		6. Please elaborate below:	Free response
		7. Please provide any other comments about what it felt like for your partner to guide your hand movements while you were trying to perceive the objects:	Free response
Guidance	Guiding	5. How confident were you in guiding your partner's hand so that they could discriminate the objects?	Likert (1-10)
		6. Please elaborate on your confidence level during guidance below:	Free response
		7. Please provide any comments about what it felt like for you to guide your partner's hand movements in feeling the objects, without being able to feel the object yourself:	Free Response
Embodiment	All	8. It felt like my hand movements were caused by my partner completely	Likert (1-10)
		9. It felt like my hand movements were caused by me completely	Likert (1-10)
		10. My hand movements were influencing my partner's hand movements	Likert (1-10)
		11. It felt as if my partner's hand movements became my own hand movements	Likert (1-10)
	Guided	12. Having my partner guide my hand felt natural, as if I were moving my own hand	Likert (1-10)
	Guiding	12. Guiding my partner's hand felt natural, as if I were moving my own hand	Likert (1-10)
		13. I felt as if my sense of where my hand was extended beyond my own and into my partner's hand	Likert (1-10)
		14. It seemed as if I might have more than one right hand	Likert (1-10)
		15. I felt out of my body at some point during the experiment	Likert (1-10)
		16. It felt like I was touching the objects	Likert (1-10)

and guided participants. It was hypothesized that results for self-causation in question 8 would be high for the guiding hand and low for the guided hand, while questions 9 and 10 regarding external causation would show the inverse. Finally, questions 11-16 were adapted from established frameworks such as the Embodiment Questionnaire (EQ), which investigates sensations of ownership, location, and agency of a rubber hand during the rubber hand illusion [183], and the Virtual Embodiment Questionnaire (VEQ), used to assess sensations of virtual embodiment with an avatar through three factors (ownership perception, agency perception, and change in body schema) [184]. These items served as an exploratory investigation into how guided hand movements may affect sensations of body ownership and motor agency over one's movements.

5.3.8 Supplemental Analyses

Additional analyses are reported in the supplementary material. This includes 1) comprehensive summary statistics of our captured data for accuracy and confidence judgments (Table 5.2); 2) overall mean accuracy and confidence judgments per participant, as well as separated by category (presented in Fig. 5.7); 3) comprehensive analysis of GLME models across solo and coupled conditions, including interaction effects for Condition x Category (Tables 5.3, 5.5) and post-hoc pairwise comparisons (Tables 5.4, 5.6); and 4) a linear mixed effects (LME) model analysis for confidence judgments across solo and coupled conditions, including interaction effects for Condition x Category (Table 5.7) and post-hoc pairwise comparisons (Table 5.8).

5.4 Results

5.4.1 Discrimination Accuracy

Mean shape discrimination accuracy in the solo (S-C) and guided (C-G) condition was 80.4% and 68.2%, respectively. Accuracy was significantly greater in the solo condition than the coupled condition (GLME: $p = 0.007, F(1, 520) = 7.3$). Accuracy in both conditions was significantly greater than chance performance of 50% (S-C: $p < 10^{-5}, F(1, 520) = 98$, C-G: $p < 10^{-5}, F(1, 520) = 23.3$).

5.4.2 Discrimination Sensitivity (d') and Response Bias (c)

Results for S-C and C-G discrimination sensitivity (d') and response bias (c) metrics are depicted in Fig. 5.4. Mean d' values in the solo (S-C) and coupled (C-G) conditions were 1.734 and 0.94, respectively. These differences were significant (Mann-Whitney: $p = 0.047, U = 3.0, r = 0.786$). In the coupled condition, d' was approximately one standard deviation from chance; in the solo condition, it was over 1.5 standard deviations above chance.

Mean c values in the solo (S-C) and coupled (C-G) conditions were -0.027 and 0.131, respectively. Response bias in the solo condition skewed slightly negative (negligible tendency towards responding “different”) and in the coupled condition skewed slightly positive (negligible tendency towards responding “same”). These differences were not significant (Mann-Whitney: $p = 0.636, U = 17.0, r = 0.214$).

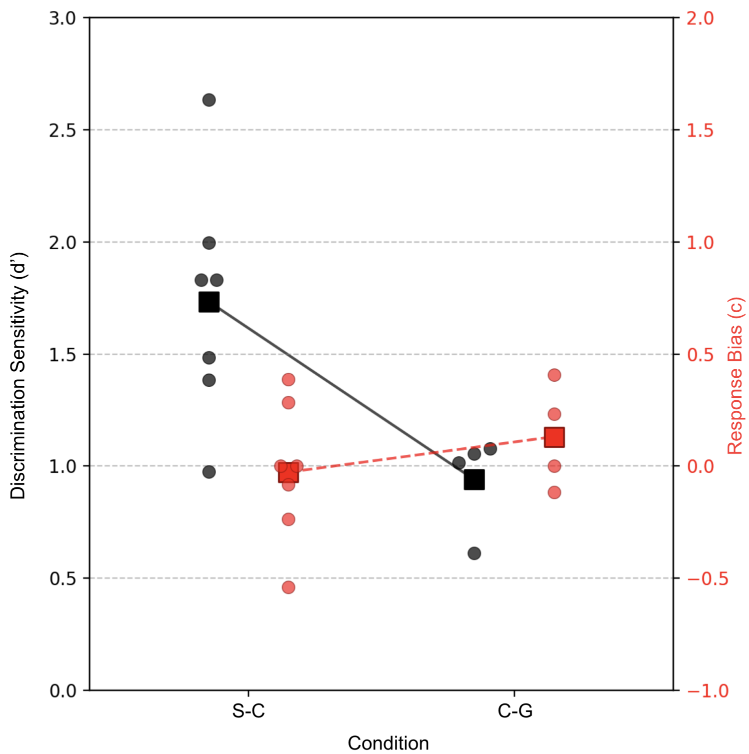

Figure 5.4: **Discrimination Sensitivity (d') and Response Bias (c) – S-C and C-G :** We compute mean discrimination sensitivity (d') and mean response bias (c) metrics per participant, as well as across each group. Here, discrimination sensitivity is higher in the solo-controlled (n=7) versus coupled-guided (n=4) conditions. However, coupled-guided discrimination sensitivity remains about one standard deviation higher than chance accuracy. Mean response bias between solo and coupled conditions is similar.

5.4.3 Subjective Questionnaire

5.4.3.1 Likert-Scale Questions

Participant responses to questions 1, 3, 5, and 8-16 (all Likert responses, scale 1-10) are depicted in Fig. 5.5.

For question 1 (comfort of the exoskeleton), both guided and guiding participants rated the device as highly comfortable ($\text{Mean}_{\text{guided}} = 8.50, \text{SD}_{\text{guided}} = 0.577, \text{Mean}_{\text{guiding}} = 7.75, \text{SD}_{\text{guiding}} = 0.957$). For question 2 (mental effort during the task), guided participants rated their effort as moderately significant ($\text{Mean}_{\text{guided}} = 7.00, \text{SD}_{\text{guided}} =$

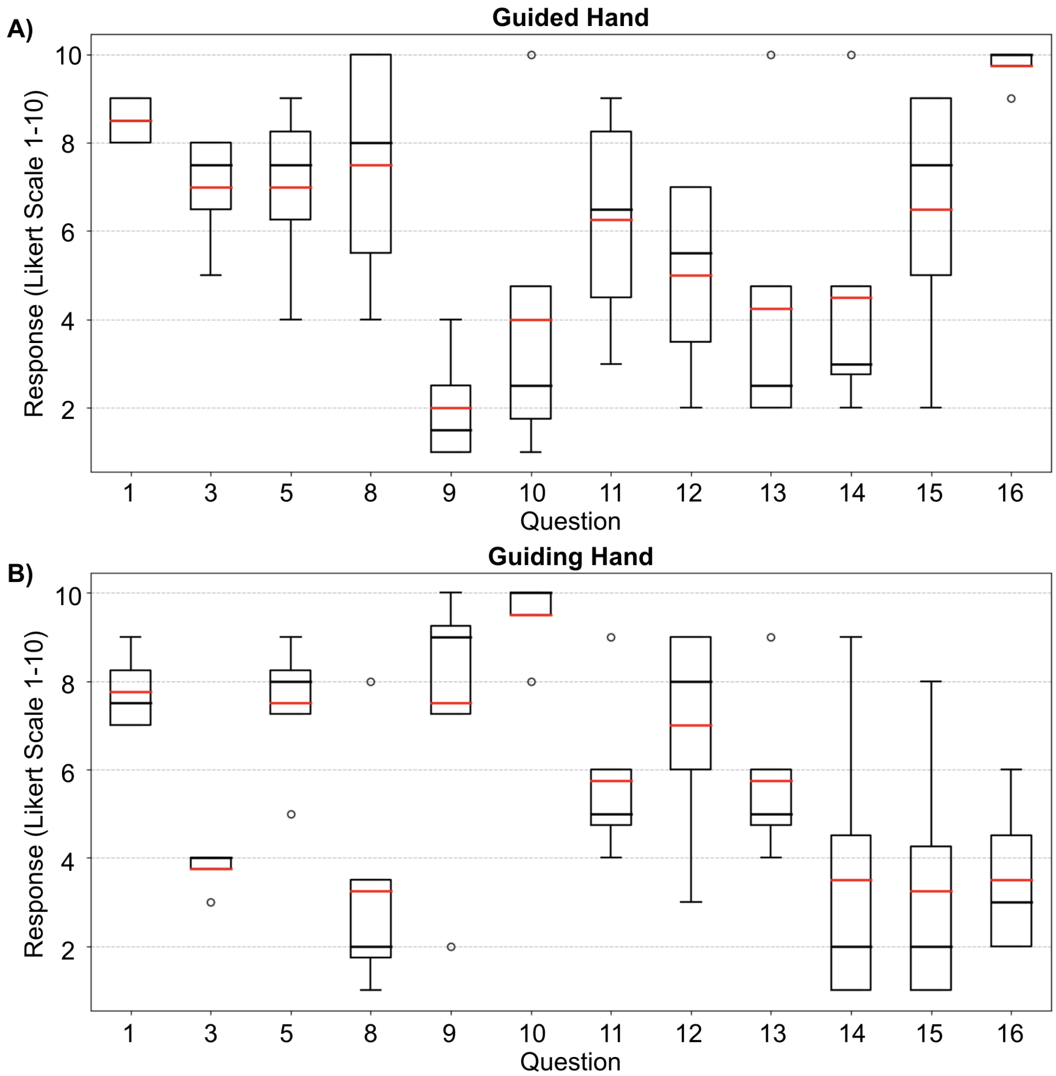

Figure 5.5: **Questionnaire responses (Likert scale):** We present results from Likert scale responses on our subjective questionnaire for the coupled-guided exploration condition, with guided hand results shown in A) and guiding hand shown presented in B). Question 1 represents comfort of the exoskeleton; question 3 represents mental effort during the task; question 5 assesses perceived effects of either guiding movements or being guided; questions 8-10 represent experiences of origination of hand movements; questions 11-16 are exploratory and ask about feelings of body ownership and agency during the experiment.

1.414, whereas guiding participants rated their effort as moderately low ($\text{Mean}_{\text{guiding}} = 3.75, \text{SD}_{\text{guiding}} = 0.50$).

For question 5 (guidance helped or hindered), administered to the guided hand participants, the received guidance was rated as moderately helpful for perceptual judgments ($\text{Mean}_{\text{guided}} = 7.00, \text{SD}_{\text{guided}} = 2.161$). For question 5 (confidence in guidance), administered to the guiding hand, most participants were moderately confident in their provided guidance ($\text{Mean}_{\text{guiding}} = 7.50, \text{SD}_{\text{guiding}} = 1.732$), with one outlier observed (response of 5).

For question 8 (hand movements were caused by my partner completely), guided participants rated this as moderately high ($\text{Mean}_{\text{guided}} = 7.50, \text{SD}_{\text{guided}} = 3.00$) and guiding participants rated this as moderately low ($\text{Mean}_{\text{guiding}} = 3.25, \text{SD}_{\text{guiding}} = 3.202$), as expected. However, there was an outlier data point in the guiding hand (response of 8), which we interpret to be a misunderstanding of the Likert scale response or phrasing of the question.

For question 9 (hand movements were caused by me completely), guided participant responses were very low ($\text{Mean}_{\text{guided}} = 2.00, \text{SD}_{\text{guided}} = 1.414$). On the other hand, guiding participant responses were moderately high ($\text{Mean}_{\text{guiding}} = 7.50, \text{SD}_{\text{guiding}} = 3.697$). Here, there is another outlier point (response of 2), which we interpret again to be a misunderstanding of the Likert scale response or phrasing of the question.

For question 10 (my hand movements were influencing my partner's hand movements), guided participant responses were moderately low ($\text{Mean}_{\text{guided}} = 4.00, \text{SD}_{\text{guided}} = 4.083$), with an outlier observed (response = 10), which we again attribute to either a misinterpretation of the question or the Likert scale. Guiding participant responses were very high ($\text{Mean}_{\text{guiding}} = 9.50, \text{SD}_{\text{guiding}} = 1.00$), as expected.

The results from questions 8-10, when removing outlier responses, indicate that the inter-manual exoskeleton is performing as intended – enabling one person to guide the hand movements of another person.

For question 11 (it felt as if my partner's hand movements became my own hand movements), both guided and guiding participants slightly agreed ($\text{Mean}_{\text{guided}} = 6.25, \text{SD}_{\text{guided}} =$

$2.753, \mathrm{Mean}_{\mathrm{guiding}} = 5.75, \mathrm{SD}_{\mathrm{guiding}} = 2.217$). This indicates that there was some blending of sensations of agency (i.e., control) over the performed hand movements, which occurs via the haptic system for the guided hand, and via the visual system for the guiding hand.

For question 12 (either providing or receiving guidance felt natural, like moving my own hand), guided participants were neutral in their response for receiving guidance ($\mathrm{Mean}_{\mathrm{guided}} = 5.00, \mathrm{SD}_{\mathrm{guided}} = 2.449$). On the other hand, guiding participants rated the sensation of providing guidance as moderately natural ($\mathrm{Mean}_{\mathrm{guiding}} = 7.00, \mathrm{SD}_{\mathrm{guiding}} = 2.828$). This indicates that the experience felt more natural to guiding hand participants than guided hand participants.

For question 13 (sense of hand extended into partner's hand), guided participants slightly disagreed ($\mathrm{Mean}_{\mathrm{guided}} = 4.25, \mathrm{SD}_{\mathrm{guided}} = 3.862$) and guiding participants slightly agreed ($\mathrm{Mean}_{\mathrm{guiding}} = 5.75, \mathrm{SD}_{\mathrm{guiding}} = 2.217$). There was one outlier in both conditions with high ratings (guiding = 9, guided = 10). Our results indicate that some participants may experience a slight alteration of body ownership during the coupling experience.

For question 14 (sense of having more than one right hand), both guiding and guided participants slightly disagreed ($\mathrm{Mean}_{\mathrm{guided}} = 4.50, \mathrm{SD}_{\mathrm{guided}} = 3.697, \mathrm{Mean}_{\mathrm{guiding}} = 3.50, \mathrm{SD}_{\mathrm{guiding}} = 3.786$). This indicates that our participants (both guiding and guided) did not experience the sensation of having more than two hands.

For question 15 (I felt out of my body at some point), guided participants responded with moderately agree ($\mathrm{Mean}_{\mathrm{guided}} = 6.50, \mathrm{SD}_{\mathrm{guided}} = 3.317$) and guiding participants responded with moderately disagree ($\mathrm{Mean}_{\mathrm{guiding}} = 3.25, \mathrm{SD}_{\mathrm{guiding}} = 3.304$). This indicates that guided participants may feel a slight change of their body awareness.

For question 16 (It felt like I was touching the objects), guided participants responded with completely agree ($\mathrm{Mean}_{\mathrm{guided}} = 9.75, \mathrm{SD}_{\mathrm{guided}} = 0.50$), and guiding participants responded with moderately disagree ($\mathrm{Mean}_{\mathrm{guiding}} = 3.50, \mathrm{SD}_{\mathrm{guiding}} = 1.914$). These expected results indicate that cutaneous sensation of the objects was intact for guided participants but not for guiding participants, which is the intended experience via the inter-manual exoskeleton.

5.4.3.2 Free Response

Both guided and guiding participants' free responses to comfort of the exoskeleton (question 2) indicated that the device was generally comfortable. Some participants (n = 2) noted slight fatigue and discomfort in the upper arm/shoulder over time, as a result of maintaining a similar posture. Some participants (n = 3) described the sensation as “weird” or “unfamiliar” but not uncomfortable. Some participants (n = 4) noted slight pulling sensations at the thumb nail that were mildly uncomfortable at times, but tolerable, due to the configuration of the thumb coupling mechanism.

In response to their mental effort during the task (question 4), guided hand participants reported a significant amount of concentration and mental effort needed to perform the task. They had to create a “mental map” of the objects based on the guided movements and incoming cutaneous sensations, and they needed to retain this in working memory when feeling the comparison stimulus. One guided participant described the inability to fully explore the object by themselves as hindering their judgments, as they required more effort and focus to perform the task.

In response to their mental effort during the task (question 4), guiding hand participants reported higher mental effort at the beginning of the task, as it took a couple of trials to understand the range of motion of the device and how to properly convey distinguishing features in the allotted time. However, all participants (n = 4) reported that the mental effort decreased to minimal once they adjusted to movements with the device.

In response to question 6, half of the guided participants (n = 2) responded that the guidance was extremely helpful for perceiving the objects, but the other half (n = 2) indicated that it hindered their ability to perceive specific features that they wanted more time to feel. In response to question 6, all guiding hand participants reported high confidence in guiding their partner's hands, especially after they adjusted to the device (n = 4). One participant reported that they felt most confident when the use of the thumb provided the most salient distinguishing features (such as conveying general size of the stimuli).

In response to question 7, most of the guided participants (n = 3) responded that in some cases, the way their partner was moving their hand was counter to the ways in which they would have directed their hand. In response to question 7, one guiding participant described the experience as "like a video game," and another guiding participant described their partner's fingers as "moving in a manner that I'd imagine I would my move fingers if I was under some kind of local anesthetic. Just not fully in control." One participant described it as difficult to guide their partner due to interference from the rings of the medial and proximal phalanges, having to rely on guiding only the fingertips.

5.5 Discussion

It is expected that haptic discrimination accuracy during self-directed hand movements (S-C condition) is above chance. However, our finding that haptic discrimination under guided movement (C-G condition) results in above-chance accuracy indicates that guided movements support haptic perception, which contributes to the understanding of how hand movements inform haptic perception of object properties in three dimensions.

We additionally found that haptic discrimination accuracy and sensitivity under guided movement conditions is lower than self-directed movement conditions. This may indicate that deliberate motor intention and coordination, as seen with self-directed hand movements, may be more helpful when discriminating between objects with complex features, such as the bell pepper stimuli employed in this experiment. Furthermore, it could reflect variability in the guiding movements provided to the guided participant – some guiding participants relied on stroking movements across the surfaces of the object, some guiding participants only directed the bottom hand towards visually distinct features, and some guiding participants attempted to convey general shape to the guided hand by performing enclosure movements, all within a five-second time window.

However, the observed disparities may also be attributed to the mechanical constraints of the inter-manual exoskeleton. The integration of 3D-printed linkages and rings on the medial and proximal phalanges introduces potential occlusion of the skin from receiving cutaneous feedback; in fact, this was reported by participants in the subsequent questionnaire. Furthermore, the increased thickness of the distal phalanges, caused by the fingertip linkages, may alter the effective morphology of the digit, potentially limiting the ability to feel inset topographical features of the stimuli. Despite these potential confounds, the persistence of above-chance performance in the guided movement condition underscores the finding that hand movements need not be self-directed to inform haptic perception.

We did not find any significant differences in response bias (c) between self-directed and guided movement conditions, indicating that the effect of the inter-manual exoskeleton did not affect tendencies towards “same” or “different” responses. This consistency in response bias across groups underscores the device’s ability to be used in perceptual experiments.

Results from our questionnaire indicate that there may be slight changes in body awareness and agency with guided hand participants only (out-of-body sensations, guided movements feeling as if they are self-directed), whereas guiding participants do not experience these changes. These results are all exploratory, and more comprehensive investigations of these experiences should be investigated with other methodologies. However, they present an interesting avenue for investigation into how a shared haptic experience between two people, through inter-manual, multi-finger guidance, can potentially affect aspects of embodiment in the guided hand.

5.6 Conclusion

This study represents the first investigation into the ability to haptically discriminate realistic and complex three-dimensional objects under multi-finger (including thumb), guided movement conditions (i.e., hand movements are not self-directed but are instead guided by another person). Here, an inter-manual exoskeleton [182] enables one person to guide the whole-hand movements of another person. We compared haptic discrimination accuracy, discrimination sensitivity, and response bias on a two-alternative forced choice task between self-directed movement (i.e., solo-controlled, with exoskeleton brace) and guided movement (i.e., coupled-guided exploration, with exoskeleton) conditions. This builds off of prior literature in haptic perception of object properties [20, 21, 18, 53, 52] using similar stimulus sets from prior haptic perception experiments [5, 4, 6].

We show that despite a short time window to explore two objects (5 seconds each), participants in the guided movement condition (with exoskeleton; C-G condition) achieved above-chance discrimination accuracy, but lower discrimination accuracy when compared to solo (self-directed movement) conditions. Corroborating these results, discrimination sensitivity (d') in guided movement conditions were also found to be significantly different from self-directed movement conditions. Taken together, these results indicate that even when finger movements are externally-directed (here, guided by another person), the somatosensory system can effectively extract perceptually salient features of objects with complex geometry. We can further extrapolate that the internal predictive models, usually employed to coordinate and self-direct human hand movements, may not be necessary for haptic perception of exact shape, although further investigation is necessary.

The inter-manual exoskeleton presented here contributes to recent research where haptic guidance devices engage the whole hand, rather than relying on single-digit force-feedback. With the rise of robotic hand exoskeletons for guiding the human hand in haptic manual interactions, our results show promise for the utility of whole-hand guidance devices without significantly impairing haptic perceptual abilities. This is critical for motor learning and rehabilitation, two areas in which such haptic whole-hand exoskeletons show immense promise [174, 144, 117, 92, 171]. We further highlight the effectiveness of such whole-hand haptic devices for guidance in examining underlying mechanisms for sensation and action, building on two-dimensional experimental platforms such as the TDS [55].

Future work will address mechanical limitations of the device, including limits to range of motion and lateral interference from finger linkages, as well as explore haptic perception of other object properties via whole-hand guidance, including weight and compliance, which utilize other manual exploratory procedures. Such future work will further clarify whether exploratory procedures need to be self-directed when perceiving objects and their properties.

5.7 Acknowledgements

The authors thank Max Linnander, Cole Bentley, Gregory Reardon, and Rebecca Reynolds. The authors acknowledge support from the University of California, Office of the President, National Science Foundation (NSF) Fellowship No. 2139319 to Dinulescu, and NSF award 1751348 to Visell. Any opinion, findings, and conclusions or recommendations expressed in this material are those of the authors and do not necessarily reflect the views of the NSF.

5.8 Supplementary Material

5.8.1 Supplemental Experimental Group – Solo (Free Hand)

As a supplemental experimental group, we recruited 6 participants for the Solo-Free (S-F) condition (mean age = 29.333, SD = 7.474, 3 female and 3 male participants). Here, participants freely interacted with the stimuli as seen in Fig. 5.6. We conducted the same two-alternative forced-choice task with this group to investigate whether the brace and forearm components of the coupling exoskeleton, experienced in the Solo-Controlled and Coupled-Guided cases, affect haptic discrimination accuracy. Results from this condition are additionally reported below.

Figure 5.6: **Free Exploration Experimental Condition:** A participant in the solo-free hand condition retains the ability to self-direct movements during the two-alternative forced-choice discrimination task.

5.8.2 Summary Statistics

We computed summary statistics of our two captured metrics (accuracy and confidence judgments) across all three captured conditions: Solo-Free Hand (S-F), Solo-Controlled (S-C), and Coupled-Guided (C-G). Summary statistics are reported in Table

5.2.

Table 5.2: Descriptive Statistics for Accuracy and Completion Time Metrics across Experimental Conditions

Condition	Metric	Mean	SD	Min	Max
S-F	accuracy	0.774	0.076	0.625	0.833
	confidence	73.826	7.775	65.208	83.438
S-C	accuracy	0.804	0.078	0.688	0.917
	confidence	65.640	6.912	57.083	76.562
C-G	accuracy	0.682	0.039	0.625	0.708
	confidence	67.891	3.905	63.958	71.979

5.8.3 Discrimination Accuracy and Confidence Ratings across Experimental Groups

We depict the distribution, center, and spread for each of our captured metrics (accuracy and confidence judgment) in Fig. 5.7. Per-participant accuracy (Fig. 5.7A) and confidence ratings (Fig. 5.7B) are computed across 48 trials and represented by black circles. Overall mean accuracy and confidence ratings are computed across all participants in each experimental group (S-F: n = 6, S-C: n = 7, C-G: n = 4 pairs). Mean accuracy in the guided movement condition (C-G) appears to be lower than either solo conditions (S-F or S-C). Mean confidence judgments appear similar across experimental groups.

We additionally present per-participant and within-group mean accuracy (Fig. 5.7C) and confidence judgments (Fig. 5.7D) across 12 trials within a stimulus/orientation presentation category (Dif/Dif, Dif/Same, Same/Dif, Same/Same) for all experimental conditions. Participant discrimination accuracy in the C-G condition on the Same/Dif presentation category was found to be notably lower than all other categories, indicating possible difficulties in discriminating orientation when the haptic stimuli are the same. Participant confidence ratings across conditions and categories appear similar across S-C and C-G conditions, but higher in the S-F condition, indicating that perceived confidence in perceptual judgments may be impaired by wearing components of the haptic exoskeleton device.

5.8.4 Statistical Analysis

All statistical testing was completed with Matlab R2025b and the Statistics and Machine Learning toolkit.

5.8.4.1 Solo (Controlled) versus Solo (Free Hand) Discrimination Accuracy

We analyzed whether discrimination accuracy in the S-C condition (solo, controlled with device) was significantly different from discrimination accuracy in the S-F condition (solo, free hand). We conducted this analysis to give us a better understanding of the effects of wearing the brace component of the device, which restricts wrist extension/flexion and partially occludes the palm of the hand with a semi-rigid handle strap.

We ran a generalized linear mixed effects model (GLME) on per-trial discrimination accuracy. We included Condition (S-F and S-C) and Category (Dif/Dif, Dif/Same, Same/Dif, Same/Same) as fixed effects, with Subject (i.e. participant or participant pair) included as a random effect. The GLME model fit statistics included an AIC of 2931.9, a BIC of 2971.8, a LogLikelihood of -1457, and a Deviance of 2913.9.

We conducted an ANOVA test for significance on the GLME model for accuracy in the two solo conditions and report the results in Table 5.3. We observed no significant main effect for Condition ($F(1,616) = 0.580, p = 0.447$). This indicates that participant discrimination accuracy is similar under free hand (no device) and controlled (with wrist and palm restrictions from the device) self-directed movement conditions. This result further indicates that our solo-control condition (S-C) is an appropriate baseline for

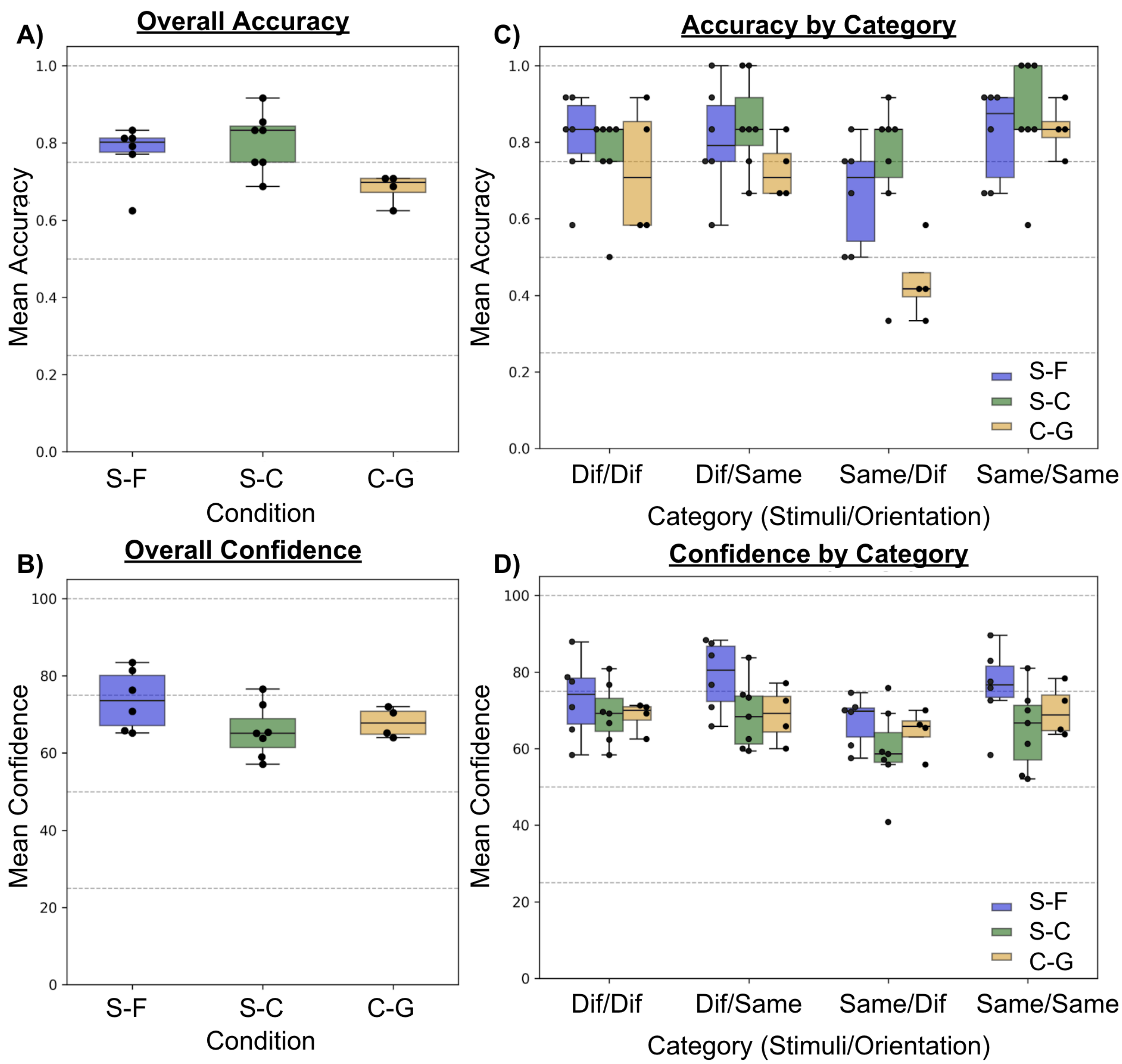

Figure 5.7: **Discrimination Accuracy and Confidence Judgments (By Condition and Category):** We present results for mean discrimination accuracy (A) and mean confidence judgments (B) across all 48 trials. Performance in the C-G condition is lower than the S-F and S-C conditions. We further present mean discrimination accuracy (C) and confidence judgments (D) across 12 trials for each of the four stimulus/orientation presentation categories for all conditions. C-G discrimination accuracy in the Same/Dif category was notable lower than the other categories. Confidence judgments in the S-F condition were higher than S-C and C-G conditions.

Table 5.3: ANOVA Marginal Tests for Solo-Controlled and Solo-Free GLME Accuracy Model

Term	F-**stat**	df_1	df_2	p-**val**
(Intercept)	123.000	1	616	**3.471e-26**
Condition	0.580	1	616	.447
Category	3.638	3	616	**.013**
Condition × Category	0.573	3	616	.633
Random Effects	**Group**	**Parameter**		**Estimate**
Subject ($n = 13$)	Intercept	SD		0.247
Error	Residual	$\sqrt{}$(Dispersion)		1.000

comparison with the coupled-guided (C-G) condition in the main manuscript.

We observed a significant difference for the main effect of Category between S-F and S-C conditions ($F(3, 616) = 3.638, p = 0.013$), but there was no significant interaction effect for Condition x Category ($F(3, 616) = 0.573, p = 0.633$). This indicates that in all conditions, participants performed with higher accuracy in some categories than others.

We conducted post-hoc pairwise comparisons across categories (presented in Table 5.4) to further investigate the main effect of category observed above. We observed a significant difference in discrimination accuracy between Same/Dif and Same/Same categories ($F(1, 616) = 8.738, p = 0.019$), indicating that across both solo groups (S-C and S-F), participants had difficulty identifying that the same peppers in different orientations are the same. There were no other significant effects for Category ($p > 0.05$).

Table 5.4: Post-hoc Pairwise Comparisons Across Categories for Solo-Controlled and Solo-Free GLME Accuracy Model

Comparison	F-**stat**	df_1	df_2	**Raw** p	**Adj.** p_c
Dif/Dif vs. Dif/Same	0.859	1	616	0.354	0.709
Dif/Dif vs. Same/Dif	2.638	1	616	0.105	0.419
Dif/Dif vs. Same/Same	1.915	1	616	0.167	0.501
Dif/Same vs. Same/Dif	6.383	1	616	0.012	0.059
Dif/Same vs. Same/Same	0.217	1	616	0.642	0.642
Same/Dif vs. Same/Same	8.738	1	616	0.003	**0.019**

5.8.4.2 Solo (Controlled) versus Coupled (Guided) Discrimination Accuracy

To determine whether discrimination accuracy in the C-G condition (coupled, guided exploration with device) was significantly different from discrimination accuracy in the S-C condition (solo, controlled with device) across stimulus/orientation presentation categories, we used a generalized linear mixed effects model (GLME) as desribed in the methodology in the main manuscript. The GLME model fit statistics include an AIC of 2467.6, a BIC of 2506, a LogLikelihood of -1224.8, and a Deviance of 2449.6.

Table 5.5: ANOVA Marginal Tests for Solo-Controlled and Coupled-Guided GLME Accuracy Model

Term	***F*-stat**	df_1	df_2	p
(Intercept)	101.860	1	520	**5.419e-22**
Condition	7.344	1	520	**6.953e-3**
Category	7.108	3	520	**1.094e-4**
Condition × Category	1.549	3	520	.201
Random Effects	**Group**	**Parameter**		**Estimate**
Subject ($n = 11$)	Intercept	SD		0.089
Error	Residual	$\sqrt{}$(Dispersion)		1.000

To test for significance, we conducted a one-way ANOVA on the GLME model for per-trial discrimination accuracy by Condition and Category; results are reported in Table 5.5. We observed significant differences for the main effect of Condition ($F(1, 520) = 7.344, p = 0.007$) and Category ($F(3, 520) = 7.108, p < 0.001$). The observed main effect of Condition indicates that participant performance is lower in the C-G case, where lack of ability to self-direct movements results in lower haptic discrimination accuracy. The observed main effect of Category indicates that some stimuli were harder for participants to discriminate than others. We found no significant interaction effects for Condition x Category ($F(3, 520) = 1.549, p = 0.201$), indicating that the diminished accuracy observed in the coupling case was consistent across stimuli/orientation presentation categories.

We further conducted post-hoc pairwise comparisons across categories (Table 5.6) to investigate which stimuli were harder for participants to discriminate between. We observed a significant difference in discrimination accuracy between Dif/Same and Same/Dif categories ($F(1, 520) = 10.570, p = 0.006$), as well as between Same/Dif and Same/Same categories ($F(1, 520) = 18.420, p < 0.001$). These results indicate that haptic stimuli, presented in different orientations, were confusing for participants. There were no other significant effects for Category ($p > 0.05$).

Table 5.6: Post-hoc Pairwise Comparisons Across Categories for Solo-Controlled and Coupled-Guided GLME Accuracy Model

Comparison	F**-stat**	df_1	df_2	**Raw** p	**Adj.** p_c
Dif/Dif vs. Dif/Same	0.777	1	520	0.378	0.378
Dif/Dif vs. Same/Dif	5.904	1	520	0.015	0.062
Dif/Dif vs. Same/Same	4.271	1	520	0.039	0.118
Dif/Same vs. Same/Dif	10.570	1	520	0.001	**0.006**
Dif/Same vs. Same/Same	1.468	1	520	0.226	0.452
Same/Dif vs. Same/Same	18.420	1	520	2.114e-5	**1.268e-4**

5.8.4.3 Linear Mixed Effects Model – Solo (Controlled) versus Coupled (Guided Exploration) Confidence Ratings

We analyzed whether confidence judgments in the C-G condition (coupled, guided exploration with device) were significantly different from confidence judgments in the S-C condition (solo, controlled with device), across stimulus/orientation presentation categories. This analysis gives us a better understanding of how participant confidence in their perceptual judgments differs based on Condition and Category.

We employed a linear mixed effects model (LME) on per-trial confidence ratings, as confidence is a continuous variable from 0 to 100 (%). We included Condition (S-F and S-C) and Category (Dif/Dif, Dif/Same, Same/Dif, Same/Same) as fixed effects, with Subject (i.e. participant or participant pair) included as a random effect. The

LME model fit statistics included an AIC of 4565.6, a BIC of 4608.3, a LogLikelihood of -2272.8, and a Deviance of 4545.6.

Table 5.7: ANOVA Marginal Tests for Solo-Controlled and Coupled-Guided LME Confidence Model

Term	**F-statistic**	df_1	df_2	**p-value**
(Intercept)	1501.800	1	520	**1.898e-155**
Condition	0.427	1	520	.514
Category	4.207	3	520	**.006**
Condition × Category	0.850	3	520	.467
Random Effects	**Group**	**Parameter**		**Estimate**
Subject ($n = 11$)	Intercept	SD		4.8731
Error	Residual	SD		17.629

We conducted an ANOVA test for significance on the LME model for per-trial confidence ratings by Condition and Category; results are reported in Table 5.7. We observed a significant main effect of Category, indicating that confidence across some stimulus presentation categories were higher than others ($F(3, 520) = 4.207, p = 0.006$). There is no observed significant main effect on condition, indicating no observed difference in confidence ratings between S-C and C-G conditions ($p > 0.05$). Surprisingly, guided participants (externally-driven hand movements) reported similar confidence levels to solo participants (self-directed hand movements). We observed no significant interaction effects of Condition x Category ($p > 0.05$).

We further conducted post-hoc pairwise comparisons of confidence ratings across categories to investigate the main effect observed above; results are reported in Table 5.8. We observed a significant difference in confidence judgments between Dif/Dif and Same/Dif categories ($F(1, 520) = 9.151, p = 0.013$), as well as between Dif/Same and Same/Dif categories ($F(1, 520) = 9.295, p = 0.014$). This indicates that some stimuli, presented with different orientations, felt harder to discriminate between for participants across all conditions.

Table 5.8: Post-hoc Pairwise Comparisons across Categories for Solo-Controlled and Coupled-Guided LME Confidence Model

Comparison	***F*-stat**	df_1	df_2	**Raw** p	**Adj.** p
Dif/Dif vs. Dif/Same	0.001	1	520	0.981	0.981
Dif/Dif vs. Same/Dif	9.151	1	520	0.003	**0.013**
Dif/Dif vs. Same/Same	0.288	1	520	0.591	1.000
Dif/Same vs. Same/Dif	9.295	1	520	0.002	**0.014**
Dif/Same vs. Same/Same	0.315	1	520	0.575	1.000
Same/Dif vs. Same/Same	6.190	1	520	0.013	0.053

5.8.5 Extended Discussion

Our supplementary analyses included more extensive investigation of participant performance across two captured metrics (discrimination accuracy and confidence in perceptual judgments) during the two-alternative forced-choice haptic experiment. Performance across stimulus presentation categories (object shape and orientation) was additionally investigated. An additional condition (solo, without the device as a control) was presented to determine whether wearing the brace component of the exoskeleton device affected haptic discrimination abilities compared to a completely free hand.

We did not find a significant difference in discrimination accuracy between our two solo conditions, indicating that wearing the brace component of the device, which constrains the wrist and partially occludes the palm, did not have an effect on haptic discrimination ability.

All results from the extended statistical analysis indicated a significant effect of stimulus presentation category on both discrimination accuracy or confidence judgments. This shows a consistent trend, where participants had difficulty discriminating between some haptic stimuli. Most prominently, the effect of orientation was confusing for participants. In one stimulus presentation category (Same/Dif), coupled participants (C-G condition) performed with lower-than-chance accuracy, indicating difficulties judging objects as “same” when the orientations of the objects are presented differently. This was not observed in the self-directed condition.

In conclusion, we present the general finding that guided hand movements are still useful for haptic discrimination of object shape. We are the first to investigate the role of whole-hand guidance (reproducing finger and thumb movements), through an inter-manual exoskeleton coupling the hands of two people, on the ability to discriminate three-dimensional objects that have complex variations in surface features. Future work in this domain should address mechanical limitations of the device (range of motion, less interference from linkages on the fingers) and investigate other object properties, such as weight, surface texture, and compliance, which require other types of hand movements (i.e., exploratory procedures). Furthermore, the effect of stimulus orientation can be further investigated under guided movement conditions. Our findings point towards a promising area of research in which collaborative guidance paradigms, such as the inter-manual exoskeleton employed here, can serve as experimental platforms for decoupling intentional motor control from haptic interactions.

Chapter 6

Conclusion

One of the primary ways in which we interact with our environment is through the sense of touch. More specifically, we use the hand – a sophisticated sensory organ and a highly dexterous tool for manipulation – to perceive features of the environment and to functionally interact with objects [12, 11, 42, 17, 18]. Furthermore, touch is critical for social development and is commonly used to communicate with those around us [185, 32]. Touch can be interpersonally subjective, such as conveying support via squeezing the shoulder of a friend, or highly semantic and categorized, such as communicating words, phrases, and sentences through tactile sign languages.

This dissertation presents an overarching vision of sharing our unique and rich touch experiences through haptic technologies. The dissertation contributes two haptic devices for sharing touch experiences and advances our understanding of haptic perception and action. The first device is a smart bracelet, presented in the third chapter, which transforms the skin into an input device for transcribing touch communication via tactile sign languages. The second device is an inter-manual exoskeleton, employed in the fourth and fifth chapters, which enables the shared experience of touching and manipulating objects by transmitting whole-hand movements between a guiding and a guided person. Here, fundamental, normally-coupled components of the haptic sense are partitioned across two nervous systems, enabling experimental investigations into haptic perception and action under guided (passive movement), multi-finger conditions. These devices contribute towards the broader goal of sharing touch experiences with others, presenting platforms for scientific inquiry of the human haptic sense.

6.1 Summary of Findings

The first chapter presented the overarching goal of enabling shared touch experiences between people and contextualized the current challenges preventing this goal. Predominantly, touch is an active, exploratory sense that is context-dependent and relies on deliberately-performed hand movements, which are kinematically complex.

The second chapter provided an interdisciplinary review of relevant research in the fields of neuroscience, perception, psychophysics, and haptic engineering, to contextualize our understanding of the human haptic sense for the subsequent chapters of the dissertation. It further provided considerations for the design of wearable and assistive haptic devices that interface with the skin, which were used to design the wearable technologies presented subsequently.

The third chapter transformed the skin into a haptic input device for transcribing and translating tactile communication into the digital domain. The smart bracelet presented here accurately classified tactile sign language letters, signed on the palm and fingers of the hand, by remote sensing at the wrist. This device addressed a current need for transcription and translation of tactile communication for those with multi-sensory impairments, who rely on tactile sign languages for interpersonal communication and social connection. The contributions of this chapter point towards a future where wearable sensing devices can bridge the haptic digital divide.

The fourth chapter examined a shared haptic experience via an inter-manual exoskeleton, worn by two people, which enabled one hand to guide the movements of another hand. An unusual method for sharing physical haptic interactions, this device enabled guided movements of all five fingers, including the more complex range of motion of the thumb, of one person's hand by another person's hand. Furthermore, the device was designed to partition components of the human haptic sense across two people during guided interactions with objects. Here, the guiding hand retained the ability to coordinate, plan, and execute whole-hand movements, but could not directly feel the objects being manipulated. In contrast, the guided hand could feel the objects but could not self-direct hand movements. The functional design of the inter-manual exoskeleton was validated by experiments on grasping and manipulation of small objects (peg-in-hole and shape-stacking tasks) under guided conditions.

The fifth chapter presented results from an experimental investigation into human haptic perception of three-dimensional objects under guided multi-finger movements. Employing the inter-manual exoskeleton presented in the previous chapter, results indicated that guided movements support complex three-dimensional object perception, although performance in the guided condition was lower than in the self-directed movement conditions. Furthermore, subjective experiences under guided movements with the exoskeleton indicated potential changes in body awareness and agency for guided hand participants. This device serves as a platform for investigation into haptic perception under guided, multi-finger movement conditions, and presents a myriad of future research opportunities to illuminate further questions about the human haptic sense.

6.2 Future Research

This dissertation fosters promising avenues for future research opportunities, towards the goal of facilitating technologies for sharing haptic experiences. These opportunities are explored below.

6.2.1 Towards Digital Haptic Interpersonal Communication via Tactile Sign Languages

Moving forward from the work presented in the third chapter, there are several promising research avenues to fully enable digital communication through tactile sign languages. These opportunities include:

- Facilitating real-time, letter-by-letter translation of tactile sign language. Here, signal processing, feature extraction, and classification must occur instantaneously (i.e., as a user is providing input) and be robust to individual signing differences.
- Using natural language processing and speech-to-text methods, which are phoneme-based rather than letter-based, to improve classification of tactile sign languages.
- Collecting large datasets from multiple tactile sign language communicators and interpreters to improve the ability of the model to classify tactile sign language, robust to individual differences (such as speed of sign, shorthand notations, etc.).
- Directly working with Deafblind users to evaluate such real-time transcription devices.
- Integrating such sensing (i.e., input) devices with methods for actuating (i.e., outputting) tactile sign language on the hand (for example, with devices such as the HaptiComm [149]).

6.2.2 Towards Capturing and Replaying Whole-Hand Touch Interactions With Objects

The findings in the fourth and fifth chapters open up several future research opportunities to explore via this inter-manual guidance exoskeleton:

- Investigate guided haptic perception of other object properties, such as weight, compliance, or texture.

- Investigate guided haptic manipulation during tasks that involve more complex motor planning and coordination. For example, writing with a pen or typing on a keyboard, where cutaneous sensation may be more critical for appropriate functional manipulation.

- Improve comfort and mechanical ergonomics of the device, such as preventing lateral interference from the mechanism.

- Investigate more constraining mechanisms to restrict the orientation of the guided thumb tip relative to the guiding thumb tip.

- Develop a methodology for verifying that the guided participant remains compliant, rather than relying on subjective metrics.

- Further investigation into feelings of embodiment (such as body ownership, feelings of agency, and body awareness) under such guided conditions. Our initial results indicate that such an experience may influence body awareness, ownership, and feelings of agency for guided hand participants.

Moving forward from this specific design of the inter-manual exoskeleton, there is an opportunity for developing technologies where whole-hand movements can be captured and replayed, outside of the context in which they were originally experienced. Here, instead of two hands being physically coupled via mechanical linkages, a capture system and a replay system, developed via robotically actuated components and multiple sensing channels, can be designed to appropriately capture whole-hand movements (multi-finger, including thumb) and replay them for a separate user – either synchronously, or at a later time. Such a system would enable the archival and asynchronous transmission of physical expertise, allowing high-fidelity motor skills and tactile sensations to be experienced outside of their original temporal or spatial contexts. Similarly to how the digitization of audio and visual information revolutionized human communication, the ability to store, share, and revisit complex haptic interactions suggests a future where human touch becomes a persistent, transmissible digital asset, fundamentally altering the landscape of remote collaboration, skill transfer, and avenues for other scientific inquiries into the human haptic sense.

6.2.3 Considerations and Implications for Shared Haptic Experiences

When designing technologies for facilitating shared haptic experiences, there must be careful consideration towards a user's sense of agency over body movements, sense of self, and feelings of body ownership, which are deeply rooted in multisensory integration—specifically the congruence between internal motor commands (efferent signals) and sensory feedback (afferent signals) [186, 1]. Qualitative findings from experiments employing the inter-manual exoskeleton (Chapters 4 and 5) suggest that such shared experiences may affect these aspects, especially for the guided hand. Some guided participants explicitly stated that they preferred to have agency over moving their own hand, describing their experiences with the words "interesting," "strange," and "invasive" (Chapter 4). Therefore, technologies that significantly alter natural sensorimotor integration of the body may produce adverse psychological, emotional, or physical effects on the user. Further research into such effects during manual guidance merits significant consideration, and it is therefore pertinent to consider the contexts and consequences where such shared experiences can be helpful, and when they can become disruptive to a user's bodily autonomy.

Sharing haptic experiences may be helpful in pedagogical, rehabilitative, product-development, or high-risk settings, where a certain aspect of a haptic interaction is desired to be transferred from the guider to the receiver. Examples include:

- Sharing the experience of achieving a stable grip, versus the feeling of an unstable grip, during teleoperation training of novice users. Applications that involve teleoperation include high-risk tasks such as bomb diffusion, waste management, and disaster response.

- Learning the haptic properties of manual crafts, sports, and other skills through feeling the experiences shared by a skilled user. For example, an experienced pilot can share how it feels to control their paraglider in different wind conditions, or can simulate sensations of what incidents with a paraglider could feel like during SIV (Simulation d'Incidents en Vol) trainings, to novice users.

- Informing the control algorithms for robotic prosthetic appendages or motor rehabilitation exoskeleton devices via human-guided movements, using capture and replay methodologies. This could yield more effective techniques for rebuilding neural connections in the brain, informed by natural hand movements.

- Maintaining haptic archives, recorded from one person, that can be revisited by anyone. This could include archival data of a company's products, where users can feel certain products before buying them (such as the texture of a piece of clothing, the size and weight of a laptop, the resistance in the keys of a piano, or the stiffness of the joysticks in a gaming controller).

However, there are contexts through which shared haptic experiences may disrupt a user's sense of agency and autonomy, or a user can be otherwise put at risk. Examples could include:

- Overwhelming of the tactile sense with externally-produced sensorimotor information by haptic technologies. Indeed, certain individuals may already be more sensitive to touch, so the feedback provided during shared touch experiences should be adaptable to fit the user's needs.

- Increased risk for bodily harm or injury due to parts failure or misuse of such devices.

- Violation of a user's peripersonal space, which is the space surrounding the body where we can reach out to contact people or objects, and is informed by multisensory integration [187]. Technologies for sharing haptic experiences collapse this zone, interfacing directly with the skin. When technologies are driven by externally produced movements, this may produce effects similar to being touched without consent in the physical world.

- Overreliance and dependence on the technology, rather than prioritizing physical experiences. This could result in overconfidence in trained skills through such technologies, which may have serious implications for the personal safety of the user.

Overreliance and dependence have also been seen with existing personal devices, such as cell phones, smart watches, computers, and other technologies. Our cell phones and laptops serve as extensions of our memory capacity, able to store terabytes of information such as phone numbers, addresses, photographs, videos, text documents, voice recordings, and many others. They also serve as direct lines of communication to billions of people across the world, and enable us to access real-time updates about world affairs and emergencies. These technologies, particularly the cell phone [188], are being increasingly incorporated into the sense of self, which yields both positive and negative effects on the user. When designing technologies for shared haptic experiences, these consequences must also be considered.

Another concern, prevalent with current technologies such as cell phones, smart watches, and ring devices, includes maintaining the security and privacy of stored biometric data. Personal devices can already track habits such as sleep, physical activity, heart rate, and stress levels. Capture and replay systems for shared haptic experiences could store data, including temporal and kinematic properties of performed hand movements and mechanical skin responses, which are highly personal and potentially identifiable. Maintaining the privacy and security of haptic biodata is a consideration that must be addressed, as the misuse or sale of such data may pose a significant risk to the individual.

Taken as a whole, designers for technologies that share haptic experiences should consider the context in which the devices will be used, the amount of kinesthetic and cutaneous feedback that is transmitted to the hand (and offering opportunities to fine-tune feedback), and the potentials for risk – including physical harm, misuse of data, changes to sense of agency, and alterations to peripersonal space.

Bibliography

[1] J. W. Moore, *What is the sense of agency and why does it matter?*, *Frontiers in psychology* **7** (2016) 1272.

[2] J. F. Norman and A. N. Bartholomew, *Blindness enhances tactile acuity and haptic 3-d shape discrimination*, *Attention, Perception, & Psychophysics* **73** (2011), no. 7 2323–2331.

[3] J. F. Norman, F. Phillips, J. S. Holmin, H. F. Norman, A. M. Beers, A. M. Boswell, J. R. Cheeseman, A. G. Stethen, and C. Ronning, *Solid shape discrimination from vision and haptics: Natural objects (capsicum annuum) and gibson's "feelies"*, *Experimental brain research* **222** (2012), no. 3 321–332.

[4] J. F. Norman, J. R. Cheeseman, O. C. Adkins, A. G. Cox, C. E. Rogers, C. J. Dowell, M. W. Baxter, H. F. Norman, and C. M. Reyes, *Aging and solid shape recognition: Vision and haptics*, *Vision Research* **115** (2015) 113–118.

[5] J. F. Norman, F. Phillips, J. R. Cheeseman, K. E. Thomason, C. Ronning, K. Behari, K. Kleinman, A. B. Calloway, and D. Lamirande, *Perceiving object shape from specular highlight deformation, boundary contour deformation, and active haptic manipulation*, *PLoS One* **11** (2016), no. 2 e0149058.

[6] C. J. Dowell, J. F. Norman, J. R. Moment, L. M. Shain, H. F. Norman, F. Phillips, and A. M. Kappers, *Haptic shape discrimination and interhemispheric communication*, *Scientific Reports* **8** (2018), no. 1 377.

[7] J. F. Norman, J. M. Dukes, and T. N. Palmore, *Aging and haptic shape discrimination: the effects of variations in size*, *Scientific Reports* **10** (2020), no. 1 14690.

[8] J. F. Norman, H. F. Norman, A. M. Clayton, J. Lianekhammy, and G. Zielke, *The visual and haptic perception of natural object shape*, *Perception & psychophysics* **66** (2004), no. 2 342–351.

[9] R. L. Klatzky and S. J. Lederman, *Touch*, in *Handbook of Psychology: Experimental Psychology*, pp. 152–178. John Wiley & Sons, Inc., 2nd ed., 2013.

[10] H. Li and L. Cheng, *A systematic review on hand exoskeletons from the mechatronics aspect*, *IEEE/ASME Transactions on Mechatronics* (2024).

[11] L. A. Jones and S. J. Lederman, *Human hand function*. Oxford university press, 2006.

[12] V. Mountcastle, *The Sensory Hand: Neural Mechanisms of Somatic Sensation*. Harvard University Press, 2005.

[13] H. P. Saal and S. J. Bensmaia, *Touch is a team effort: interplay of submodalities in cutaneous sensibility*, *Trends in neurosciences* **37** (2014), no. 12 689–697.

[14] R. S. Johansson and J. R. Flanagan, *Coding and use of tactile signals from the fingertips in object manipulation tasks*, *Nature Reviews Neuroscience* **10** (2009), no. 5 345–359.

[15] R. S. Johansson, J. R. Flanagan, and R. S. Johansson, *Sensory control of object manipulation*, *Sensorimotor control of grasping: Physiology and pathophysiology* (2009) 141–160.

[16] D. M. Wolpert and J. R. Flanagan, *Motor prediction*, *Current biology* **11** (2001), no. 18 R729–R732.

[17] R. L. Klatzky, *Haptic perception and its relation to action*, *Annual review of psychology* **76** (2025), no. 1 227–250.

[18] A. M. Kappers and W. M. Bergmann Tiest, *Haptic perception*, *Wiley Interdisciplinary Reviews: Cognitive Science* **4** (2013), no. 4 357–374.

[19] N. Lepora, *Active tactile perception*, in *Scholarpedia of Touch*, pp. 151–159. Springer, 2016.

[20] S. J. Lederman and R. L. Klatzky, *Hand movements: A window into haptic object recognition*, *Cognitive psychology* **19** (1987), no. 3 342–368.

[21] S. J. Lederman and R. L. Klatzky, *Extracting object properties through haptic exploration*, *Acta psychologica* **84** (1993), no. 1 29–40.

[22] R. L. Klatzky and S. J. Lederman, *Identifying objects from a haptic glance*, *Perception & Psychophysics* **57** (1995), no. 8 1111–1123.

[23] R. Klatzky and C. L. Reed, *Haptic exploration*, in *Scholarpedia of Touch*, pp. 177–183. Springer, 2016.

[24] N. F. Vaibhav, V. S. Mohit, and A. A. Anilesh, *Applications of haptics technology in advance robotics*, in *INTERACT-2010*, pp. 273–277, IEEE, 2010.

[25] P. Culmer, A. Alazmani, F. Mushtaq, W. Cross, and D. Jayne, *Haptics in surgical robots*, in *Handbook of robotic and Image-Guided surgery*, pp. 239–263. Elsevier, 2020.

[26] K. Pacheco-Barrios, J. Ortega-Márquez, and F. Fregni, *Haptic technology: Exploring its underexplored clinical applications—a systematic review*, *Biomedicines* **12** (2024), no. 12 2802.

[27] W. Barfield, *The use of haptic display technology in education*, *Themes in science and technology education* **2** (2010), no. 1-2 11–30.

[28] A. Moscatelli, M. B. 0002, A. Serio, A. Bicchi, and M. O. Ernst, *Sensorymotor synergies: Fusion of cutaneous touch and proprioception in the perceived hand kinematics*, in *Human and Robot Hands - Sensorimotor Synergies to Bridge the Gap Between Neuroscience and Robotics* (M. B. 0002 and A. Moscatelli, eds.), pp. 87–98. Springer, 2016.

[29] B. P. Delhaye, F. Schiltz, F. Crevecoeur, J.-L. Thonnard, and P. Lefèvre, *Fast grip force adaptation to friction relies on localized fingerpad strains*, *Science advances* **10** (2024), no. 3 eadh9344.

[30] S. J. Lederman and M. M. Taylor, *Fingertip force, surface geometry, and the perception of roughness by active touch*, *Perception & psychophysics* **12** (1972), no. 5 401–408.

[31] B. P. Delhaye, K. H. Long, and S. J. Bensmaia, *Neural basis of touch and proprioception in primate cortex*, *Comprehensive physiology* **8** (2018), no. 4 1575–1602.

[32] A. Montagu, *The skin, touch, and human development*, *Clinics in Dermatology* **2** (1984), no. 4 17–26.

[33] A. R. Sobinov and S. J. Bensmaia, *The neural mechanisms of manual dexterity*, *Nature Reviews Neuroscience* **22** (2021), no. 12 741–757.

[34] A. B. Schwartz, *Movement: how the brain communicates with the world*, *Cell* **164** (2016), no. 6 1122–1135.

[35] A. Leo, G. Handjaras, H. Marino, M. Bianchi, P. Pietrini, and E. Ricciardi, *The motor control of hand movements in the human brain: Toward the definition of a cortical representation of postural synergies*, in *Human and Robot Hands: Sensorimotor Synergies to Bridge the Gap Between Neuroscience and Robotics*, pp. 41–60. Springer, 2016.

[36] Y. Yan, J. M. Goodman, D. D. Moore, S. A. Solla, and S. J. Bensmaia, *Unexpected complexity of everyday manual behaviors*, *Nature communications* **11** (2020), no. 1 3564.

[37] D. M. Wolpert, Z. Ghahramani, and M. I. Jordan, *An internal model for sensorimotor integration*, *Science* **269** (1995), no. 5232 1880–1882.

[38] R. S. Johansson and B. B. Edin, *Predictive feed-forward sensory control during grasping and manipulation in man*, *BIOMEDICAL RESEARCH-TOKYO-* **14** (1993) 95–95.

[39] I. Panek, T. Bui, A. Wright, and R. Brownstone, *Cutaneous afferent regulation of motor function*, *Acta neurobiologiae experimentalis* **74** (2014), no. 2 158–171.

[40] A. M. Ebied, G. J. Kemp, and S. P. Frostick, *The role of cutaneous sensation in the motor function of the hand*, *Journal of Orthopaedic Research* **22** (2004), no. 4 862–866.

[41] A.-S. Augurelle, A. M. Smith, T. Lejeune, and J.-L. Thonnard, *Importance of cutaneous feedback in maintaining a secure grip during manipulation of hand-held objects*, *Journal of neurophysiology* **89** (2003), no. 2 665–671.

[42] J. R. Flanagan and R. S. Johansson, *Hand movements*, *Encyclopedia of the human brain* **2** (2002) 399–414.

[43] A. Carteron, K. McPartlan, C. Gioeli, E. Reid, M. Turturro, B. Hahn, C. Benson, and W. Zhang, *Temporary nerve block at selected digits revealed hand motor deficits in grasping tasks*, *Frontiers in Human Neuroscience* **10** (2016) 596.

[44] A. Kavounoudias, J. P. Roll, J. Anton, B. Nazarian, M. Roth, and R. Roll, *Proprio-tactile integration for kinesthetic perception: an fmri study*, *Neuropsychologia* **46** (2008), no. 2 567–575.

[45] S. E. Jansen, W. M. B. Tiest, and A. M. Kappers, *Identifying haptic exploratory procedures by analyzing hand dynamics and contact force*, *IEEE Transactions on Haptics* **6** (2013), no. 4 464–472.

[46] T. Cooke, C. Wallraven, and H. H. Bülthoff, *Multidimensional scaling analysis of haptic exploratory procedures*, *ACM Transactions on Applied Perception (TAP)* **7** (2010), no. 1 1–17.

[47] J. J. Gibson, *Observations on active touch.*, *Psychological review* **69** (1962), no. 6 477.

[48] C. Simões-Franklin, T. A. Whitaker, and F. N. Newell, *Active and passive touch differentially activate somatosensory cortex in texture perception*, *Human brain mapping* **32** (2011), no. 7 1067–1080.

[49] J. R. Cheeseman, J. F. Norman, and A. M. Kappers, *Dynamic cutaneous information is sufficient for precise curvature discrimination*, *Scientific Reports* **6** (2016), no. 1 1–7.

[50] B. J. Van der Horst and A. M. Kappers, *Haptic curvature comparison of convex and concave shapes*, *Perception* **37** (2008), no. 8 1137–1151.

[51] W. M. Bergmann Tiest and A. M. L. Kappers, *Cues for haptic perception of compliance*, *IEEE Transactions on Haptics* **2** (2009), no. 4 189–199.

[52] A. M. Kappers and W. M. B. Tiest, *Haptic Perception of Material Properties*, ch. 10, pp. 225–249. John Wiley and Sons, Ltd, 2017. https://onlinelibrary.wiley.com/doi/pdf/10.1002/9783527690534.ch10.

[53] A. M. Kappers, *Human perception of shape from touch*, *Philosophical Transactions of the Royal Society B: Biological Sciences* **366** (2011), no. 1581 3106–3114.

[54] V. Hayward, *Haptic shape cues, invariants, priors and interface design*, in *Human haptic perception: Basics and applications*, pp. 381–392. Springer, 2008.

[55] B. Richardson, M. Symmons, and R. Accardi, *The tds: A new device for comparing active and passive-guided touch*, *IEEE Transactions on Rehabilitation Engineering* **8** (2000), no. 3 414–417.

[56] M. A. Symmons, B. L. Richardson, and D. B. Wuillemin, *Intrasensory attention: kinaesthetic versus cutaneous inputs*, *Perception* **36** (2007), no. 6 880–887.

[57] M. A. Symmons, B. L. Richardson, and D. B. Wuillemin, *Components of haptic information: Skin rivals kinaesthesis*, *Perception* **37** (2008), no. 10 1596–1604.

[58] G. H. Van Doorn, J. Hohwy, and M. A. Symmons, *Capture of kinesthesis by a competing cutaneous input*, *Attention, Perception, & Psychophysics* **74** (2012), no. 7 1539–1551.

[59] M. A. Heller, *Active and passive touch: The influence of exploration time on form recognition*, *The Journal of General Psychology* **110** (1984), no. 2 243–249.

[60] M. A. Symmons, B. L. Richardson, D. B. Wuillemin, and G. H. VanDoorn, *Active versus passive touch in three dimensions*, in *First Joint Eurohaptics Conference and Symposium on Haptic Interfaces for Virtual Environment and Teleoperator Systems. World Haptics Conference*, pp. 108–113, IEEE, 2005.

[61] N. Braun, S. Debener, N. Spychala, E. Bongartz, P. Sörös, H. H. Müller, and A. Philipsen, *The senses of agency and ownership: a review*, *Frontiers in psychology* **9** (2018) 535.

[62] H. Limerick, D. Coyle, and J. W. Moore, *The experience of agency in human-computer interactions: a review*, *Frontiers in Human Neuroscience* **8** (2014) 643.

[63] K. Kilteni, P. Engeler, and H. H. Ehrsson, *Efference copy is necessary for the attenuation of self-generated touch*, *IScience* **23** (2020), no. 2 100843.

[64] S.-J. Blakemore, D. M. Wolpert, and C. D. Frith, *Central cancellation of self-produced tickle sensation*, *Nature neuroscience* **1** (1998), no. 7 635–640.

[65] P. Haggard, S. Clark, and J. Kalogeras, *Voluntary action and conscious awareness*, *Nature neuroscience* **5** (2002), no. 4 382–385.

[66] D. M. Wegner and T. Wheatley, *Apparent mental causation: Sources of the experience of will.*, *American psychologist* **54** (1999), no. 7 480.

[67] C. D. Frith, *The cognitive neuropsychology of schizophrenia*. Psychology press, 1992.

[68] M. Zhu, S. Biswas, S. I. Dinulescu, N. Kastor, E. W. Hawkes, and Y. Visell, *Soft, wearable robotics and haptics: Technologies, trends, and emerging applications*, *Proceedings of the IEEE* **110** (2022), no. 2 246–272.

[69] C. Pacchierotti, S. Sinclair, M. Solazzi, A. Frisoli, V. Hayward, and D. Prattichizzo, *Wearable haptic systems for the fingertip and the hand: taxonomy, review, and perspectives*, *IEEE transactions on haptics* **10** (2017), no. 4 580–600.

[70] A. Atalay, V. Sanchez, O. Atalay, D. M. Vogt, F. Haufe, R. J. Wood, and C. J. Walsh, *Batch fabrication of customizable silicone-textile composite capacitive strain sensors for human motion tracking*, *Advanced Materials Technologies* **2** (2017), no. 9 1700136, [https://onlinelibrary.wiley.com/doi/pdf/10.1002/admt.201700136].

[71] S. Yao and Y. Zhu, *Wearable multifunctional sensors using printed stretchable conductors made of silver nanowires*, *Nanoscale* **6** (2014) 2345–2352.

[72] C. Harrison, D. Tan, and D. Morris, *Skinput: appropriating the skin as an interactive canvas*, *Communications of the ACM* **54** (2011), no. 8 111–118.

[73] Y. Shao, H. Hu, and Y. Visell, *A wearable tactile sensor array for large area remote vibration sensing in the hand*, *IEEE Sensors Journal* **20** (2020), no. 12 6612–6623.

[74] S. Choi and K. J. Kuchenbecker, *Vibrotactile display: Perception, technology, and applications*, *Proceedings of the IEEE* **101** (2012), no. 9 2093–2104.

[75] A. U. Alahakone and S. A. Senanayake, *Vibrotactile feedback systems: Current trends in rehabilitation, sports and information display*, in *2009 IEEE/ASME International Conference on Advanced Intelligent Mechatronics*, pp. 1148–1153, IEEE, 2009.

[76] P. Kourtesis, F. Argelaguet, S. Vizcay, M. Marchal, and C. Pacchierotti, *Electrotactile feedback applications for hand and arm interactions: A systematic review, meta-analysis, and future directions*, *IEEE transactions on haptics* **15** (2022), no. 3 479–496.

[77] Z. Zhou, Y. Yang, J. Liu, J. Zeng, X. Wang, and H. Liu, *Electrotactile perception properties and its applications: A review*, *IEEE transactions on haptics* **15** (2022), no. 3 464–478.

[78] E. Battaglia, J. P. Clark, M. Bianchi, M. G. Catalano, A. Bicchi, and M. K. O'Malley, *The rice haptic rocker: skin stretch haptic feedback with the pisa/iit softhand*, in *2017 IEEE World Haptics Conference (WHC)*, pp. 7–12, IEEE, 2017.

[79] C. Fang, Y. Zhang, M. Dworman, and C. Harrison, *Wireality: Enabling complex tangible geometries in virtual reality with worn multi-string haptics*, in *Proceedings of the 2020 CHI Conference on Human Factors in Computing Systems*, pp. 1–10, 2020.

[80] M. Zhu, T. N. Do, E. Hawkes, and Y. Visell, *Fluidic fabric muscle sheets for wearable and soft robotics*, *Soft robotics* **7** (2020), no. 2 179–197.

[81] S. Martin and N. Hillier, *Characterisation of the novint falcon haptic device for application as a robot manipulator*, in *Australasian Conference on Robotics and Automation (ACRA)*, pp. 291–292, Citeseer Sydney, Australia, 2009.

[82] S. Grange, F. Conti, P. Rouiller, P. Helmer, and C. Baur, *The delta haptic device*, *Mecatronics 2001* (2001).

[83] T. H. Massie and J. K. Salisbury, *The phantom haptic interface: A device for probing virtual objects*, in *ASME International Mechanical Engineering Congress and Exposition*, vol. 14147, pp. 295–301, American Society of Mechanical Engineers, 1994.

[84] J. E. Colgate, P. E. Grafing, M. C. Stanley, and G. Schenkel, *Implementation of stiff virtual walls in force-reflecting interfaces*, in *Proceedings of IEEE virtual reality annual international symposium*, pp. 202–208, IEEE, 1993.

[85] B. L. Richardson, D. B. Wuillemin, and G. J. MacKintosh, *Can passive touch be better than active touch? a comparison of active and passive tactile maze learning*, *British Journal of Psychology* **72** (1981), no. 3 353–362.

[86] P. Tran, S. Jeong, K. R. Herrin, and J. P. Desai, *Hand exoskeleton systems, clinical rehabilitation practices, and future prospects*, *IEEE Transactions on Medical Robotics and Bionics* **3** (2021), no. 3 606–622.

[87] T. Du Plessis, K. Djouani, and C. Oosthuizen, *A review of active hand exoskeletons for rehabilitation and assistance*, *Robotics* **10** (2021), no. 1 40.

[88] C. N. Schabowsky, S. B. Godfrey, R. J. Holley, and P. S. Lum, *Development and pilot testing of hexorr: Hand exoskeleton rehabilitation robot*, *Journal of NeuroEngineering and Rehabilitation* **7** (2010), no. 1 1–16.

[89] N. Ho, K. Tong, X. Hu, K. Fung, X. Wei, W. Rong, and E. Susanto, *An emg-driven exoskeleton hand robotic training device on chronic stroke subjects: Task training system for stroke rehabilitation*, in *2011 IEEE international conference on rehabilitation robotics*, pp. 1–5, IEEE, 2011.

[90] S. Ueki, H. Kawasaki, S. Ito, Y. Nishimoto, M. Abe, T. Aoki, Y. Ishigure, T. Ojika, and T. Mouri, *Development of a hand-assist robot with multi-degrees-of-freedom for rehabilitation therapy*, *IEEE/ASME Transactions on Mechatronics* **17** (2012), no. 1 136–146.

[91] P. Ben-Tzvi and Z. Ma, *Sensing and force-feedback exoskeleton (safe) robotic glove*, *IEEE Transactions on Neural Systems and Rehabilitation Engineering* **23** (2014), no. 6 992–1002.

[92] D. Leonardis, M. Barsotti, C. Loconsole, M. Solazzi, M. Troncossi, C. Mazzotti, V. P. Castelli, C. Procopio, G. Lamola, C. Chisari, *et. al.*, *An emg-controlled robotic hand exoskeleton for bilateral rehabilitation*, *IEEE transactions on haptics* **8** (2015), no. 2 140–151.

[93] I. Jo and J. Bae, *Design and control of a wearable and force-controllable hand exoskeleton system*, *mechatronics* **41** (2017) 90–101.

[94] M. Sarac, M. Solazzi, and A. Frisoli, *Design requirements of generic hand exoskeletons and survey of hand exoskeletons for rehabilitation, assistive, or haptic use*, *IEEE transactions on haptics* **12** (2019), no. 4 400–413.

[95] M. Gabardi, M. Solazzi, D. Leonardis, and A. Frisoli, *Design and evaluation of a novel 5 dof underactuated thumb-exoskeleton*, *IEEE Robotics and Automation Letters* **3** (2018), no. 3 2322–2329.

[96] M. B. Hong, S. J. Kim, Y. S. Ihn, G.-C. Jeong, and K. Kim, *Kulex-hand: An underactuated wearable hand for grasping power assistance*, *IEEE Transactions on Robotics* **35** (2019), no. 2 420–432.

[97] I. Jo, Y. Park, J. Lee, and J. Bae, *A portable and spring-guided hand exoskeleton for exercising flexion/extension of the fingers*, *Mechanism and Machine Theory* **135** (2019) 176–191.

[98] G. Li, L. Cheng, Z. Gao, X. Xia, and J. Jiang, *Development of an untethered adaptive thumb exoskeleton for delicate rehabilitation assistance*, *IEEE Transactions on Robotics* **38** (2022), no. 6 3514–3529.

[99] H. Li, L. Cheng, N. Sun, and R. Cao, *Design and control of an underactuated finger exoskeleton for assisting activities of daily living*, *IEEE/ASME Transactions on Mechatronics* **27** (2021), no. 5 2699–2709.

[100] L. Yang, F. Zhang, J. Zhu, and Y. Fu, *A portable device for hand rehabilitation with force cognition: Design, interaction, and experiment*, *IEEE Transactions on Cognitive and Developmental Systems* **14** (2021), no. 2 599–607.

[101] W. Xu, Y. Guo, C. Bravo, and P. Ben-Tzvi, *Design, control, and experimental evaluation of a novel robotic glove system for patients with brachial plexus injuries*, *IEEE Transactions on Robotics* **39** (2022), no. 2 1637–1652.

[102] J. Lai and A. Song, *Design and characterization of a novel compact hand exoskeleton robot for telerehabilitation and muscle spasticity assessment*, *IEEE/ASME Transactions on Mechatronics* **29** (2023), no. 4 2416–2427.

[103] R. Michikawa, T. Endo, and F. Matsuno, *A multi-dof exoskeleton haptic device for the grasping of a compliant object adapting to a user's motion using jamming transitions*, *IEEE Transactions on Robotics* **39** (2022), no. 1 373–385.

[104] R. Liang, Q. Zhang, W. Yang, L. Li, and B. He, *Opposition movement of the little finger enhances the grasping function of robotic hands*, *IEEE Robotics and Automation Letters* **9** (2024), no. 4 3743–3750.

[105] M. Dragusanu, M. Z. Iqbal, T. L. Baldi, D. Prattichizzo, and M. Malvezzi, *Design, development, and control of a hand/wrist exoskeleton for rehabilitation and training*, *IEEE Transactions on Robotics* **38** (2022), no. 3 1472–1488.

[106] J. Li, R. Zheng, Y. Zhang, and J. Yao, *ihandrehab: An interactive hand exoskeleton for active and passive rehabilitation*, in *2011 IEEE International Conference on Rehabilitation Robotics*, pp. 1–6, IEEE, 2011.

[107] A. Chiri, N. Vitiello, F. Giovacchini, S. Roccella, F. Vecchi, and M. C. Carrozza, *Mechatronic design and characterization of the index finger module of a hand exoskeleton for post-stroke rehabilitation*, *IEEE/ASME Transactions on Mechatronics* **17** (2012), no. 5 884–894.

[108] C. L. Jones, F. Wang, R. Morrison, N. Sarkar, and D. G. Kamper, *Design and development of the cable actuated finger exoskeleton for hand rehabilitation following stroke*, *IEEE/ASME Transactions on Mechatronics* **19** (2014), no. 1 131–140.

[109] Z. Ma and P. Ben-Tzvi, *Rml glove—an exoskeleton glove mechanism with haptics feedback*, *IEEE/ASME Transactions on Mechatronics* **20** (2015), no. 2 641–652.

[110] M. Cempini, M. Cortese, and N. Vitiello, *A powered finger–thumb wearable hand exoskeleton with self-aligning joint axes*, *IEEE/ASME Transactions on Mechatronics* **20** (2015), no. 2 705–716.

[111] P. Agarwal, J. Fox, Y. Yun, M. K. O'Malley, and A. D. Deshpande, *An index finger exoskeleton with series elastic actuation for rehabilitation: Design, control and performance characterization*, *The International Journal of Robotics Research* **34** (2015), no. 14 1747–1772.

[112] D. Popov, I. Gaponov, and J.-H. Ryu, *Portable exoskeleton glove with soft structure for hand assistance in activities of daily living*, *IEEE/ASME Transactions on Mechatronics* **22** (2017), no. 2 865–875.

[113] C. G. Rose and M. K. O'Malley, *Hybrid rigid-soft hand exoskeleton to assist functional dexterity*, *IEEE Robotics and Automation Letters* **4** (2019), no. 1 73–80.

[114] B. B. Kang, H. Choi, H. Lee, and K.-J. Cho, *Exo-glove poly ii: A polymer-based soft wearable robot for the hand with a tendon-driven actuation system*, *Soft robotics* **6** (2019), no. 2 214–227.

[115] S.-W. Pu, Y.-C. Pei, and J.-Y. Chang, *Decoupling finger joint motion in an exoskeletal hand: A design for robot-assisted rehabilitation*, *IEEE Transactions on Industrial Electronics* **67** (2019), no. 1 686–697.

[116] N. Sun, G. Li, and L. Cheng, *Design and validation of a self-aligning index finger exoskeleton for post-stroke rehabilitation*, *IEEE Transactions on Neural Systems and Rehabilitation Engineering* **29** (2021) 1513–1523.

[117] T. Bützer, O. Lambercy, J. Arata, and R. Gassert, *Fully wearable actuated soft exoskeleton for grasping assistance in everyday activities*, *Soft robotics* **8** (2021), no. 2 128–143.

[118] P. Tran, S. Jeong, F. Lyu, K. Herrin, S. Bhatia, D. Elliott, S. Kozin, and J. P. Desai, *Flexotendon glove-iii: Voice-controlled soft robotic hand exoskeleton with novel fabrication method and admittance grasping control*, *IEEE/ASME Transactions on Mechatronics* **27** (2022), no. 5 3920–3931.

[119] W. Chen, G. Li, N. Li, W. Wang, P. Yu, R. Wang, X. Xue, X. Zhao, and L. Liu, *Soft exoskeleton with fully actuated thumb movements for grasping assistance*, *IEEE Transactions on Robotics* **38** (2022), no. 4 2194–2207.

[120] D. H. Kim, Y. Lee, and H.-S. Park, *Bioinspired high-degrees of freedom soft robotic glove for restoring versatile and comfortable manipulation*, *Soft robotics* **9** (2022), no. 4 734–744.

[121] M. Sui, Y. Ouyang, H. Jin, Z. Chai, C. Wei, J. Li, M. Xu, W. Li, L. Wang, and S. Zhang, *A soft-packaged and portable rehabilitation glove capable of closed-loop fine motor skills*, *Nature Machine Intelligence* **5** (2023), no. 10 1149–1160.

[122] G. Li, L. Cheng, and C. Zhang, *Design and modeling of a bioinspired flexible finger exoskeleton for strength augmentation*, *IEEE/ASME Transactions on Mechatronics* **29** (2024), no. 6 4389–4400.

[123] P. Daemi, Y. Zhou, M. D. Naish, A. D. Price, and A. L. Trejos, *Comprehensive kinematic model of a tendon-driven wearable tremor suppression device*, *IEEE Transactions on Robotics* **40** (2023) 421–437.

[124] K. Tadano, M. Akai, K. Kadota, and K. Kawashima, *Development of grip amplified glove using bi-articular mechanism with pneumatic artificial rubber muscle*, in *2010 IEEE International Conference on Robotics and Automation*, pp. 2363–2368, 2010.

[125] P. Polygerinos, Z. Wang, K. C. Galloway, R. J. Wood, and C. J. Walsh, *Soft robotic glove for combined assistance and at-home rehabilitation*, *Robotics and autonomous systems* **73** (2015) 135–143.

[126] H. Zhao, J. Jalving, R. Huang, R. Knepper, A. Ruina, and R. Shepherd, *A helping hand: Soft orthosis with integrated optical strain sensors and emg control*, *IEEE Robotics & Automation Magazine* **23** (2016), no. 3 55–64.

[127] H. K. Yap, P. M. Khin, T. H. Koh, Y. Sun, X. Liang, J. H. Lim, and C.-H. Yeow, *A fully fabric-based bidirectional soft robotic glove for assistance and rehabilitation of hand impaired patients*, *IEEE Robotics and Automation Letters* **2** (2017), no. 3 1383–1390.

[128] S.-S. Yun, B. B. Kang, and K.-J. Cho, *Exo-glove pm: An easily customizable modularized pneumatic assistive glove*, *IEEE Robotics and Automation Letters* **2** (2017), no. 3 1725–1732.

[129] J. Wang, Y. Fei, and W. Pang, *Design, modeling, and testing of a soft pneumatic glove with segmented pneunets bending actuators*, *Ieee/asme transactions on mechatronics* **24** (2019), no. 3 990–1001.

[130] K. H. Heung, R. K. Tong, A. T. Lau, and Z. Li, *Robotic glove with soft-elastic composite actuators for assisting activities of daily living*, *Soft robotics* **6** (2019), no. 2 289–304.

[131] N. Takahashi, S. Furuya, and H. Koike, *Soft exoskeleton glove with human anatomical architecture: Production of dexterous finger movements and skillful piano performance*, *IEEE Transactions on Haptics* **13** (2020), no. 4 679–690.

[132] Z. Wang, D. Wang, Y. Zhang, J. Liu, L. Wen, W. Xu, and Y. Zhang, *A three-fingered force feedback glove using fiber-reinforced soft bending actuators*, *IEEE Transactions on Industrial Electronics* **67** (2020), no. 9 7681–7690.

[133] L. Ge, F. Chen, D. Wang, Y. Zhang, D. Han, T. Wang, and G. Gu, *Design, modeling, and evaluation of fabric-based pneumatic actuators for soft wearable assistive gloves*, *Soft robotics* **7** (2020), no. 5 583–596.

[134] W. Kim, B. Seo, S. Y. Yu, and K.-J. Cho, *Deployable soft pneumatic networks (d-pneunets) actuator with dual-morphing origami chambers for high-compactness*, *IEEE Robotics and Automation Letters* **7** (2021), no. 2 1262–1269.

[135] M. Feng, D. Yang, and G. Gu, *High-force fabric-based pneumatic actuators with asymmetric chambers and interference-reinforced structure for soft wearable assistive gloves*, *IEEE Robotics and Automation Letters* **6** (April, 2021) 3105–3111.

[136] H. Li, L. Cheng, Z. Li, and W. Xue, *Active disturbance rejection control for a fluid-driven hand rehabilitation device*, *IEEE/ASME Transactions on Mechatronics* **26** (April, 2021) 841–853.

[137] S. Jadhav, M. R. A. Majit, B. Shih, J. P. Schulze, and M. T. Tolley, *Variable stiffness devices using fiber jamming for application in soft robotics and wearable haptics*, *Soft Robotics* **9** (Feb, 2022) 173–186.

[138] L. Gerez, G. Gorjup, Y. Zhou, and M. Liarokapis, *A hybrid, soft robotic exoskeleton glove with inflatable, telescopic structures and a shared control operation scheme*, in *2022 International Conference on Robotics and Automation (ICRA)*, pp. 5693–5699, May, 2022.

[139] J. Lai, A. Song, J. Wang, Y. Lu, T. Wu, H. Li, B. Xu, and X. Wei, *A novel soft glove utilizing honeycomb pneumatic actuators (hpas) for assisting activities of daily living*, *IEEE Transactions on Neural Systems and Rehabilitation Engineering* **31** (2023) 3223–3233.

[140] Z. Wang, X. Zhou, Z. Zhou, Y. Zhang, Y. Zhang, and D. Wang, *Matejam: Multi-material teeth-clutching layer jamming actuation for soft haptic glove*, *IEEE Transactions on Haptics* **16** (2023), no. 2 276–286.

[141] Y. Liu, Y. Wang, H. Gao, Q. Wang, and H. Zhao, *From skin movement to wearable robotics: The case of robotic gloves*, *IEEE/ASME Transactions on Mechatronics* **29** (Dec, 2024) 4108–4119.

[142] G. Mashud, S. Hasan, and N. Alam, *Advances in control techniques for rehabilitation exoskeleton robots: A systematic review.*, in *Actuators*, vol. 14, 2025.

[143] S. Lei and K. Huang, *Research on design strategies of wearable devices for the visually impaired*, in *2024 International Conference on Humanities, Arts, Education and Social Development (HAESD 2024)*, pp. 107–115, Atlantis Press, 2024.

[144] T. Bützer, J. Dittli, J. Lieber, H. J. van Hedel, A. Meyer-Heim, O. Lambercy, and R. Gassert, *Pexo-a pediatric whole hand exoskeleton for grasping assistance in task-oriented training*, in *2019 IEEE 16th International Conference on Rehabilitation Robotics (ICORR)*, pp. 108–114, IEEE, 2019.

[145] G. Salvietti, L. Franco, M. Tschiersky, G. Wolterink, M. Bianchi, A. Bicchi, F. Barontini, M. Catalano, G. Grioli, M. Poggiani, *et. al.*, *Integration of a passive exoskeleton and a robotic supernumerary finger for grasping compensation in chronic stroke patients: The softpro wearable system*, *Frontiers in Robotics and AI* **8** (2021) 661354.

[146] E. Battaglia, J. P. Clark, M. Bianchi, M. G. Catalano, A. Bicchi, and M. K. O'Malley, *Skin stretch haptic feedback to convey closure information in anthropomorphic, under-actuated upper limb soft prostheses*, *IEEE Transactions on Haptics* **12** (2019), no. 4 508–520.

[147] J. P. Clark, S. Y. Kim, and M. K. O'Malley, *The rice haptic rocker: Comparing longitudinal and lateral upper-limb skin stretch perception*, in *International Conference on Human Haptic Sensing and Touch Enabled Computer Applications*, pp. 125–134, Springer, 2018.

[148] J. P. Clark, S. Y. Kim, and M. K. O'Malley, *The rice haptic rocker: Altering the perception of skin stretch through mapping and geometric design*, in *2018 IEEE Haptics Symposium (HAPTICS)*, pp. 192–197, IEEE, 2018.

[149] B. Duvernoy, S. Topp, and V. Hayward, *Hapticomm, a haptic communicator device for deafblind communication*, in *International AsiaHaptics conference*, pp. 112–115, Springer, 2018.

[150] B. Duvernoy, I. Farkhatdinov, S. Topp, and V. Hayward, *Electromagnetic actuator for tactile communication*, in *International Conference on Human Haptic Sensing and Touch Enabled Computer Applications*, pp. 14–24, Springer, 2018.

[151] S. Dinulescu, N. Tummala, G. Reardon, B. Dandu, D. Goetz, S. Topp, and Y. Visell, *A smart bracelet supporting tactile communication and interaction*, in *2022 IEEE Haptics Symposium (HAPTICS)*, pp. 1–7, IEEE, 2022.

[152] C. M. Reed, W. M. Rabinowitz, N. I. Durlach, L. D. Braida, S. Conway-Fithian, and M. C. Schultz, *Research on the tadoma method of speech communication*, *The Journal of the Acoustical Society of America* **77** (1985), no. 1 247–257, [https://doi.org/10.1121/1.392266].

[153] C. M. Reed, L. A. Delhorne, and N. I. Durlach, *Tactile reception of fingerspelling and sign language*, *The Journal of the Acoustical Society of America* **82** (1987), no. S1 S24–S24, [https://doi.org/10.1121/1.2024713].

[154] J. M. Loomis, *On the tangibility of letters and braille*, *Perception & Psychophysics* **29** (Jan., 1981) 37–46.

[155] H. Nicolau, K. Montague, T. Guerreiro, A. Rodrigues, and V. L. Hanson, *Holibraille: Multipoint vibrotactile feedback on mobile devices*, in *Proceedings of the 12th International Web for All Conference*, pp. 1–4, 2015.

[156] U. Gollner, T. Bieling, and G. Joost, *Mobile lorm glove: introducing a communication device for deaf-blind people*, in *Proceedings of the sixth international conference on tangible, embedded and embodied interaction*, pp. 127–130, 2012.

[157] H. Z. Tan, C. M. Reed, Y. Jiao, Z. D. Perez, E. C. Wilson, J. Jung, J. S. Martinez, and F. M. Severgnini, *Acquisition of 500 english words through a tactile phonemic sleeve (taps)*, *IEEE Transactions on Haptics* **13** (2020), no. 4 745–760.

[158] C. Vogler and D. Metaxas, *Parallel hidden markov models for american sign language recognition*, in *Proceedings of the Seventh IEEE International Conference on Computer Vision*, vol. 1, pp. 116–122 vol.1, 1999.

[159] A. Theil, L. Buchweitz, J. Gay, E. Lindell, L. Guo, N.-K. Persson, and O. Korn, *Tactile board: A multimodal augmentative and alternative communication device for individuals with deafblindness*, in *19th International Conference on Mobile and Ubiquitous Multimedia*, MUM 2020, (New York, NY, USA), p. 223–228, Association for Computing Machinery, 2020.

[160] Y. Shao, V. Hayward, and Y. Visell, *Spatial patterns of cutaneous vibration during whole-hand haptic interactions*, *Proceedings of the National Academy of Sciences* **113** (2016), no. 15 4188–4193.

[161] Y. Shao, V. Hayward, and Y. Visell, *Compression of dynamic tactile information in the human hand*, *Science advances* **6** (2020), no. 16 eaaz1158.

[162] X. Libouton, O. Barbier, Y. Berger, L. Plaghki, and J.-L. Thonnard, *Tactile roughness discrimination of the finger pad relies primarily on vibration sensitive afferents not necessarily located in the hand*, *Behavioural brain research* **229** (2012), no. 1 273–279.

[163] K. O. Sofia and L. Jones, *Mechanical and psychophysical studies of surface wave propagation during vibrotactile stimulation*, *IEEE transactions on haptics* **6** (2013), no. 3 320–329.

[164] A. Mujibiya, X. Cao, D. S. Tan, D. Morris, S. N. Patel, and J. Rekimoto, *The sound of touch: on-body touch and gesture sensing based on transdermal ultrasound propagation*, in *Proceedings of the 2013 ACM international conference on Interactive tabletops and surfaces*, pp. 189–198, 2013.

[165] Y. Zhang, W. Kienzle, Y. Ma, S. S. Ng, H. Benko, and C. Harrison, *Actitouch: Robust touch detection for on-skin ar/vr interfaces*, in *Proceedings of the 32nd Annual ACM Symposium on User Interface Software and Technology*, pp. 1151–1159, 2019.

[166] S. Sundaram, P. Kellnhofer, Y. Li, J.-Y. Zhu, A. Torralba, and W. Matusik, *Learning the signatures of the human grasp using a scalable tactile glove*, *Nature* **569** (2019), no. 7758 698–702.

[167] R. Booth and P. Goldsmith, *A wrist-worn piezoelectric sensor array for gesture input*, *Journal of Medical and Biological Engineering* **38** (2018), no. 2 284–295.

[168] R. S. Johansson and G. Westling, *Signals in tactile afferents from the fingers eliciting adaptive motor responses during precision grip*, *Experimental brain research* **66** (1987), no. 1 141–154.

[169] L. Marchal-Crespo and D. J. Reinkensmeyer, *Review of control strategies for robotic movement training after neurologic injury*, *Journal of neuroengineering and rehabilitation* **6** (2009), no. 1 20.

[170] P. S. Lum, S. B. Godfrey, E. B. Brokaw, R. J. Holley, and D. Nichols, *Robotic approaches for rehabilitation of hand function after stroke*, *American journal of physical medicine & rehabilitation* **91** (2012), no. 11 S242–S254.

[171] E. M. Refour, B. Sebastian, R. J. Chauhan, and P. Ben-Tzvi, *A general purpose robotic hand exoskeleton with series elastic actuation*, *Journal of mechanisms and robotics* **11** (2019), no. 6 060902.

[172] S. M. Steinl and L. Johannsen, *Interpersonal interactions for haptic guidance during maximum forward reaching*, *Gait & posture* **53** (2017) 17–24.

[173] E. J. A. Mireles, J. Zenzeri, V. Squeri, P. Morasso, and D. De Santis, *Skill learning and skill transfer mediated by cooperative haptic interaction*, *IEEE Transactions on Neural Systems and Rehabilitation Engineering* **25** (2017), no. 7 832–843.

[174] J. Nishida, Y. Tanaka, R. Nith, and P. Lopes, *Digitusync: A dual-user passive exoskeleton glove that adaptively shares hand gestures*, in *Proceedings of the 35th Annual ACM Symposium on User Interface Software and Technology*, pp. 1–12, 2022.

[175] N. M. Oomen, R. B. Graham, and S. L. Fischer, *Exploring the role of task on kinematic variability and assessing consistency in individual responses across repetitive manual tasks*, *Ergonomics* **66** (2023), no. 6 749–761.

[176] G. M. Johansson and C. K. Häger, *A modified standardized nine hole peg test for valid and reliable kinematic assessment of dexterity post-stroke*, *Journal of neuroengineering and rehabilitation* **16** (2019), no. 1 8.

[177] P. Feys, I. Lamers, G. Francis, R. Benedict, G. Phillips, N. LaRocca, L. D. Hudson, R. Rudick, and M. S. O. A. Consortium, *The nine-hole peg test as a manual dexterity performance measure for multiple sclerosis*, *Multiple Sclerosis Journal* **23** (2017), no. 5 711–720.

[178] P. Jenmalm and R. S. Johansson, *Visual and somatosensory information about object shape control manipulative fingertip forces*, *Journal of Neuroscience* **17** (1997), no. 11 4486–4499.

[179] J. M. Goodman and S. J. Bensmaia, *The neural basis of haptic perception*, *Stevens' handbook of experimental psychology and cognitive neuroscience* **2** (2018) 201–240.

[180] R. W. Angel, *Efference copy in the control of movement*, *Neurology* **26** (1976), no. 12 1164–1164.

[181] T. Froese and G. U. Ortiz-Garin, *Where is the action in perception? an exploratory study with a haptic sensory substitution device*, *Frontiers in psychology* **11** (2020) 809.

[182] S. Dinulescu, D. Goetz, N. Tummala, S. Lee, J. Carpino, and Y. Visell, "An inter-manual exoskeleton that facilitates guided multi-finger grasping and manipulation." Unpublished, March, 2026.

[183] M. R. Longo, F. Schüür, M. P. Kammers, M. Tsakiris, and P. Haggard, *What is embodiment? a psychometric approach*, *Cognition* **107** (2008), no. 3 978–998.

[184] D. Roth and M. E. Latoschik, *Construction of the virtual embodiment questionnaire (veq)*, *IEEE transactions on visualization and computer graphics* **26** (2020), no. 12 3546–3556.

[185] A. Gallace and C. Spence, *The science of interpersonal touch: an overview*, *Neuroscience & Biobehavioral Reviews* **34** (2010), no. 2 246–259.

[186] M. Pyasik, T. Furlanetto, and L. Pia, *The role of body-related afferent signals in human sense of agency*, *Journal of Experimental Neuroscience* **13** (2019) 1179069519849907.

[187] D. Rabellino, P. A. Frewen, M. C. McKinnon, and R. A. Lanius, *Peripersonal space and bodily self-consciousness: implications for psychological trauma-related disorders*, *Frontiers in Neuroscience* **14** (2020) 586605.

[188] C. S. Park and B. K. Kaye, *Smartphone and self-extension: Functionally, anthropomorphically, and ontologically extending self via the smartphone*, *Mobile Media & Communication* **7** (2019), no. 2 215–231.